M.A.G.T. van den Hoop

ELECTROCHEMICAL METAL SPECIATION

IN NATURAL AND MODEL POLYELECTROLYTE SYSTEMS

M.A.G.T. van den Hoop

ELECTROCHEMICAL METAL SPECIATION

IN NATURAL AND MODEL POLYELECTROLYTE SYSTEMS

Proefschrift
ter verkrijging van de graad van doctor
in de landbouw- en milieuwetenschappen
op gezag van de rector magnificus,
dr. C.M. Karssen
in het openbaar te verdedigen
op vrijdag 21 januari 1994
des namiddags te vier uur in de Aula
van de Landbouwuniversiteit te Wageningen

Stellingen

1) De binding van (zware) metalen aan natuurlijke macromoleculen verschilt aanzienlijk van die aan synthetische polyzuren, zoals polymethacrylzuur.

Dit proefschrift.

2) De protolytische omstandigheden in een metaal/polyelectroliet systeem worden niet uitsluitend gedefinieerd door de pH.

Dit proefschrift.

3) Bij de afleiding van milieukwaliteitsdoelstellingen voor sedimenten dient in het geval van zware metalen rekening gehouden te worden met het Acid Volatile Sulfide gehalte.

M.A.G.T. van den Hoop and H.A. den Hollander,
RIVM report, draft version December 1993.

4) De term biobeschikbaarheid kan in veel gevallen aan betekenis winnen als er een nadere omschrijving aan toe wordt gevoegd.

5) Het benadrukken van andermans fouten in wetenschappelijke geschriften, zoals dat regelmatig gebeurt in stellingen bij proefschriften, is gemakkelijk. Die wetenschapper die de positieve aspecten van andermans werk naar voren brengt, verdient waardering.

6) Bedrijven, organisaties en afdelingen krijgen de leidinggevenden die zij verdienen.

7) Mensen die de uitdrukking "praat me er niet van" gebruiken, gaan meestal op de praatstoel zitten.

8) Stellingen bij proefschriften moeten óf getuigen van enige grootsheid óf een ludiek karakter hebben.

9) Chaos is een vorm van orde.

James Gleick, Chaos: making a new science.
New York etc., Viking, 1987.

Stellingen behorende bij het proefschrift "Electrochemical metal speciation in natural and model polyelectrolyte systems".
Marc van den Hoop, Wageningen, 21 januari 1994.

Voor Paletti

EEN WOORD VOORAF

Het is zover. Ik kan u nu eindelijk laten zien en lezen waar ik mij de afgelopen jaren mee bezig heb gehouden. Dit proefschrift geeft u echter slechts een indruk van mijn wetenschappelijke werkzaamheden. Jammer, want ik heb mij niet alleen kunnen ontwikkelen op wetenschappelijk gebied, maar ook op persoonlijk vlak. Dit was mogelijk door de mensen om mij heen.

Op de vakgroep heerste een zeer gemoedelijke sfeer, waar ik het bijzonder naar mijn zin heb gehad. Een tijd, waarin gewerkt moest worden aan de inhoud van dit proefschrift, maar waarin tevens een haast onmetelijke vrijheid bestond. Van mijn begeleiders kreeg ik wetenschappelijke vrijheid; (externe) financiële bijdragen gaven mij bewegingsvrijheid; door flexibele werktijden had ik de vrijheid om ook aan andere overdag plaatsvindende activiteiten deel te nemen. In mijn werkomgeving had ik de vrijheid om mijn verhalen kwijt te kunnen, niet alleen in de koffiekamer, maar ook in de gangen, het lab, down town en bij het secretariaat.

Het is waarschijnlijk overbodig u te vertellen dat ik met veel plezier op reis ging. Hierdoor kreeg ik de mogelijkheid om buitenlandse collega's te ontmoeten, andere culturen en werelden te ontdekken, te genieten van natuurschoon en het leven in de plaatselijke kroegen. De buitenlandse collega's hebben mij geholpen door meetapparatuur beschikbaar te stellen en door discussies over wetenschappelijke en minder wetenschappelijke zaken. Samen met hen heb ik publicaties geschreven en zal dat in de toekomst blijven doen. Bovendien heb ik hier ook nog goede vrienden aan overgehouden.

Op hun eigen manier motiveren mensen uit mijn nabije omgeving, zoals familie, vrienden, afdelingsgenoten, buren, volkshuisvesters en (nieuwe) collega's, mij aan mijn leven een positieve invulling te geven. Hun belangstelling voor mij en mijn dagelijkse activiteiten, geven mij energie om dit te realiseren. In mijn leven neemt mijn levensgezel een bijzondere plaats in. Zij weet mij steeds weer door haar liefde en doortastendheid te stimuleren niet stil te staan, maar door te gaan met ontwikkelen.

Al deze mensen bedank ik alvast hierbij. Maar liever doe ik dat onder het genot van een goed glas.

1. INTRODUCTION

2. CONDUCTOMETRIC ANALYSIS OF METAL/POLYELECTROLYTE SYSTEMS

3. STRIPPING VOLTAMMETRY OF METAL COMPLEXES WITH MACROMOLECULAR LIGANDS

4. CONDUCTOMETRIC VERSUS VOLTAMMETRIC SPECIATION

5. CONDUCTOMETRY AND VOLTAMMETRY OF METAL COMPLEXES OF SYNTHETIC POLYACIDS

6. PRETREATMENT AND CHARACTERIZATION OF HUMIC ACIDS

7. CONDUCTOMETRY AND VOLTAMMETRY OF METAL COMPLEXES WITH NATURAL POLYACIDS

CHAPTER 1

Introduction

1.1 Metal speciation in aquatic systems

Nowadays, metal speciation is a well-known term used for the determination of the distribution of metal ions over different chemical and/or physico-chemical forms, and for the distribution itself. In natural systems, physico-chemical forms of metal ions include: the free (hydrated) metal ion; complexes of metal with simple inorganic species, such as chloride and carbonate; complexes of metal with macromolecular ligands, like humic and fulvic acids; metal ions adsorbed on a variety of colloidal particles, for example clay minerals and (hydr)oxides of iron, manganese or aluminium; and precipitate metal compounds, such as heavy metal sulfides. All these species can co-exist and, hence, the prediction of the metal ion distribution in these systems may be quite complicated. With respect to the bio-availability of (heavy) metals, knowledge of their speciation is of great significance, both from the viewpoint of their essentiality for various life forms, which is the case for e.g. zinc, potassium and calcium, and with respect to their toxicity, as is the case of e.g. cadmium and lead. It is well-known that toxic effects of heavy metals may be reduced in the presence of complexing agents [e.g. 1-4]. Obviously, under these conditions the metals may be less available for uptake by organisms. In general, many chemical and biological properties of metals in natural waters can hardly be explained on the basis of total metal concentrations. The understanding of these properties greatly improves by taking into account the actual speciation of the metals. Extensive lists of references to studies of (heavy) metal speciation in natural systems are available in the literature and support the great importance of the current subject [5-7].

In order to limitate the immense field of metal speciation, we will focus in the present study on the distribution of (heavy) metals over the free and bound states in aquatic systems containing macromolecular complexants of natural origin, in particular dissolved organic matter, such as humic and fulvic acids. These polyacids belong to the major natural complexants of metals and play an important role in their circulation in aquatic systems [8]. Due to binding of metals by the macromolecules, the availability of the metals for organisms may decrease, whereas, on the other hand, the mobility of the metals may increase, because the complexing agents are quite soluble in aquatic systems. In marine and fresh waters typical concentrations of dissolved organic carbon are found to be in the range of $10 \ \mu g.l^{-1}$ up to $10 \ mg.l^{-1}$ [5].

Humic material results from chemical and biochemical transformations of the products of decay, desintegration, and microbial action. Due to the great differences in origin it has a very complex and heterogeneous structure. Because of the structural complexities and varieties, the exact composition is not definable; it depends primarily on the source of the humic material (i.e. sea, estuary, lake, or soil) [5]. Although the global structural formula is different for various humic acids, their chemical structures and properties are quite similar. Humic and fulvic acids have many functional groups, predominantly carboxylic and phenolic hydroxylic, and these are subject to dissociation. Hence, these polyacids are generally charged and therefore they are often referred to as (bio)polyelectrolytes. Due to chemical and electrostatic interactions, humic substances are able to bind heavy metals and, hence, to influence or even control the distribution of these metal ions in natural systems.

1.2 (Bio)polyelectrolytes and counterion distribution

Polyelectrolytes may be denoted as a class of macromolecules, which contain a large number of chargeable groups on the macromolecular chain. Polyacids in aqueous solution are generally able to dissociate into negatively charged polyions and protons. One way of classifying these macromolecules is according to the strength of the groups into strong and weak polyelectrolytes. For the former group of polyacids, the dissociation may reach its maximum value at any pH, whereas for the latter the (spontaneous) degree of dissociation may be quite low for relative low pH. Examples of weak polyelectrolytes are polyacrylic acid, polymethacrylic acid and humic acid. Polystyrenesulfonic acid is an example of a strong polyelectrolyte. Several reviews on polyelectrolytes and their properties are available in the literature [9-13].

One of the crucial properties of multiply charged polyelectrolytic species is their interaction with counterions. The electrostatic interaction between charged sites on the polyelectrolyte is generally responsible for a speciation pattern of counterions that is quite different from that for mono-functional electrolytes such as acetate [13]. The following specific features may play major roles in metal speciation in polyelectrolyte systems:

(i)   The polyionic charge density is a basic parameter that controls the distribution of counterions over the free and bound state. For example, Cleven [14] has studied the binding of divalent metal ions with a variety of (bio)polyelectrolytes and found that the stabilities of metal/polyion complexes increase with increasing degree of neutralization, which is related to the charge density of the polyelectrolyte. These results are in

agreement with the observations in a number of other studies [15-17]. Generally, the association of counterions with polyelectrolytes increases with increasing charge density on the polyion.

(ii)   Furthermore, the association of divalent metals with polyelectrolytes is in several ways affected by the presence of monovalent counterions. First, in the case of a large excess of monovalent counterions over divalent ones, the former ions are mainly responsible for the ionic strength. Hence, they control the magnitude of the Debye screening length and thus the resulting effective charge density of the polyelectrolyte. Second, electrostatic interaction of monovalent counterions with the polyion may give rise to competition effects with respect to the divalent counterions and thus affect the speciation patterns of the metals involved. For example, Cabaniss and Shuman [18] observed a 10-fold increase in copper activity by increasing the $NaClO_4$ concentration from 0.005 to 0.05 mol.l^{-1} for a Suwannee River fulvic acid sample at a constant pH of 7. For other polyelectrolytes, such as polyacrylic acid and polygalacturonic acid, a similar decrease in the extent of binding of divalent counterions has been found upon increasing concentrations of monovalent counterions [19,20].

(iii)   For naturally occurring polyelectrolytes, the chemical heterogeneity with respect to binding sites on the polyelectrolyte is another important parameter. Different types of sites may have different affinities for counterions. Commonly, this is referred to as the polyfunctional character of the macromolecules. To each single type of site a single intrinsic binding constant may be assigned. In addition, the overall stability of the metal/complex is also affected by electrostatic interactions among the sites as met in (i). In these cases, the association of counterions can no longer be described by one single stability. This has led to the introduction of equilibrium affinity distribution functions [8,21,22], which depend on the metal/complexing site ratio [23-25].

(iv)   Finally, the conformation of the polyelectrolyte may change as the result of variations in the charge density and the degree of hydration of the macromolecule. For example, the stabilized, hypercoiled conformation of polymethacrylic acid at low pH values disappears with increasing charge density on the polymeric chain [26], which may result in changes of the speciation pattern of counterions. O'Neill *et al*. [27] and Morawetz and Kandanian [28] have found that the binding of Cu^{2+} and Mg^{2+} with polymethacrylic acid is quite different for the isotactic conformation compared to the syndiotactic one.

1.3 Electrochemical methods

Considering various electrochemical techniques, potentiometry is certainly the most attractive for speciation. The observed potential is a direct measure of the activity of free (hydrated) metal species. In the absence of any significant interference with other ions, the speciation information can easily be obtained through a Nernst-type equation. However, the selectivity is rather limited, especially if chemically similar ions are present in the sample. For natural samples another serious limitation arises. The detection limit is not far below 10^{-6} mol.l^{-1}. Finally, the poor precision of potentiometry reduces its applicability under conditions where accurate measurements are required. Therefore, electrochemical methods such as polarography and voltammetry are widely used in trace element speciation in natural water systems, because of their metal-specificity, their high sensitivity and the allowance of direct speciation [5,29-31]. Although the specific potentialities of voltammetric techniques for the characterization of all kinds of homogeneous complexation reactions of electroactive metal ions have been recognized for a long period [32], application of voltammetry to speciation in polyelectrolytic systems is quite recent [14,31,33,34].

For metal-complexes with sufficiently large association/dissociation rate constants, the voltammetric response will be a function of the diffusion of both the free metal ion and the bound metal. In many speciation studies, the diffusion coefficients of the free and the bound metal have been assumed to be equal [see e.g. 35, 36], which is a reasonable assumption in the case of small complexing agents. However, for macromolecules, such as polymethacrylic acid and humic material, the diffusion coefficient of the polyacid is much smaller compared to that of the free metal ion [37]. Ignoring this difference will lead to misinterpretation of voltammetric data if the complexes are labile. The problem, however, can be tackled by considering the average diffusion coefficient, which takes into account the diffusion coefficients of both the free and bound metal for simultaneously diffusing labile species. The concept of an average diffusion coefficient was already put forward in the early fifties, firstly in the frame of experimental studies [38,39] and later on a theoretical basis [40]; the combination of this concept with finite complex association/dissociation rates became available in the eighties [33,34].

However, the applicability of the recent developped theory is *a priori* limited to direct voltammetric techniques, such as normal pulse polarography, differential pulse polarography or ac polarography. Extension to stripping techniques like differential pulse anodic stripping voltammetry is not an obvious matter, since the influence of the effective diffusion coefficient

on the (pre-electrolysis) current depends on the hydrodynamic and geometrical conditions. Although accurate theory is not (yet) available for stripping voltammetries, one may suppose that for labile metal complexes the voltammetric current is still a function of the mean diffusion coefficient to some power p, which incorporates the mass transport conditions. On a more operational level, analysis is then performed by fitting the experimentally obtained voltammetric response to this postulated functionality. The present study is concerned with the application of this approach to metal ion binding studies in solutions of well-defined synthetic polyelectrolytes and naturally occurring ones.

Although less sensitive than voltammetric methods, conductometry has been shown to be a valuable supporting tool in the analysis of metal/polyelectrolyte systems [14,19,41-46]. The applicability of conductometry to speciation in polyelectrolytic systems has been known for years [41,42]. Conductometry measures the total ionic transport of all charged species in the system, but is unable to distinguish directly between the various contributions. For the case of monovalent counterions, this problem was first tackled by Eisenberg [41], who varied the nature of the counterion, which enabled the estimation of the distribution of counterions over the free and bound states. Conductometric analysis of mixed metal/polyelectrolyte systems in terms of free and bound counterions became possible by applying the conductivity excess function [14,19], which is defined as the negative difference between the specific conductivity of a mixed metal/polyelectrolyte system and the sum of the conductivities of the metal salt and the poly-electrolyte solution before mixing. So far the interpretation of data using this function remained more or less qualitative [14]. However, a combination of the Eisenberg procedure together with the conductivity excess function does allow the computation of fractions of both monovalent and divalent bound counterions [14]. The theoretical treatment of the conductivity of poly-electrolyte solutions is generally based on a two-state approximation, i.e. the counterions are assumed to be either bound to the polyion or free in solution [11,47]. Although this approach is an oversimplification of the real situation, it may be operationally helpful and in many practical situations it is efficacious. Part of this study will therefore be concerned with the interpretation of conductometrically measured counterion distributions in terms of a two-state counterion distribution model.

1.4 Outline of this thesis

The aim of the present study is to investigate the applicability of conductometric and voltam-
metric techniques in obtaining information on the speciation of metals in systems containing
macromolecules. Available theory from the literature is validated. For this purpose, the
interaction of zinc and cadmium with synthetic and naturally occurring polyacids is studied by
both electrochemical methods. Polymethacrylic and polyacrylic acids are used as model poly-
electrolytes, whereas humic acids are chosen as examples of complexing agents in natural waters.
The content of the different chapters is given below.

In chapter 2, the present state of the theory of conductometric analysis of metal/polyelectrolyte
systems is described. Special attention is paid to the relation between the conductometrically
measured counterion distribution and the two-state counterion distribution. Furthermore, the
treatment of conductometric data, resulting into fractions of free and bound counterions, is
developed for systems containing both monovalent and divalent counterions.

Chapter 3 deals with the voltammetric speciation of metal/complexes in systems containing
macromolecular ligands. An electroanalytical procedure for determining the stability of labile
metal/polyacid complexes under natural conditions is described. The procedure presented takes
into account diffusion of free and bound metal ions. The influence of two interfering phenomena,
i.e. adsorption of metal ions on vessel material and protolysis of the macromolecular ligand, are
discussed in some detail.

A comparison between conductometric speciation and voltammetric speciation is made in
chapter 4. For both electrochemical techniques, the typical ranges of application are derived.
From the analysis of conductometric and voltammetric data for the $Zn(II)$/polymethacrylate
system, it is shown that the two methods are to some extent complementary.

In chapter 5, conductometric and voltammetric speciation data are presented for some
metal/polyacrylate and metal/polymethacrylate systems. Conductometric fractions of free and
bound monovalent and divalent counterions are compared to theoretical predictions computed
from a recently proposed extended counterion condensation model [48]. Stabilities obtained
from voltammetric complexation curves are presented and discussed with respect to the influence
of (i) the molar mass of the macromolecules, (ii) the supporting electrolyte concentration, and
(iii) the charge density of the polyion.

Chapter 6 deals with the purification and characterization of humic acids. Pretreatment and fractionation (based on pH solubility) procedures for the humic acids are described. The humic acids are characterized in terms of chargeable groups by conductometric titration and molar mass distributions by flow field-flow-fractionation.

For naturally occurring polyelectrolytes, i.e. humic acids, experimental speciation data are presented in chapter 7. The structure of this chapter is similar to that of chapter 5. Analysis of conductometric acid-base titrations of humic acids shows that the polyelectrolytic nature of these polyacids is (much) less pronounced compared to the synthetic polyelectrolytes PMA and PAA. Voltammetric speciation data confirm this behaviour, which is tentatively explained in terms of the distribution of charges on the humic acids. Finally the need for future activities in this field is outlined.

1.5 References

1. W.G. Sunda and J.A.M. Lewis, Limnol. Oceanogr., 23 (1978) 870.
2. Y.K. Chau, R. Gacther and K. Lum-Shue-Chang, J. Fish Res. Board Can., 31 (1974) 1515.
3. B.S. Khangarot and P.K. Ray, Ecotoxicol. Environ. Saf., 18 (1989) 109.
4. N. Corp and A.J. Morgan, Environ. Pollut., 74 (1991) 39.
5. J. Buffle, Complexation Reactions in Aquatic Systems: An Analytical Approach, Ellis Horwood Ltd, Chichester, 1988.
6. C.J.M. Kramer and J.C. Duinker (Eds), Complexation of Trace Metals in Natural Waters, Nijhoff-Junk, The Hague, 1984.
7. J.R. Kramer and H.E. Allen (Eds), Metal Speciation: theory, analysis and application, Lewis Publishers Inc., Chelsea, 1988.
8. J. Buffle, Circulation of Metals in the Environment, in H. Sigel (Ed.), Natural Organic Matter and Metal-Organic Interactions in Aquatic Systems, Series: Metal Ions in Biological Systems, Vol. 18, M. Dekker, New York, 1984.
9. C. Tanford, Physical Chemistry of Macromolecules, John Wiley & Sons Inc., New York, 1961.
10. S.A. Rice and M. Nagasawa, Polyelectrolyte Solutions, Academic Press, London, 1961.
11. F. Oosawa, Polyelectrolytes, Marcel Dekker Inc., New York, 1970.
12. H. Eisenberg, Biological Macromolecules and Polyelectrolytes in Solution, Clarendon Press, Oxford, 1976.
13. M. Mandel, in Encyclopedia of Polymer Science and Engineering, Vol. 11, Wiley, New York (1988) 739.
14. R.F.M.J. Cleven, PhD Thesis, Agricultural University, Wageningen, 1984.
15. D.E. Wilson and P. Kinney, Limnol. Oceanogr., 22 (1977) 281.
16. J.A. Marinsky and M.M. Reddy, Org. Geochem., 17 (1984) 207, 215.
17. S. Kawaguchi, T. Kitano, K. Ito and A. Minakata, Macromolecules, 24 (1991) 6335.
18. S.E. Cabaniss and M.S. Shuman, Geochim. Cosmochim. Acta, 52 (1988) 185.
19. H.G. de Jong, J. Lyklema and H.P. van Leeuwen, Biophys. Chem. 27 (1987) 173.
20. C. Qian, M.R. Asdjodi, H.G. Spencer and G.B. Savitsky, Macromolecules, 22 (1989) 995.
21. D.S. Gamble and C.H. Langford, Environ. Sci. Technol., 22 (1988) 1325.
22. M.M. Nederlof, PhD Thesis, Agricultural University, Wageningen, 1992.

8

23. J. Buffle and R.S. Altmann, in W. Stumm (Ed.), Aquatic Surface Chemistry: chemical processes at the particle-water interface, Wiley, New York (1987) 351.
24. M. Filella, J. Buffle and H.P. van Leeuwen, Anal. Chim. Acta, 232 (1990) 209.
25. J.P. Pinheiro, A.M. Mota and M.L. Simões Gonçalves, Anal. Chim. Acta, in press.
26. J.C. Leyte and M. Mandel, J. Polym. Sci. Part A, 2 (1964) 1879.
27. J.J. O'Neill, E.M. Loebl, A.Y. Kandanian and H. Morawetz, J. Polym. Sci. A, 3 (1965) 4201.
28. H. Morawetz and A.Y. Kandanian, J. Phys. Chem., 70 (1966) 2995.
29. M. Whitfield and D. Jagner (Eds.), Marine Electrochemistry. A Practical Introduction, Wiley, New York, 1981.
30. T.M. Florence, Analyst, 111 (1986) 489.
31. H.P. van Leeuwen, R.F.M.J. Cleven and J. Buffle, Pure Appl. Chem., 61 (1989) 255.
32. J. Heyrovsky, Polarographie, Springer, Wien, 1941.
33. R.F.M.J. Cleven, H.G. de Jong and H.P. van Leeuwen, J. Electroanal. Chem., 202 (1986) 57.
34. H.G. de Jong, H.P. van Leeuwen and K. Holub, J. Electroanal. Chem., 234 (1987) 1, 17; 235 (1987); 260 (1989) 213.
35. D.R. Turner and M. Whitfield, J. Electroanal. Chem., 103 (1979) 43, 61.
36. B. Raspor, H.W. Nürnberg, P. Valenta and M. Branica, Mar. Chem., 15 (1984) 231.
37. P.K. Cornel, R.S. Summers and P.V. Roberts, J. Colloid Interface Sci., 110 (1986) 149.
38. V. Hanus and R. Brdicka, Chem. Listy, 44 (1950) 291.
39. V. Kacena and L. Matousek, Chem. Listy, 46 (1952) 525.
40. J. Koutecky, Collect. Czech. Chem. Commun., 19 (1954) 857.
41. H. Eisenberg, J. Polym. Sci., 30 (1958) 47.
42. T. Kurucsev and B.J. Steel, Pure Appl. Chem., 17 (1969) 149.
43. W.P.J.T. van der Drift, PhD Thesis, State University Utrecht, 1975.
44. G.S. Manning, J. Phys. Chem., 79 (1975) 262.
45. G.S. Manning, Q. Rev. Biophys., 11 (1978) 179.
46. H.P. van Leeuwen, R.F.M.J. Cleven and P. Valenta, Pure Appl. Chem., 63 (1991) 1251.
47. G.S. Manning, J. Chem. Phys., 51 (1969) 924.
48. S. Paoletti, J.C. Benegas, A. Cesàro, G. Manzini, F. Fogolari and V. Crescenzi, Biophys. Chem., 41 (1991) 73.

CHAPTER 2

Conductometric analysis of metal/polyelectrolyte systems

2.1 Introduction

Conductometry has become an important tool in the analysis of physicochemical properties of polyelectrolyte solutions [1-8]. Classical work up to the mid sixties has been reviewed by Kurucsev and Steel [9]. Conductometry measures the transport of *all* charged species in the system studied. The conductance of polyelectrolyte solutions is affected by association of counterions with the polyion, which obviously is of primary interest for metal speciation in polyelectrolytic systems. However, due to the lack of adequate theory, for quite some time the interpretation of conductivity data has remained mainly descriptive. For example, in conductometric titration curves of humic matter, distinguishable parts have been interpreted as reflecting the existence of different types of functional groups [4,10,11], thereby ignoring the electrostatic interactions typical of polyelectrolytes. In the seventies, substantial progress has been made in the development of the theory of polyelectrolytes, in particular with respect to counterion binding and conductivity [2,12,13]. The theoretical developments concerning ion association phenomena in relation to their implications for conductivities of polyelectrolyte solutions have been recently reviewed by Van Leeuwen *et al.* [14]. The interpretation of a number of titration curves for practical systems could be improved on the basis of the recent theoretical results. For monovalent counterions, it is now possible to estimate the distribution of the counterions over the free and bound states and to find the conductivity contribution of the polyion-counterion associate (λ_p) by varying the nature of the counterion [2]. This procedure has been successfully applied to polyelectrolytes in mixed electrolyte solutions [6,15].

For linear polyelectrolytes of infinite length, the theoretical analysis of the distribution of small ions around the polyion can be roughly classified into two categories. One is based on the Poisson equation and the Boltzmann distribution, and it gives an hyperbolic tangent decrease of the ion concentration as a function of distance from the polyelectrolyte chain [e.g. 16,17]. The second is based on a two-state concept, in which the counterions are considered either bound to the polyion or free in solution [18,19]. The two approaches have been critically compared by Mandel [20]. Although the first approach is more realistic, its practical application is somewhat limited by the absence of an analytical solution of the Poisson-Boltzmann equation, except for some

special cases [20]. We will mainly follow the two-state concept for cylindrical geometry and use Manning's counterion condensation theory [19]. This theory, together with its treatment of conductivity, is attractive because it introduces easily applicable concepts and leads to simple analytical expressions for various quantities under a variety of different conditions.

In this chapter we will describe the present state of the theory of conductivity characteristics of counterion-polyion systems with special emphasis on association phenomena. As part of it, attention will be paid to the relation between the conductometrically measured counterion distribution and the two-state counterion distribution.

2.2 Theory

2.2.1 Conductometry and counterion distribution

One may formally express the molar conductivity Λ of a salt-free polyelectrolyte solution as

$$\Lambda = f(\lambda_i^\circ + \lambda_p) \tag{2.1}$$

where λ_i° and λ_p represent the ionic conductivities of the free counterion in pure solvent and the polyion, respectively, and where f is a parameter ($0 \leq f \leq 1$) which expresses the extent of reduction of the conductivity due to association between the counterions and the polyion. In terms of a two-state representation of the counterion distribution, one might refer to f as to the "conductometrically free" fraction of counterions [6]. This is helpful in practice, but should not lead us to ignore the real situation where the degree of interaction between the polyion and the counterions gradually varies as a function of distance.

In the most general situation, where counterion condensation may occur, the counterion distribution is characterized by the range

electrostatically trapped ("condensed") ------→ constituent of diffuse ------→ free ion at infinite distance
by polyion (if sufficiently charged)   counterionic atmosphere   from polyion

In the case of a salt-free polyelectrolytic system, the state of the free ion is just the limit for the "outer" ions in the counterionic atmosphere.

One of the main issues in treating the conductivity of polyelectrolyte solutions is the quantification of the contribution from the ions in the diffuse counterionic atmosphere. Manning [19] tackled this by starting from the Nernst-Planck equation for the migration of the counterions, taking into account the radial part of the inhomogeneity of the electric field around the polyions and the steady ionic movement under the influence of the external field. Ignoring the possible mobility of condensed counterions along the chain, it was found that for $\xi > |z_i|^{-1}$

$$f_i = 0.866 \, | z_i |^{-1} \, \xi^{-1} \qquad\qquad (\xi \ge | z_i |^{-1}) \qquad\qquad (2.2)$$

where z_i is the valency of the counterion and ξ is the structural charge density parameter defined by

$$\xi = l_B / l \qquad\qquad (2.3)$$

In equation (2.3), l represents the spacing between charged sites on the linear polyion. The Bjerrum length l_B is defined as the distance between two charges at which the electrostatic interaction energy equals kT:

$$l_B = F^2 / 4\pi\varepsilon\varepsilon_0 RT \qquad\qquad (2.4)$$

where e is the elementary charge, $\varepsilon\varepsilon_0$ the permittivity of the solution, k the Boltzmann constant and T the absolute temperature.

The dimensionless coefficient 0.866 in equation (2.2) results from the numerical evaluation of the components of the radially inhomogeneous electric field around the linear polyion with smeared-out charge. For polyions with $\xi < 1$ and monovalent counterions, the functionality of f is a different one (with for $\xi = 1$ again $f = 0.866$)

$$f_1 = 1 - \frac{0.55\xi^2}{\pi + \xi} \qquad\qquad (\xi \le 1) \qquad\qquad (2.5)$$

At this point it is useful to emphasize the difference between condensed counterions and conductometrically bound counterions. According to the counterion condensation concept [19],
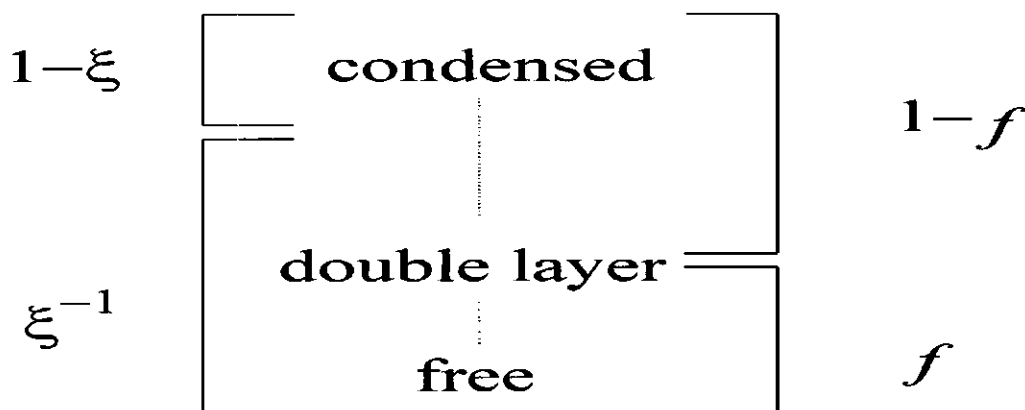
systems are thermodynamically unstable if the charge density exceeds a certain critical value:

$$\xi_{crit} = |z_i|^{-1} \tag{2.6}$$

The instability is resolved by association of counterions with the polyelectrolyte chain to such an extent that the net value of ξ is reduced to the critical value $|z_i|^{-1}$. The condensed fraction, r_i, then equals

$$r_i = z_i^{-1}(1 - 1/z_i\xi) \qquad\qquad \xi \geq \xi_{crit} \tag{2.7}$$

and hence the remaining fraction $1-r_i$ includes both the ions in the diffuse double layer and the free ions. The conductometrically bound ions include (at least in Manning's theory) *all* condensed ions, *plus* some part of the diffuse layer ions. Thus, in the case of monovalent counterions, the "free fraction" f is always some fraction of ξ^{-1} and the bound fraction $(1-f)$ is always larger than $(1-\xi^{-1})$. In a scheme:

$$
1-\xi \quad
\begin{array}{c}
\boxed{\text{condensed}} \\[2em]
\boxed{\text{double layer}} \\[1em]
\text{free}
\end{array}
\quad
\begin{array}{c}
1-f \\[3em]
f
\end{array}
$$

The expressions for f may be used in combination with equation (2.1) and thus serve as analytical working equations. Just for illustration, we have titrated several polymethacrylic acid (PMA) solutions with LiOH, NaOH and KOH solutions, respectively, in the absence of additional salt. In figure 2.1, plots of the molar conductivity of the polyelectrolyte solution Λ versus λ_i^o, so-called Eisenberg plots [1], are presented for various values of ξ with $[PMA]=2.5*10^{-3}$ mol.l^{-1}. In accordance with equation (2.1) a straight line is obtained, indicating that the interaction of alkali metal ions and the polymethacrylate anion is of a non-specific nature. The slopes and the

intercepts of the lines in figure 2.1 equal f and $f\lambda_p$, respectively. In figure 2.2, the resulting f values are presented as a function of ξ for various concentrations of PMA. The decrease of f and, hence the increase of the fraction condensed counterions with increasing charge density of the polyelectrolyte is in agreement with equation (2.7). Furthermore, the independence of f with respect to the PMA concentration confirms the typical polyelectrolytic behaviour of the alkali polymethacrylate system.
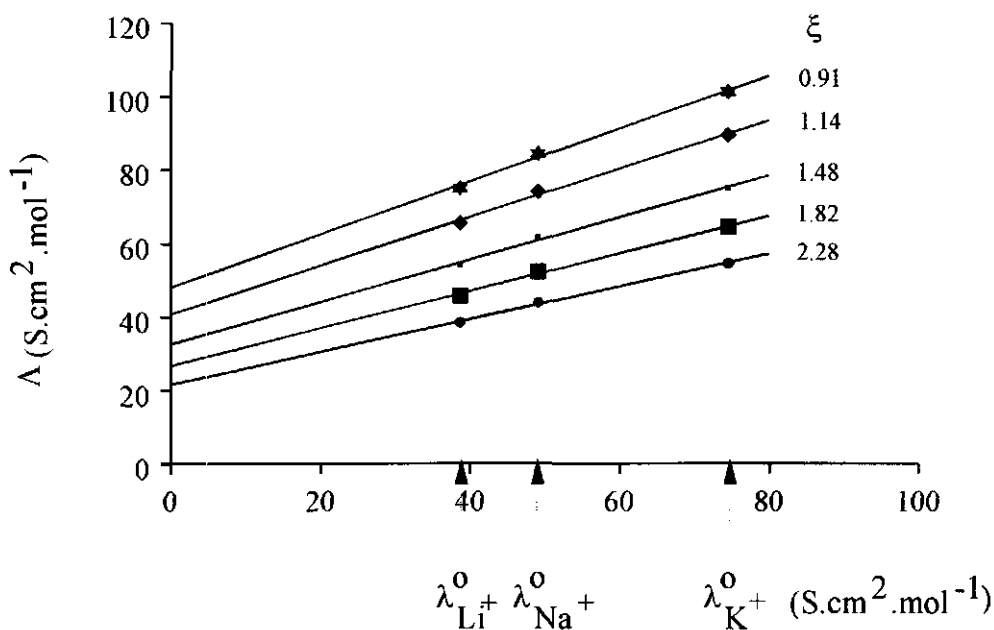
Figure 2.1: Plot of the molar conductivity of alkali polyacrylate solutions vs. the molar conductivity of the corresponding monovalent counterion for various charge densities of the polymethacrylate anion with [PMA]=2.5*10^{-3} mol.l^{-1}.

In figure 2.2, the solid curve represents the fraction conductometrically-free monovalent counterions computed with equations (2.2) and (2.5), whereas the dotted curve equals the fraction of free counterions according to the condensation approach, i.e. 1-r_i. For ξ values smaller than 1, the experimental values are well below the theoretical ones. For this range of values of ξ, the concentration of free protons may be rather high and, hence, their contribution to the overall conductance may become substantial, which is not taken into account in the Eisenberg analysis. Furthermore, in this range of ξ values the polymethacrylate anion is subject to a conformational

transition [21]. For very high values of ξ, the contribution free hydroxyl ions to the conductivity starts to participate too. However, under these conditions the problem is less severe, since the molar conductivity of OH⁻ is much smaller than that of H⁺. Nevertheless, for intermediate charge density values, the experimental f values seem to be in fair agreement with the theoretical predictions. In comparison with the scheme presented for higher charge density values, experimental f values approach the fraction free counterions according to the CC concept. This can be explained by considering the fact that the conformation of the polyelectrolyte expands and, hence, the experimental conditions better correspond to the theoretical geometrical assumption, i.e a cylindrical array of charges.
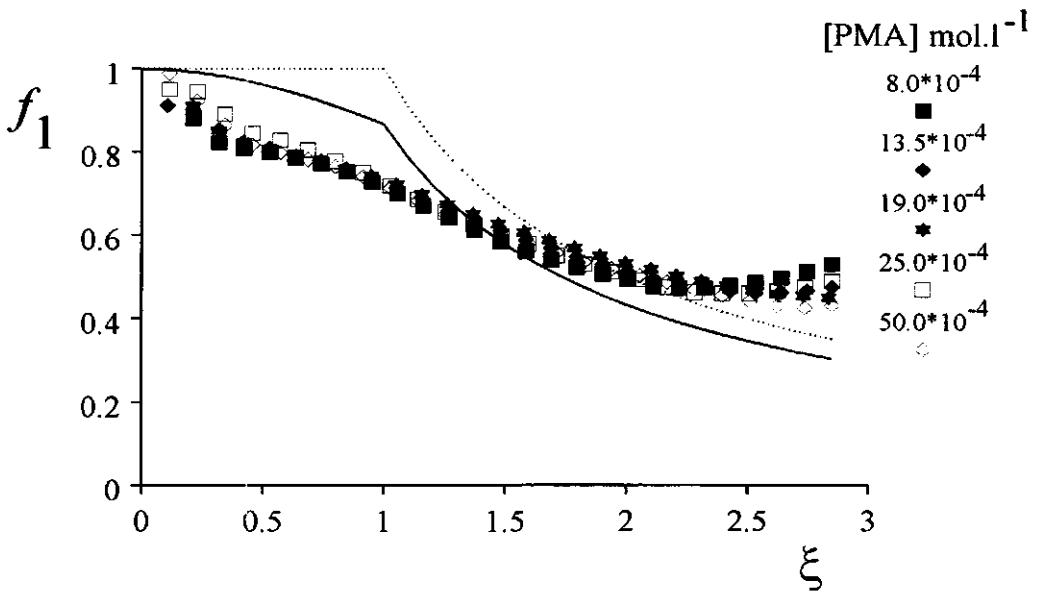
Figure 2.2: Experimental values (symbols) and theoretical values of f_1 as a function of ξ for various concentrations of PMA. Solid curve, conductometrically free counterions; dotted curve: free counterions according to the counterion condensation approach.

One may also utilize equations (2.2) and (2.5) for f to derive an analytical expression for λ_p. This can be done by considering that for $\xi > 1$ and monovalent counterions, a fraction $0.866\xi^{-1}$ of the counterions moves "freely" in the applied field, whereas a fraction of $(1-0.866)\xi^{-1}$ migrates in the opposite direction with the same mobility as the polyion [12]. This may be formulated as

$$\frac{E_{\text{eff}}}{E} = 0.866 - 0.134 \frac{u_p^\circ}{u_i^\circ} \tag{2.8}$$

where E and E_{eff} are the applied and the effective field, respectively, and u_p° and u_i° are the electric mobilities of the free polyion and the free counterion, respectively. Thus, with u_p being the effective mobility of the polyion in the polyelectrolytic system, with $u_p / u_p^\circ = E_{\text{eff}} / E$, we have

$$u_p = \frac{0.866 u_p^\circ}{1 + 0.134 u_p^\circ / u_i^\circ} \tag{2.9}$$

For the case that $u_p^\circ \approx \frac{2\varepsilon\varepsilon_0\zeta^\circ}{3\eta}$ (randomly orientated, infinitely long cylinders; ζ° is the electrokinetic potential of the free polyion and η is the viscosity of the solvent) and dilute electrolyte systems ($\kappa a \ll 1$) we end up with

$$\lambda_p = \frac{0.866 H \lambda_i^\circ |\ln \kappa' a|}{|z_i| \lambda_i^\circ + 0.134 H |\ln \kappa' a|} \tag{2.10}$$

where κ' is a modified screening length given by:

$$(\kappa')^2 = \frac{F^2}{\varepsilon\varepsilon_0 RT} \xi^{-1} c_p \tag{2.11}$$

Here, a is the radius of the polyion cylinder, and H is a standard electrophoretic mobility factor defined by:

$$H = \frac{4\varepsilon\varepsilon_0}{3\eta} RT \tag{2.12}$$

where F is the Faraday constant and R the gas constant. In equation (2.11), c_p represents the equivalent volume concentration of deprotonated groups on the polyion (which equals the degree of dissociation α_d times the total concentration of groups c_T).

It is perhaps useful to note from equation (2.10) that one of the main assumptions in the phenomenological approach, viz. that λ_p be independent of the nature of the counterion, is experimentally supported by the success of the Eisenberg plots [1]. The term $0.134H \mid \ln \kappa' a \mid$ in the denominator is of second order and usually less than 10% of the term $|z_i|\lambda_i^\circ$. Hence, λ_i° practically cancels in equation (2.10) and the use of the relationship $\Lambda = f(\lambda_i^\circ + \lambda_p)$ is justified.

2.2.2 Counterion condensation in systems with ionic mixtures

So far the connection between the conductometrically measured counterion distribution and the two-state distribution has been discussed for the salt-free case in the presence of either monovalent or divalent counterions. In this section we will extend the theoretical treatment of the two-state approximation to polyelectrolyte systems in the presence of mixtures of counterions with different valencies. The treatment of conductivity data of these systems will be elucidated in the final section of this chapter.

For the calculation of the fractions of free monovalent and divalent cations, we use the model recently proposed by Paoletti *et al.* [22], which basically follows the model of counterion condensation of linear polyelectrolytes as firstly developed by Manning [23]. Briefly, it amounts to splitting the polyelectrolytic contribution, g^{ion}, to the total reduced molar excess Gibbs energy into two main contributions:

- a purely electrostatic term, g^{el}, and
- a reduced molar Gibbs energy of mixing of the non-polyionic species, g^{mix}.

$$g^{ion} = g^{el} + g^{mix} \tag{2.13}$$

The reduced molar Gibbs energy is defined as:

$$g = \frac{G}{n_p RT} \tag{2.14}$$

where n_p is the number of moles of polyionic charged groups (assuming univalency), i.e. c_p times the volume of the solution. Expressions for g^{el} and g^{mix} are presented in the Appendix. The reference state is a solution at the same temperature, pressure and in the same solvent, containing the same type and concentration of all ions, but with the fixed ions being mobile. It is assumed that in the presence of counterions with different valencies the total fraction of condensed counterions, r, is given by:

$$r = r_1 + r_2 = 2 - f_1 - f_2 \tag{2.15}$$

with $r_1 = rx_1$ and $r_2 = rx_2$. As before, f_1 and f_2 are the fractions of free monovalent and divalent counterions, respectively, and x_i is the mol fraction in the condensation volume according to:

$$x_i = \frac{r_i}{r} = \frac{1 - f_i}{2 - f_1 - f_2} \tag{2.16}$$

which implies that $\sum_i x_i = 1$. In the case of monovalent and divalent counterions the effective charge is given by:

$$q_{eff} = 1 - r[x_1 + 2(1 - x_1)] = 1 - r(2 - x_1) \tag{2.17}$$

The system is fully defined by the state variables (temperature, pressure, concentrations of solutes), and characterized by the two independent variables r and x, and by the molar condensation volume, V_p, expressed in litres per mole of fixed charge (see Appendix). For the determination of r, x and V_p it was found convenient to resort to a Gibbs energy minimisation procedure, similar to the original one in the treatment of Manning [23]. The minimisation conditions have been defined as:

$$(\partial g^{ion}/\partial r)_x = 0 \tag{2.18}$$

and

$$(\partial g^{ion}/\partial x)_r = 0 \tag{2.19}$$

Equations (2.18) and (2.19) are independent. The minimisation of equation (2.18) results in values for V_p and r as a limiting law, which are used to obtain x according to condition (2.19). From equation (2.18) it can be derived that in the limit $c_p \to 0$ stability is retained if:

$$r = \frac{1}{(2 - x)} \left(1 - \frac{1}{\xi(2 - x)} \right) \tag{2.20}$$

It can be easily verified that equation (2.20) reduces to the well-known limiting conditions for the two extreme cases of purely monovalent (x=1) and purely divalent counterion (x=0) (cf. equation (2.7)). The two variables r and x, can be obtained by the simultaneous solution of equations (2.19) and (2.20).

2.2.3 Treating conductometric data

As stated before, the central assumption in our theoretical treatment is that, conductometrically speaking, counterions are either bound to the polyelectrolyte or free in solution: the so-called two-state approximation. According to this model [24], the specific conductivity K_s of a polyelectrolyte solution, which consists of negatively charged polyions and several types of counterions and co-ions, is formally written as:

$$K_s = \sum_i f_i \lambda_i^\circ c_i + \sum_j (\lambda_-^\circ)_j (c_-)_j + f_p \lambda_p c_p \qquad (2.21)$$

where c_i and $(c_-)_j$ denote the analytical molar concentrations of counterions of type i, and co-ions of type j, respectively; as before, c_p is the equivalent volume concentration of deprotonated groups on the polyion; λ_i° and $(\lambda_-^\circ)_j$ are the molar conductivities of counterions of type i and co-ions of type j in pure solvent, respectively; as before, λ_p is the molar conductivity of the polyion (per mole of deprotonated monomers); f_i and f_p are fractional distribution parameters. Equation (2.21) implies that the co-ions are assumed not be involved in any association reaction and are behaving ideally. This means that interactions with the polyions and activity effects are negligible, which are reasonable assumptions for dilute solutions and highly charged polyelectrolytes.

It is useful to introduce the degree of coverage, Θ_i, which is defined here as the number of conductometrically bound counter charges per charged group on the polyion:

$$\Theta_i = \frac{z_i(1 - f_i)c_i}{c_p} \qquad (2.22)$$

with the charge balance requirement

$$f_p = 1 - \sum_i \Theta_i \qquad (2.23)$$

Note that in a salt-free polyelectrolyte solution $c_p = c_1$ or $c_p = \frac{1}{2}c_2$ for monovalent or divalent counterions, respectively.

We will now consider two cases: (1) the conductivity of polyelectrolyte solutions with either monovalent or divalent counterions under salt-free conditions, and (2) the conductivity of polyelectrolyte solutions with ionic mixtures in the presence of co-ions.

The latter case is of importance for studying the competitive behaviour of counterions with different valencies in polyelectrolytic systems. The conditions of the former case are often met in conductometric acid-base titrations aiming at the determination of the total number of chargeable groups of polyions. For example, polyacid solutions may be titrated with either monovalent or divalent metal hydroxide solutions. In addition, the number of apparently bound counter charges per charged group on the polyion can be obtained from the titration data. For not too strong polyacids, there is a pH range where neither H^+- nor OH^--ions are present at significant levels. Under these conditions, the neutralization reaction for the supposedly monovalent groups with monovalent metal hydroxide solutions can be represented as:

$$PH + M^+ + OH^- \rightarrow (PM_{\Theta_1})^{\Theta_1 - 1} + (1 - \Theta_1)M^+ + H_2O \qquad (2.24)$$
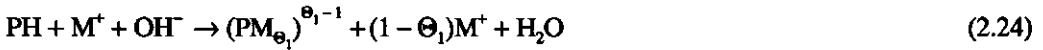
For the free metal concentration $[M^+]$ in the salt-free system, $[M^+]=(1-\Theta_1)c_p$. Then K_s can be expressed as:

$$K_s = (1 - \Theta_1)c_p(\lambda_p + \lambda_1^0) \qquad (2.25)$$

Dividing K_s by $c_1(=c_p)$ gives the molar conductivity Λ of the salt-free solution as expressed by equation (2.1).

For natural water systems, the case of ionic mixtures is of importance and, therefore, we will focus here on the titration of an aqueous polyelectrolyte solution (with a monovalent counterion) with a solution of a divalent metal salt. For the sake of clarity, according to equation (2.21) the specific conductivity for a polyelectrolyte solution containing both monovalent and divalent counterions will become:

$$K_s = f_1\lambda_1^0 c_1 + f_2\lambda_2^0 c_2 + f_p\lambda_p c_p + \lambda_j^0 c_j \qquad (2.26)$$

where the subscripts 1 and 2 denote the valencies of the counterions and subscript j refers to the

co-ion. As discussed before, in the case of purely electrostatic (i.e. non-specific) interactions, f_1 and λ_p values can be determined from Eisenberg plots. Values of f_2 can be calculated from the conductivity excess function ΔK_s, defined as the negative difference between the specific conductivity of a mixed metal/polyelectrolyte system and the sum of the conductivities of the metal salt solution and the polyelectrolyte solution before mixing. For the case of adding $Me(NO_3)_2$ to an alkali metal polycarboxylate solution we have:

$$\Delta K_s = (f_{1,0} - f_1)(\lambda_1^\circ + \lambda_p)c_1 + (1 - f_2)(\lambda_2^\circ + 2\lambda_p)c_2 \tag{2.27}$$

where $f_{1,0}$ is the fraction of conductometrically free monovalent counterions in the polyelectrolyte solution without added 2:1 salt. The first term on the r.h.s. in equation (2.27) accounts for the liberation of monovalent ions and the second one represents the effects of binding divalent ions.

With a sufficiently constant λ_p, the M^+/M^{2+} exchange ratio v is easily computed using

$$v_{1,2} = \frac{\Delta[(f_{1,0} - f_1)c_1]}{\Delta f_2 c_2} = \frac{\Delta r_1 c_1}{\Delta r_2 c_2} \tag{2.28}$$

This exchange ratio may be expected to be between zero and two. The former limit indicates the situation where there is no interaction of monovalent cations with the polyion and activities are unity. In terms of the counterion condensation theory, this means that $\xi < \xi_{crit}$. The latter limit will be observed in the case of complete charge compensation as e.g. predicted for the salt-free case by Manning's counterion condensation theory [13]. However, according to Paoletti et al. [22], there may be different regimes of charge density values and counterion concentrations, where both monovalent and divalent counterions are condensed. This means that under conditions of an increase of the concentration of divalent counterions, the number of released charges related to monovalent counterions is smaller than the number of charges related to condensed divalent counterions. In other words, the exchange ratio $v_{1,2}$ will often be smaller than 2.

Appendix

In the presence of excess salt and under conditions where polyion-polyion interaction is negligible, the electrostatic free energy g^{el} of a polyelectrolytic system is given by the counterion condensation theory [25]:

$$g^{el} = -\xi (q_{eff})^2 \ln(1 - e^{-\kappa d}) \tag{A2.1}$$

where q_{eff} is the net charge (i.e. site charge minus counter charge) on each ionized site on the polyelectrolyte and κ is the reciprocal Debye length. In the case of no condensation, q_{eff} equals the polyionic charge.

For g^{mix} the following contributions of the different non-polyionic species to the change of the entropy of mixing are considered:

$$g^{mix} = (g_1)^{cond} + (g_2)^{cond} + (g_1)^{free} + (g_2)^{free} + g_{coions} + g_{sol} \tag{A2.2}$$

which according to [22] are written as:

$$(g_1)^{cond} = rx_1 \ln \frac{rx_1}{(1 + R_1)V_p c_p} \tag{A2.3}$$

$$(g_2)^{cond} = rx_2 \ln \frac{rx_2}{R_2 V_p c_p} \tag{A2.3}$$

$$(g_1)^{free} = (1 + R_1 - rx_1) \ln \frac{1 + R_1 - rx_1}{(1 + R_1)(1 - V_p c_p)} \tag{A2.5}$$

$$(g_2)^{free} = (R_2 - rx_2) \ln \frac{R_2 - rx_2}{R_2(1 - V_p c_p)} \tag{A2.6}$$

$$g_{coions} = (R_1 + 2R_2) \ln \frac{1}{1 - V_p c_p} \tag{A2.7}$$

$$g_{sol} = r \tag{A2.8}$$

R_1 and R_2 stand for the analytical concentrations of the (added) 1:1 and 2:1 salt, divided by c_p. Thus, $(1+R_1)$ is the ratio between the amounts of monovalent counterions and charged groups

on the polymer. V_p is the molar condensation volume expressed in litres per mole of fixed charge. Finally, equation ($A2.8$) takes into account the lowering of the concentration of ions of the solution.

2.3 References

1. H. Eisenberg, J. Polym. Sci., 30 (1958) 47.
2. W.P.T.J. van der Drift, PhD Thesis, State University Utrecht, 1975.
3. J.C.T. Kwak and R.C. Hayes, J. Phys. Chem., 79 (1975) 265.
4. S. Arai and K. Kumuda, Geoderma, 19 (1977) 21, 307.
5. R.F.M.J. Cleven, PhD Thesis, Agricultural University, Wageningen 1984.
6. H.G. de Jong, J. Lyklema and H.P. van Leeuwen, Biophys. Chem., 27 (1987) 173.
7. M.A.G.T. van den Hoop, H.P. van Leeuwen and R.F.M.J. Cleven, Anal. Chim. Acta, 232 (1990) 141.
8. S. Kawaguchi, T. Kitano, K. Ito and A. Minakata, Macromolecules, 24 (1991) 6335.
9. T. Kurucsev and B.J. Steel, Pure Appl. Chem., 17 (1967) 149.
10. M. Schnitzer and S.I.M. Skinner, Soil Sci., 96 (1963) 86.
11. N.C. Lockhart, Clays Clay Miner., 29 (1981) 413.
12. G.S. Manning, J. Phys. Chem., 79 (1975) 262.
13. G.S. Manning, Q. Rev. Biophys., 11 (1978) 179.
14. H.P. van Leeuwen, R.F.M.J. Cleven and P. Valenta, Pure Appl. Chem., 63 (1991) 1251.
15. J.C. Benegas, S. Paoletti, A. Cesàro, M.A.G.T. van den Hoop and H.P. van Leeuwen, Biophys. Chem., 42 (1992) 297.
16. S. Lifson and A. Katchalsky, J. Polym. Sci., 13 (1954) 43.
17. M. Guéron and G. Weisbuch, Biopolymers, 19 (1980) 353.
18. F. Oosawa, Polyelectrolytes, Dekker, New York 1971.
19. G.S. Manning, J. Chem. Phys., 51 (1969) 924.
20. M. Mandel, in Encyclopedia of Polymer Science and Engineering, Vol. 11, Wiley, New York (1988) 739.
21. M. Mandel, J.C. Leyte and M.G. Stadhouder, J. Phys. Chem., 71 (1967) 603.
22. S. Paoletti, J. Benegas, A. Cesàro, G. Manzini, F. Fogolari and V. Crescenzi, Biophys. Chem., 41 (1991) 73.
23. G.S. Manning, Biophys. Chem., 7 (1977) 95.
24. G.S. Manning, Biopolymers 9 (1970) 1543.
25. G.S. Manning and B.H. Zimm, J. Chem. Phys., (43 (1965) 4250.

Stripping voltammetry of metal complexes with macromolecular ligands

3.1 Introduction

The electroanalytical chemistry of metal complexes is a classical subject. Already in the early days of polarography, the Czechoslovak school of Heyrovsky [1] drew attention to the potentialities of voltammetric techniques for the characterization of all kinds of homogeneous complexation reactions of electroactive metal ions. Nowadays voltammetry has become a most important tool in environmental metal speciation studies. This is especially true for stripping voltammetry since this technique allows direct speciation measurements in samples with metal ion concentrations down to sub-ppb levels. Generally, in voltammetric techniques the response is the result of transport of the different species to the surface of the electrode. In the case of macromolecular natural ligands, the interpretation is more difficult due to 1) differences between the diffusion coefficients of the free and the bound metal ions, 2) the chemical heterogeneity of the ensemble of ligands, 3) the possibly involved kinetics of the association/dissociation reactions and 4) possible adsorption of the ligand and the complex at the surface of the electrode. The consequences of these features will be discussed below.

The dynamic behaviour of a metal complex is determined by the ratio between the time scale of the experiment (t) and that of the association/dissociation process of the complex involved. On the basis of this ratio, three characteristic regimes can be distinguished (see figure 3.1): 1) the static, 2) the semi-dynamic and 3) the dynamic regime. In the static regime, dissociation during the period t is negligibly small and, therefore, there is no significant contribution to the current. The latter is then simply a direct measure of the free metal ion concentration in solution. This type of complexes is often called inert. When one is interested in the speciation of free ions, this would be a rather ideal situation which, unfortunately, is not frequently met with natural metal complex systems. In the semi-dynamic regime, the average life-times of the complex and the free metal have an order of magnitude comparable to that of t. For this regime the current-time relation is quite involved, as pointed out by De Jong *et al.* [2] and will be not discussed in detail here. Finally, in the dynamic regime, t largely exceeds the average life-times of the free metal ion and complex.

$$k'_a t \quad , \quad k_d t$$

$\ll 1$	≈ 1	$\gg 1$
static	kinetic	dynamic

$$\left.\frac{J_{kin}}{J_{diff}}\right] \blacktriangleright \text{lability criterion}$$

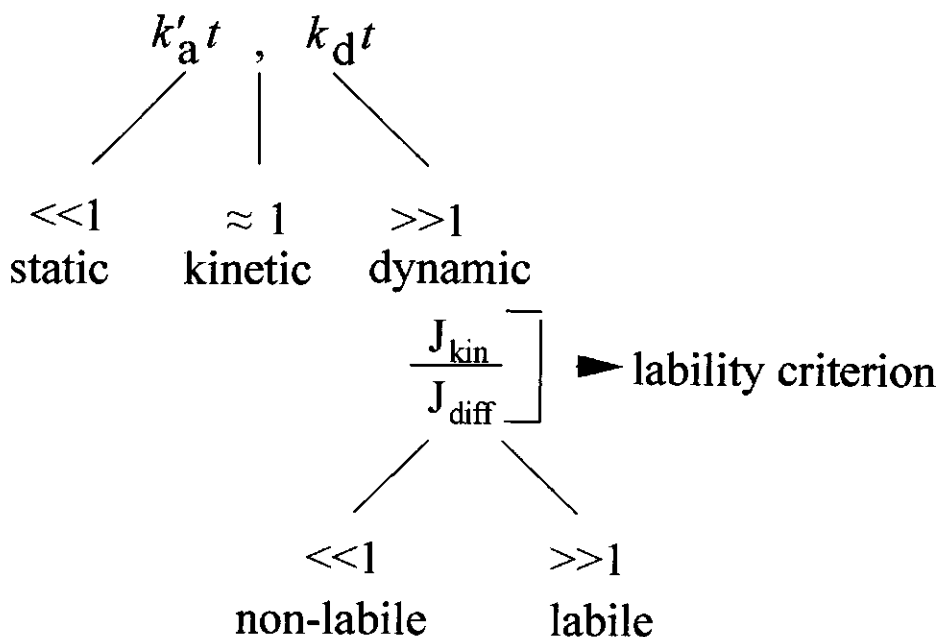|	
$\ll 1$	$\gg 1$
non-labile	labile

Figure 3.1: A schematic representation of the characteristic regimes of metal complex systems as determined by the ratio between the time scale of the experiment (t) and the association-/dissociation process of the complex involved. k'_a denotes the association rate constant multiplied by the concentration of the ligand; k_d is the dissociation rate constant; J_{kin} and J_{diff} denote the contribution to the flux under purely kinetic and purely diffusion controlled conditions, respectively. Further explanation in the text.

Here, the chemical state of the metal changes many times during the experiment. For this regime two interesting limiting cases can be observed: 1) the non-labile and 2) the labile situation, defined in figure 3.1 and further explained in the theory below. For the non-labile situation, the current has a purely kinetic character and the association/dissociation kinetics of the complex involved are crucial in the interpretation of the experimental data. Under labile conditions the current becomes purely diffusion-controlled and calls for the introduction of the mean metal diffusion coefficient of the complex system (see below). For the case of excess of ligand over total metal, De Jong et al. [2] have derived the criterion of lability of such a complex system. On the same basis, a lability criterion has been derived for the steady-state situation that holds for the usual stripping voltammetric conditions [3,4].

In the absence of any complexing agents, the voltammetric response of a metal ion solution is directly related to the diffusion coefficient of the metal ion involved. Under sufficiently acidic conditions (where hydrolysis and/or precipitation are absent) the current refers to the total metal ion concentration. In the presence of macromolecular ligands under complexing conditions, one has to deal with the simultaneous transport of the free metal ions, the complex and the ligands. This is so because the consumption of metal at the electrode surface may be accompanied by dissociation of the metal complex in the diffusion layer. As pointed out above, the voltammetric response may then become a function of both the free and the bound metal ion concentration depending on the regime. In the dynamic regime, under labile conditions where a purely diffusion-controlled current is obtained, it is mandatory to use the overall mean diffusion coefficient ($\overline{D}$) of the complex system. This is simply a weighted average of the diffusion coefficients of the different species. In this way, the differences in diffusion coefficients of the free and the bound metal ions are taken into account. Large differences in diffusion coefficients of the different species are often met in natural systems [5]. In these samples, which contain complexing agents such as fulvic and humic acids, the ligands are much larger than the free metal ions and consequently their diffusion coefficients are appreciably smaller.

Furthermore, adsorption of the metal complex at the surface of the electrode can (seriously) affect the regular shape of the voltammogram [e.g. 6,7]. As a consequence of adsorption, metal will be accumulated at the electrode and may become available for reduction. The extent to which this occurs depends on, for instance, the rate of dissociation as discussed above. Disregarding adsorption can lead to misinterpretation of the voltammetric current and may result in incorrect conclusions regarding the stability of the metal complex system. For example, in normal pulse polarography the occurrence of a maximum suggests possible adsorption as shown by Cleven [7] for the Pb-humic acid system. In this case adsorption may be avoided by using reverse pulse polarography, where the flow of a limiting current during the pre-pulse period prevents accumulation of the depolarizer at the electrode surface.

Finally, for natural samples, the complexing agents involved are often of a polyfunctional and/or polyelectrolytic nature, so that their affinity to metal ions is a function of the actual metal-to-ligand ratio. As a consequence of the this heterogeneity the complex formation cannot be described anymore by a single stability K. This problem requires the introduction of equilibrium complexation distribution functions, which describe the probability of finding a site forming a complex with a particular value of the stability constant. The final mathematical expressions

for these distribution functions depend on use of the choice of the binding spectrum used, for instance that by Freundlich. Recently, the effects of chemical heterogeneity of a metal complex system on polarographic curves have been subjected to a first analysis [8,9].

In this chapter we will present an electroanalytical procedure for determining the stability of labile heavy metal/polyacid complexes under natural conditions (i.e. low concentrations of both the metal ion and the polyacid, intermediate pH values and various concentrations of elec-tro-inactive electrolyte). Attention will be paid to the lability criterion which is essential for the voltammetric analysis of the complexes involved. The consequences of adsorption of metal ions on vessel material and protolysis of the macromolecule are also taken into account. Appropriate ways to deal with these complications will be discussed in some detail.

3.2 Theory

For the case of a reversible electrode reaction, the mass transport of metal ions from the bulk solution to the electrode surface characterizes the voltammetric conditions. We consider the simplest complexation scheme in which an electroactive metal ion (denoted as M; charge omitted for simplicity) associates with a ligand or site (L) to form an electroinactive complex (ML):

$$\mathbf{M}^0 \rightleftharpoons \mathbf{M} + \mathbf{L} \underset{k_a}{\overset{k_d}{\rightleftharpoons}} \mathbf{ML} \tag{3.1}$$

Simultaneous effects of differences in diffusion coefficients and limited association/dissociation rates have been analyzed in some detail [2]. In this complexation scheme, M^0 denotes the metal atom and k_a and k_d are the association and dissociation rate constants, respectively. The com-plexation equilibrium in the bulk is expressed by the stability K:

$$K = \frac{c_{ML}^*}{c_M^* c_L^*} \tag{3.2}$$

where c_M^*, c_L^* and c_{ML}^* denote the bulk concentrations of M, L and ML, respectively. When a large excess of ligand is present ($c_L^* \gg c_T^* (= c_M^* + c_{ML}^*)$), the association becomes quasi-monomolecular with a rate constant

$$k'_a = k_a c_L^*$$ (3.3)

The corresponding stability K' is then the ratio between bound and free metal

$$K' = \frac{k'_a}{k_d} = \frac{c_{ML}^*}{c_M^*}$$ (3.4)

Only under certain conditions can the stability be obtained from the complexation curve, i.e. the voltammetric response of a metal ion solution as a function of the ligand concentration. First, the system must be voltammetrically labile, meaning that the rates of the association/dissociation reactions (3.1) must be sufficiently fast to maintain equilibrium for any relevant value of the space and time as defined by De Jong *et al.* [2]. Second, there must be a large excess of the complexing agent over the metal. Then, a constant ratio between bound and free metal is attained over the whole voltammetric diffusion layer. This is necessary to ensure a constant (mean) diffusion coefficient from the bulk of the solution to the surface of the electrode.

For the dynamic case, the lability criterion for a complexing system with an excess of ligand is given by [2]

$$\frac{k_d^{1/2} \varepsilon^{-1/2} (\varepsilon^{-1} + K')t^{1/2}}{K'(1+K')^{1/2}} \gg 1$$ (3.5)

where $\varepsilon = D_{ML}/D_M$. Equation (3.5) expresses that the lability of the complex increases with decreasing K and decreasing ε at constant effective times of the dynamic experiment. If condition (3.5) is not fulfilled, kinetic effects resulting from limited association/dissociation rates play a (crucial) role. Then analysis of the voltammetric response becomes quite involved [2]. In the case the l.h.s. of equation (3.5) becomes $\ll 1$, the system is referred to as non-labile. Under non-labile conditions, the voltammetric response will be purely controlled by the kinetics of the system.

On the same basis, a lability criterion can be derived for the steady-state situation that holds for the usual stripping conditions. The expression parallel to equation (3.5) is [3,4]

$$\frac{k_d^{1/2}\delta}{D_M^{1/2}K'^{1/2}} \gg 1 \tag{3.6}$$

where δ is the thickness of the diffusion layer, which is a function of D_{ML}. For the case of a rotating disk electrode (RDE) and under conditions that $\varepsilon K' \gg 1$, the Levich equation [10] can be used

$$\delta = 1.61 D_{ML}^{1/3}\omega^{-1/2}\nu^{1/6} \tag{3.7}$$

where ω is the angular rotation frequency and ν the kinematic viscosity of the solution. From a theoretical point of view, planar electrodes (solid or with a thin film of mercury) are preferable over mercury drop electrodes. This is so since, in the planar case, the hydrodynamic conditions are much better defined and the low volume/area ratios of film electrodes result in favourable accumulation efficiencies. On the other hand, reproducibility of the surface is much better for the approximately spherical mercury drop electrodes. In this study, we have used the hanging mercury drop electrode (HMDE). For this geometry the exact theoretical relationship between δ and D_{ML} is uncertain, and hence, we cannot (rigourously) determine the former quantity. For this case we are using an approximate procedure.

3.2.1 Voltammetric current

Since the relationship between voltammetric current and mass transport properties under stripping voltammetric conditions with a HMDE is not yet well established, an alternative for practice is to fit the experimentally obtained current to some postulated functionality with respect to the mean diffusion coefficient ($\overline{D}$). To that end, for a labile metal complex system, the pre-electrolysis current (I_e) is formally written as:

$$I_e \propto \overline{D}^p c_T^* \tag{3.8}$$

with

$$\overline{D} = (c_M^*/c_T^*)D_M + (c_{ML}^*/c_T^*)D_{ML} \tag{3.9}$$

which actually incorporates the speciation of the available metal over the species M and ML. The power p is related to the nature of the mass transport during the pre-electrolysis step. For example, it is 1/2 for semi-infinite linear diffusion and 2/3 for laminar convective diffusion [10] (cf. equations (3.5) and (3.6), respectively). For stripping voltammetries equation (3.8) has been shown to work well enough [11]. The operational value of p varies with geometrical conditions and the mode of stirring. Usually p is found between 1/2 and 2/3 [11]. The concentration of metal inside the mercury drop, which is linearly proportional to the reoxidation peak current (I), will be also proportional to the pre-electrolysis current and time (t_e):

$$I_e t_e \propto c_{M^0} \propto I \tag{3.10}$$

Let us define Φ as the ratio between the reoxidation peak current for the complex system and the reference peak current under conditions of no complexation. Combination of equations (3.2), (3.8), (3.9) and (3.10) then gives:

$$\Phi = \left(\frac{\overline{D}}{D_M} \right)^p = \left(\frac{1 + \varepsilon K c_L^*}{1 + K c_L^*} \right)^p \tag{3.11}$$

Equation (3.11) yields dependencies of Φ on c_L^* as presented in figure 3.2. Due to increase of $K c_L^*$, Φ will decrease with increasing ligand concentration for $\varepsilon < 1$. Distinction can be made between three regions with different information content with respect to the different parameters in equation (3.11). Region A is most sensitive to the complex stability K. In fact, Φ is most sensitive to K if $K c_L^* \approx 1$ (for mathematical details see the Appendix). This implies that the applicability of the experimental procedure largely depends on the analytically feasible ranges of the concentration of the ligand involved. If ligand concentration levels of 10^{-8} to 10^{-3} mol.l^{-1} are being taken as realistic under SV experimental conditions, it means that roughly the range of $10^3 < K$ l.mol$^{-1} < 10^8$ can be covered. It is useful to note here that section A of the complexation curve is not very sensitive to p. This is of importance because it implies that uncertainties in p have only little influence on the evaluation of K. This aspect will be explained in more detail in Chapter 5. The value of p has its greatest influence on the shape of the curve in region B. The diffusion coefficient ratio ε dominates in region C, the tail of the complexation curve. From equation (3.11) it is immediately clear that for $K c_L^* \gg 1$, Φ approaches the limit ε^p:

$$\Phi(c_L^* \to \infty) = \lim_{c_L^* \to \infty} \left(\frac{1 + \varepsilon K c_L^*}{1 + K c_L^*} \right)^p = \varepsilon^p \tag{3.12}$$

In the case of macromolecular complexes with very low diffusion coefficients, D_{ML}/D_M may become so small that in region A the first term in $\overline{D}$ (see equation (3.9)) is strongly dominant. Then Φ approaches the fraction of free metal ions. Under the limiting condition that $D_{ML}=D_M$ and k_d large (indicating lability), Φ will be equal to 1 over the whole complexation curve. It is obvious that then speciation through analysis of Φ is not possible.
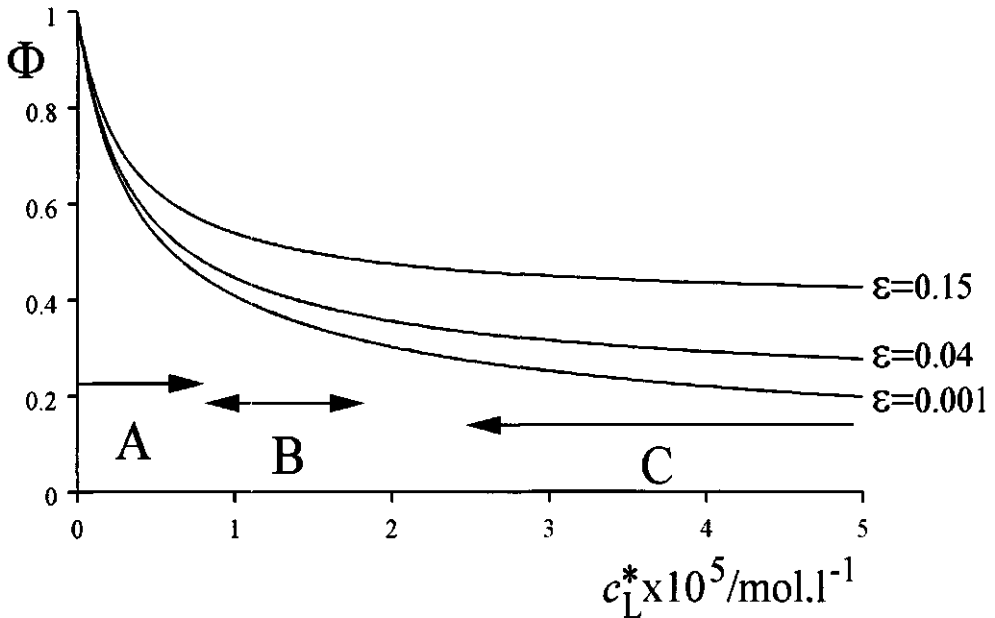

Figure 3.2: Sensitivity of the Φ, c_L^* complexation curve to the different parameters. $K=5 \times 10^5$ l.mol^{-1}, p=1/2; values of ε are indicated. Further explanation in the text.

3.2.2 Peak potential shift

In the case of a labile complex, the characteristic potential of the metal ion reduction (E_{peak}) will decrease with increasing ligand concentration. This is basically due to a lowered [M(free)]/[M^0] ratio at the mercury electrode surface compared to the ligand-free solution. The potential shift, ΔE_{peak}, can be related to the stability K [2]

$$(nF/RT)\Delta E_{peak} = -\ln(\overline{D}/D_M)^p - \ln(Kc_L^*) \qquad (3.13)$$

which is similar to the classical DeFord-Hume equation [12], and valid for the case of a large excess of ligand over $[M^0]$. In equation (3.13), n is the number of electrons in the charge transfer reaction, F the Faraday constant, R the gas constant and T the absolute temperature.

3.2.3 Heterogeneity

So far, the stripping voltammetric analysis was considered for a homogeneous metal complex system by taking into account a single stability K. However, as pointed out in the introduction, natural complexing agents are often heterogeneous with regard to their affinity to metal ions. Moreover, the electrostatic interaction of metal ions with the macromolecule is a function of the coverage of the different site types present in these systems. Hence, analysis of the complexation curve for heterogeneous metal complexes results in an average stability $\overline{K}$ which refers to a coverage approximately equal to $c_T/2c_L^*$. This is so, since $\overline{K}$ is obtained in region A of the complexation curve, where $\overline{K}c_L^* \approx 1$, and thus c_{bound}/c_{free} is of order unity. Hence, under stripping voltammetric conditions, the heterogeneity of the complex involved can be investigated by varying the metal-to-ligand ratio. In the present study, we have performed this by measuring complete Φ, c_L^* curves for different total metal ion concentrations. From the set of values of $\overline{K}$, the affinity distribution function can be obtained by analyzing the relationship between the degree of coverage and the concentration of free metal ions as discussed by Van Riemsdijk and Koopal [13].

3.3 Experimental methodology

The experimental procedure is based on adding ligand to the solution of the metal and measuring the reoxidation current. The concentration levels should be such that the values measured of Φ all refer to excess ligand while the region $Kc_L^* \approx 1$ is sufficiently covered. Under these conditions, the voltammetric response can be analysed according to equation (3.12) with the total metal concentration constant over the whole complexation curve. Unavoidable dilution resulting from the addition of the ligand solution is accounted for. Losses of metal due to adsorption onto vessel material or hydrolysis/precipitation should be avoided. This, however, sets some experimental limits to the procedure presented.

Due to the protolytic character of the macromolecular ligands used, the complexation is strongly dependent on the acidity conditions [14]. This is especially true in the case of relatively weak polyacids like poly(meth)acrylic acids and humic acids. Acidity determines the negative charge density on the polyanion via (de)protonation of the complexing groups, and this charge is responsible for the electrostatic enhancement of the stability of the complex with a positive metal ion.

In the following sections we will discuss the experimental conditions and their appropriateness in terms of the theory for obtaining the stability of heavy metal/polyacid complexes by stripping voltammetry.

3.3.1 Adsorption phenomena

As a consequence of the procedure, the metal/polyacid solution is always in contact with different surfaces e.g., the sample vessel, electrodes and stirrer. Metal ions can adsorb onto these surfaces. In determining total concentrations, adsorption on vessel walls has been avoided by the use of teflon and decreasing the pH of the sample solution to very low values [15]. In metal speciation studies, however, the distribution of heavy metals over different species in their natural environment is of interest. Changing the conditions of the sample solution would lead to changes in the original speciation and is therefore not allowed.

It has been shown [16] that under natural conditions, i.e. at very low concentrations of the heavy metal ions, adsorption on the different surfaces, present in the experimental set-up, may play an important role with respect to the voltammetric response. The extent of adsorption depends on the pH, the type of surface, the presence of supporting electrolyte and also on the concentration of complexing agent. These various aspects will be briefly discussed below. The reader is referred to ref. [17] for more details (including the experimental conditions).

Figure 3.3 shows the pH-dependence of the Differential Pulse Anodic Stripping Voltammetric (DPASV) peak current (normalized by the value obtained at a pH low enough to ensure negligible adsorption) observed for Cd(II)-solutions in a glass cell and at different concentrations of the metal. For a 10^{-5} mol.l^{-1} solution, the current is essentially constant over the pH-range covered.
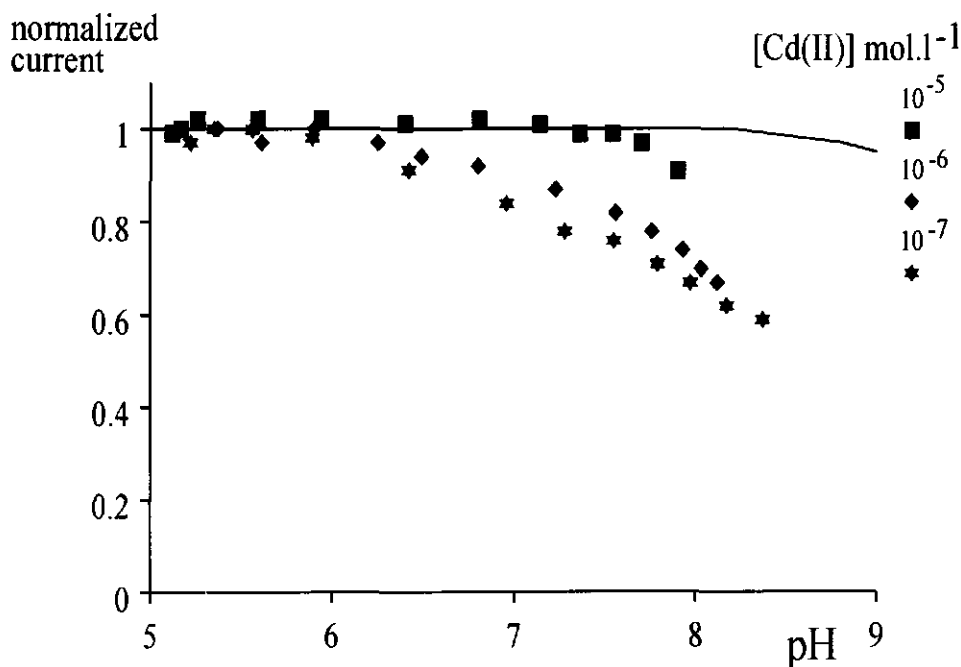
Figure 3.3: DPASV peak currents (normalized by the mean value obtained at low pH) for Cd(II) solutions as a function of pH for experiments carried out in a glass vessel in the presence of 0.01 mol.l^{-1} KNO$_3$ at different metal concentrations. The solid line denotes the free metal fraction calculated considering hydrolysis (through tabulated stability constants after [18]).

However, for lower concentrations the peak currents start to decrease dramatically with increasing pH from pH values of about 6 and higher. This effect can neither be attributed to the metal-ion hydrolysis, as indicated by the distribution diagrams of the hydrolysis species (solid curve [18]), nor to the presence of carbonates, as demonstrated by the insensitivity of the results to adding K$_2$CO$_3$. Díaz-Cruz et al. [17] have consistently shown by additional desorption experiments that this current decrease is fully due to metal adsorption onto "cell" components. Similar results have been obtained for Zn(II) [17] and Pb(II) [19].

The influence of the type of cell material on the amount of adsorption of Zn(II) as a function of the pH can be seen from figure 3.4. For polymethacrylate vessels the metal adsorption is more extensive than for glass vessels, apparently due to the relatively strong complexation with carboxylate groups present on the surface. Substantial adsorption was also observed with nylon.

Polyfluoroethylene and teflon vessels appeared to be even stronger adsorbing than glass, especially in the case of Cd(II)-ion [17], but the differences were not very large. Finally, the polystyrene vessel proved to be much less adsorbing than glass.
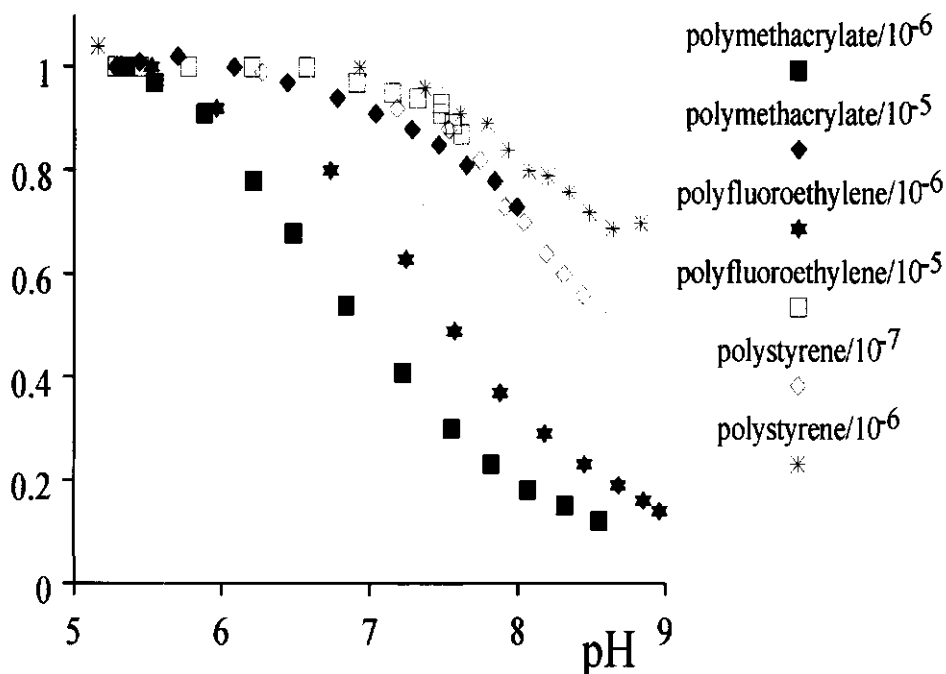
normalized
current

Figure 3.4: DPASV peak currents (normalized by the mean value obtained at low pH) for Zn(II) solutions as a function of pH for experiments performed in vessels made of different materials in the presence of 0.01 mol.l^{-1} KNO$_3$ at different metal concentrations.

Figure 3.5 reflects the adsorption rates of Zn(II)-ions on a teflon vessel and the influence of adding PMA as the complexing agent. Starting with an initially acidic Zn(II) nitrate solution, a TRIS buffer solution with pH=7.4 was added at time t=0. Due to the increase of pH, adsorption of Zn(II)-ions on the teflon vessel sets in and the voltammetric current decreases with time (step a). It has to be mentioned that the Zn(II) ions do not interfere with the TRIS buffer [17]. At t=30 min PMA is added; the immediate further decrease is primarily due to complexation, but it is also affected by the adsorption/desorption of Zn(II)-ions to/from the vessel walls (step b; see

below). After 60 min, the Zn/PMA solution is exchanged for a KNO_3 medium at low pH (step c). The current then progressively increases again due to the desorption of previously adsorbed Zn(II)-ions that were not removed from the system by the solution exchange operation.
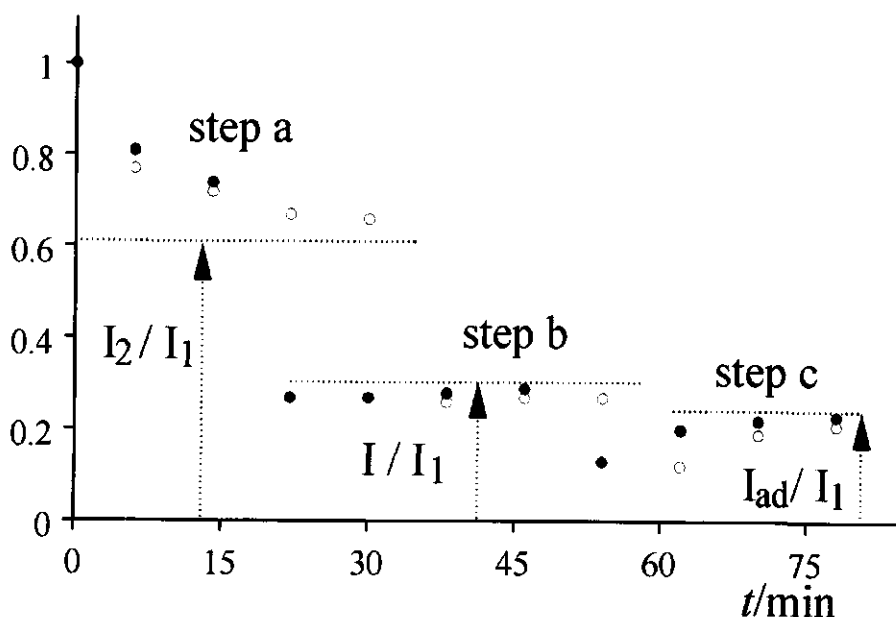

Figure 3.5: DPASV peak currents (normalized by the mean value measured at pH<5 (I_1)) for Zn(II) solutions as a function of time for exchange experiments carried out in a teflon vessel at pH 7.4 in the presence of 0.001 mol.l^{-1} TRIS buffer and 0.01 mol.l^{-1} KNO_3. Step a: initial Zn(II) solution in the presence of TRIS buffer. Step b: after adding PMA (α_n=0.8, [PMA]=5×10^{-5} mol.l^{-1} in the bulk solution). Step c: after exchange of the bulk solution by a 0.01 mol.l^{-1} KNO_3 solution at the same pH<5 as in the beginning. I is the current measured in the presence of PMA. I_2 is the current measured in the absence of PMA at a pH value equal to that attained in the presence of PMA. I_{ad} is the current measured after exchanging the Zn(II)/PMA solution for a noncomplexing medium.

From figure 3.5 it can be proved that the sum of the intensity ratios obtained at the ends of steps a and c is lower than unity. This is because during step b, complexation by PMA gives rise to partial desorption of previously adsorbed Zn(II)-ions. Considering this last phenomenon, one has to be cautious in interpreting the Φ, c_L^* relationship in terms of equation (3.11). Surprisingly, log K values obtained from the normal experimental procedure, in which a metal ion solution

is titrated with a ligand solution and I is measured, are in satisfactory agreement with those obtained from rigourously accurate, and highly time-consuming, measurements [17]. It therefore seems that for practical purposes the most convenient procedure to study such systems, consists of the usual voltammetric titrations in which the blank is measured at a pH as close as possible to that attained in the presence of the ligand. In practical measuring situations with a certain type of system, the validity of this conclusion should be checked, according to the given experimental procedure.

3.3.2 Protolytic control

The degree of neutralization (α_n) of a polyacid solution is defined as the ratio between the number of moles of KOH added to the polyacid and the total number of acidic groups

$$\alpha_n = \text{moles KOH}_{added} / \text{moles polyacid} = (L^- + OH^- - H^+) / c_c \tag{3.14}$$

where c_c denotes the analytical concentration of carboxylic groups, i.e. $HL + L^-$. More interesting than the degree of neutralization, which is an attractive operational parameter, is the degree of dissociation (α_d), defined as the ratio between the concentration of deprotonated acidic groups and the total concentration of groups c_c

$$\alpha_d = L^- / (L^- + HL) = L^- / c_c \tag{3.15}$$

For high concentrations of a relatively weak polyacid like PMA (pK_a=4.9), α_n and α_d are practically identical in the commonly used range of α_n (from 0.2 to 0.8). A voltammetric titration involves the addition of small aliquots of highly concentrated polyacid solution (with a given α_n value) to the metal ion solution and measuring the voltammetric response. During such a titration the resulting α_d can be very different from the α_n value of the polyacid solution. This is because, on the one hand, the polyacid is strongly diluted, which increases the degree of dissociation of weak acids. On the other hand, even small excesses of H^+- or OH^-- ions in the metal solution can give rise to important changes in α_d at the low polyacid concentrations involved. Furthermore, the presence of divalent cations implies the transformation of L^- groups into the complex forms ML^+. As a consequence, α_d can be affected by complexation, especially at not too low metal-to-ligand ratios. Finally, there is also the effect of the increase of the pK_a value of the polyelectrolytic acid with increasing α_d (due to the increase of the negative charge

on the macromolecule), and the possible changes in pK_a with increasing c_c [14]. This means that the actual values of α_d during a complexation titration cannot be evaluated by using a constant pK_a value.

Anyway, and in the absence of buffer solutions, α_d can be related to α_n and to the measured pH of the solution, by means of the mass balance and charge balance equations, which finally yield in the case of excess of ligand [20]

$$\alpha_d = \alpha_n + (H^+ - K_w/H^+ - H_0^+) / c_c \tag{3.16}$$

for an initially acidic metal ion solution. K_w is the ionic product of the water. $[H^+]_0$ is the initial concentration of H^+. In the case of an initially alkaline metal ion solution, the term $-[H^+]_0$ in the second term of the r.h.s. of equation (3.16) has to be replaced by $+[OH^-]_0$ ($=K_w/[H^+]_0$):

$$\alpha_d = \alpha_n + (H^+ - K_w/H^+ + K_w/H_0^+) / c_c \tag{3.17}$$

Under the experimental conditions employed, the activity coefficients of H^+- and OH^-ions are constant and for not too high ionic strengths fairly close to unity, which allows the direct determination of $[H^+]$ and $[H^+]_0$ from pH measurements. As a consequence, α_d values can be calculated for any point of a titration by applying equation (3.15).

3.3.3 Experimental procedure

Taking into account adsorption and protolysis in stripping voltammetric titrations of metal/polyacid complexes, we have used the following experimental procedure for obtaining complexation curves.

1) Prior to the experiment, the polystyrene vessel and the electrodes are held in contact with a concentrated nitric acid solution for several hours, in order to desorb all possible adsorbed metal ions.

2) The metal ion solution, prepared at a pH between 4.5 and 5.0, and with a fixed KNO_3 concentration, is placed into the vessel and, after degassing with purified nitrogen gas, some voltammetric responses are recorded to establish the reference value and its reproducibility.

3) By KOH or HNO$_3$ addition the pH is set close to the expected pH of the titration; this is usually very similar to the pH of the titrant polyacid solution. Then, some additional measurements are done till the current becomes reproducible. At this point, the peak potential should coincide with that obtained in step 2) (if not, undesired phenomena such as hydrolysis could be involved). If the currents obtained in 2) and 3) are equal, adsorption onto the vessel walls is absent or negligible and the experiment can continue. If current 3) is smaller than 2), adsorption onto the vessel surfaces may have occurred. In this case, the complexation results have to be checked against results obtained by the more laborious exchange procedure as described by Díaz-Cruz et al. [17].

4) After each addition of the complexing agent and degassing the solution for at least 1 minute, the voltammetric response is recorded.

5) Equation (3.16) or (3.17) is applied to calculate α_d from pH measurements done during the titration. If α_d remains constant, results are valid. If not, the titration must be repeated at a more convenient pH value.

6) The stability of the complex is obtained via equation (3.11) and (3.13), using the intensity and the peak potential values of the metal solution found in step 3) as a reference.

Appendix

The sensitivity of Φ with respect to K can be found after taking the derivative of equation (3.11)

$$\frac{d\Phi}{dK} = \frac{p(1 + \varepsilon K c_L^*)^{p-1} c_L^*(\varepsilon - 1)}{(1 + K c_L^*)^{p+1}} \tag{A3.1}$$

The independent variable in a complexation experiment is the ligand concentration c_L^*. The value of c_L^* where the sensitivity of Φ to K has a maximum, can be found by solving

$$d(d\Phi/dK)/dc_L^* = 0 \tag{A3.2}$$

and gives:

$$\varepsilon K^2 c_L^{*2} + pK(1+\varepsilon)c_L^* - 1 = 0 \tag{A3.3}$$

For small values of ε ($\varepsilon \to 0$) equation (A3.3) approaches

$$pK c_L^* = 1 \tag{A3.4}$$

From equation (A3.4) it can be easily seen that Φ is most sensitive to K if Kc_L^* is in order of 1.5 to 2 for p=2/3 and p=1/2, respectively. For much smaller or much higher values of Kc_L^*, Φ will be too close to unity or too small for reliable computation of K.

3.4 References

1. J. Heyrovsky, Polarographie, Springer-Verlag, Wien, 1941.
2. H.G. de Jong, H.P. van Leeuwen and K. Holub, J. Electroanal. Chem. 234 (1987) 1, 17; 235 (1987) 1; 260 (1989) 213.
3. W. Davison, J. Electroanal. Chem., 87 (1978) 395.
4. H.P. van Leeuwen, Sci. Total Environ., 60 (1987) 45.
5. J. Buffle, Complexation Reactions in Aquatic Systems: An Analytical Approach, Ellis Horwood Ltd, Chichester 1988.
6. J. Heyrovsky and J. Kuta, Principles of Polarography, Academic Press, New York, 1966.
7. R.F.M.J. Cleven, PhD Thesis, Agricultural University, Wageningen 1984.
8. M. Filella, J. Buffle and H.P. van Leeuwen, Anal. Chim. Acta, 232 (1990) 209.
9. H.P. van Leeuwen and J. Buffle, J. Electroanal. Chem., 296 (1990) 359.
10. V.G. Levich, Physicochemical Hydrodynamics, Prentice-Hall, Englewood Cliffs, NJ, USA, 1962.
11. M. Esteban, H.G. de Jong and H.P. van Leeuwen, Intern. J. Environm. Anal. Chem., 38 (1990) 75.
12. D.D. DeFord and D.N. Hume, J. Am. Chem. Soc., 73 (1951) 5321.
13. W.H. van Riemsdijk and L.K. Koopal, in J. Buffle and H.P. van Leeuwen, eds., Environmental Particles vol. 1, IUPAC Environmental Analytical and Physical Chemistry Series, Lewis Publishers, Boca Raton, 1992, p. 455-495.
14. M. Mandel, in Encyclopedia of Polymer Science and Engineering, Vol. 11, Wiley, New York (1988) 739.
15. T.S. West and H.W. Nürnberg (eds), The Determination of Trace Metals in Natural Waters, IUPAC, Commission V.6, Analytical Chem. Division, Blackwell Scientific Publications, California, USA, 1988.
16. W. Davison, S.J. de Mora, R.M. Harrison and S. Wilson, Sci. Tot. Environ., 60 (1987) 35.
17. J.M. Díaz-Cruz, M. Esteban, M.A.G.T. van den Hoop and H.P. van Leeuwen, Anal. Chem., 64 (1992) 1769.
18. C.F. Baes Jr. and R.A. Mesmer, The Hydrolysis of Cations, Wiley-Interscience, New York, 1976.
19. M.A.G.T. van den Hoop, unpublished results.
20. J.M. Díaz-Cruz, M. Esteban, M.A.G.T. van den Hoop and H.P. van Leeuwen, Anal. Chim. Acta, 264 (1992) 163.

CHAPTER 4

Conductometric versus voltammetric speciation

4.1 Introduction

As described in detail in chapters 2 and 3, the speciation of monovalent and divalent counterions in polyelectrolytic systems can be obtained from both conductometric and voltammetric experiments. In the former case, analysis of data for the conductivity excess function results in fractions of free and bound counterions as a function of the ratio between the amount of added divalent cations and the concentration of the polyelectrolyte. In the case of stripping voltammetric experiments, analysis of complexation curves leads to stability values of the metal/complex involved. Once the stability has been obtained, the distribution of metal ions over the free and bound state can be calculated for any ligand concentration.

The aim of the present chapter is to compare conductometric and voltammetric speciation data and to evaluate their meaning. The main aspects of the theoretical analysis of metal/polyelectrolyte solutions in terms of free and bound counterions by conductometry and voltammetry will be summarized. As a part of this, the ranges of applicability of the two analytical methods will be defined. For both conductometry and voltammetry, experimental data are available for zinc(II)/polyacrylate (PAA) and zinc(II)/polymethacrylate (PMA) systems [1,2]. The present problem is therefore concerned with a solution containing:

- polyacrylate or polymethacrylate polyanions with negatively charged carboxylate groups, denoted by P^{z-},
- monovalent counterions M^+,
- divalent counterions Zn^{2+}, and
- monovalent co-ions A^- (usually NO_3^-)

4.2 Conductometric speciation

Conductometry measures the sum transport of all charged species in the studied system; additional information is needed to obtain their individual contributions. For the interpretation of

conductometric titration of an aqueous polyelectrolyte solution (containing a monovalent counterion) with a solution of divalent metal salt, we follow the procedure described in detail in chapter 2. In short, the procedure includes the following basic equations and assumptions.

For the present polyelectrolytic system containing monovalent and divalent counterions (M and Zn(II), respectively), monovalent co-ions (nitrate) and PAA/PMA as complexing agent, the specific conductivity K_s can be formally written as (charges omitted for simplicity):

$$K_s = f_M \lambda_M^\circ c_M + f_{Zn} \lambda_{Zn}^\circ c_{Zn} + f_p \lambda_p c_p + \lambda_{NO_3}^\circ c_{NO_3} \tag{4.1}$$

where c_M, c_{Zn} and c_{NO_3} denote the analytical concentrations of monovalent and divalent counterions and monovalent anions, respectively. As before, c_p is the volume concentration of carboxylate groups; λ_M° denotes the molar conductivity of the monovalent counterion at infinite dilution; and f_i is the fractional distribution parameter of i. Equation (4.1) is based on a two-state approximation, i.e. the counterions are assumed to be either bound to the polyelectrolyte or free in solution. Doing this, the real situation has been simplified by disregarding the gradual change from fully free polyionic groups and counterions on one hand to a perfect associate, i.e. a state of complete annihilation of charges, on the other. However, the two-state approximation has been shown to be operationally helpful and very effective in many practical situations. Furthermore, as pointed out in chapter 2, it seems reasonable to assume that the evaluated distribution parameters f_M and f_{Zn} come close to the equilibrium fractions of free monovalent and divalent counterions. Finally, by using equation (4.1) one assumes that the conductivity of the co-ions is not affected by the polyion and deviations from ideality are only caused by polyion-counterion interactions. This assumption is assumed to be reasonable for the case of dilute polyelectrolyte solutions.

In the case of purely electrostatic (i.e. non-specific) interactions, f_M and λ_p can be determined from Eisenberg plots [3], i.e. plots of the molar conductivity Λ versus the molar conductivities of various monovalent counterions in pure solvent λ_M°. These plots are also found to be linear for the mixed systems K/Zn(II)/PAA [1] and K/Zn(II)/PMA [2]. Values of f_{Zn} can be calculated from the dependence of the conductivity excess function ΔK_s on c_M/c_{Zn}. The conductivity excess function is defined as the difference between the specific conductivity of a mixed metal/polyelectrolyte system and the sum of the conductivities of metal salt solution before mixing. For the case of adding $Zn(NO_3)_2$ to an alkali metal polycarboxylate solution we have:

$$\Delta K_s = (f_{M,0} - f_M)(\lambda_M^\circ + \lambda_p)c_M + (1 - f_{Zn})(\lambda_{Zn}^\circ + 2\lambda_p)c_{Zn} \tag{4.2}$$

where $f_{M,0}$ is the fraction of conductometrically free monovalent counterions in the pure poly-electrolyte solution. The first term on the r.h.s. in equation (4.2) is due to the liberation of monovalent ions and the second one represents the effects of binding divalent ions. Assuming a constant λ_p, the M/Zn exchange ratio ν(cond) is easily computed using

$$\nu_{MZn}(\text{cond}) = \frac{\Delta[(f_{M,0} - f_M)c_M]}{\Delta f_{Zn}c_{Zn}} \tag{4.3}$$

The conductometric analysis of mixed counterion-polyelectrolyte solutions in terms of free and bound counterions runs essentially through equation (4.2). Therefore, conductometry is most successfully applied in series of experiments where c_{Zn}/c_M is varied. Furthermore, accuracy requirements set limits to the concentration ratios to be covered. All of constituents play some role in the determination of f_{Zn} (i.e., M through f_M, P through λ_p). Hence, none of them is allowed to dominate K_s. Typically one therefore has in conductometric analysis:

$$c_{MNO_3} \approx c_{Zn} \approx c_p \tag{4.4}$$

4.3 Voltammetric speciation

The speciation of metal ions in systems containing macromolecules on the basis of a voltam-metric method has been discussed in detail in the previous chapter. However, for the purpose of the present chapter, i.e. a comparison of conductometric and voltammetric speciation data, it is useful to recall the main aspects and assumptions of the voltammetric analysis of metal/polyelectrolyte systems in terms of a stability K. Starting-point in the voltammetric treatment of metal/polyelectrolyte solutions is to consider that the voltammetric response is not only a function of the transport of the electroactive free metal ion (in the present case zinc(II)) from the bulk solution to the electrode surface, but that it also depends on the simultaneous diffusion of the electroinactive metal complex. Hence, the association/dissociation reactions of zinc(II) with the polyacrylate or polymethacrylate (denoted as P) play an important role:

$$Zn^0 \underset{-2e^-}{\overset{-2e^-}{\rightleftharpoons}} Zn(II) + P \underset{k_a}{\overset{k_d}{\rightleftharpoons}} ZnP \tag{4.5}$$

where k_a and k_d are the rate constants for association and dissociation, respectively. Charges of polyionic species are omitted for simplicity. The analysis of voltammetric data runs through [4,5]:

$$\Phi = \left(\frac{\overline{D}}{D_M}\right)^p = \left(\frac{1+\varepsilon K c_L^*}{1+K c_L^*}\right)^p \tag{4.6}$$

$$(nF/RT)\Delta E_{peak} = -\ln(\overline{D}/D_M)^p - \ln(K c_L^*) \tag{4.7}$$

where Φ is defined as the ratio between the peak current for the complex system and the reference peak current under conditions of no complexation. As before [4], p is a hydrodynamic parameter with a value in between 1/2 and 2/3 for stripping voltammetries and 1/2 for direct voltammetries and $\overline{D}$ is the mean diffusion coefficient of the Zn/P complex system, given by

$$\overline{D} = D_{Zn}\frac{c_{Zn}}{c_{ZnP}+c_{Zn}} + D_{ZnP}\frac{c_{ZnP}}{c_{ZnP}+c_{Zn}} \tag{4.8}$$

Equations (4.6)-(4.8) express that by voltammetry one can measure free metal concentrations that are very small compared to that of the bound metal. Note that this is not so for conductometry. However, the application of the presented relationships between the voltammetric current, the characteristic potential shift (ΔE_{peak}) and the stability of the complex involved is only allowed if certain conditions are obeyed. The metal/polyelectrolyte system must be voltammetrically labile, i.e., the kinetics of the association/dissociation reactions (4.5) must be sufficiently fast to maintain equilibrium for any relevant value of space and time [6]. Lability criteria for the dynamic case and for stripping voltammetries have been derived in the literature [6-8]. Furthermore, there must be a large excess of complexing agent (in the present case carboxylate groups of the polyacids PAA and PMA) over the metal, hence $c_P \gg c_{Zn}$. The reason for this condition is to be sure that the equilibrium ratio c_{ZnP}/c_{Zn} is constant over the whole voltammetric diffusion layer. This is necessary to ensure a constant mean diffusion coefficient (see equation 4.8) from the bulk of the solution to the surface of the electrode. Moreover, to render the transport number of the electroactive species negligibly small, an excess of supporting electrolyte (in the present study c_{KNO_3}) should be added to the system and thus $c_{KNO_3} \gg c_{Zn}$. Since the result of this condition is that the contribution of Zn(II) ions to the diffuse counterionic atmosphere is negligibly small,

the use of a two-state counterion distribution model for the divalent zinc(II) counterions is then less approximate. In this sense, the voltammetric results will be less approximate then the conductometric ones. Finally, in order to exclude possible diffuse double layer effects and to make the ionic strength dependent on c_{KNO_3} only, it is necessary that $c_P \ll c_{KNO_3}$. Typically one therefore has in voltammetric analysis:

$$c_{KNO_3} \gg c_P \gg c_{Zn} \tag{4.9}$$

as the typical voltammetric counterpart of the conductometric condition (4.4). It should be mentioned that for the present study, where [Zn(II)] is 10^{-7} mol.l^{-1} with conditions of a 10 to 100-fold excess of P over Zn(II) and a 10 to 100-fold excess of K$^+$ over P, it is still possible to study the metal/polyanion interaction over an ionic strength range of some 3 decades (i.e., from 10^{-3} to 1 mol.l^{-1}).

At this point it is useful to consider the electrolyte concentration dependency of the metal/polyelectrolyte complex. It is determined by the electrostatic interaction of both the monovalent and divalent counterions. This can easily be understood if one considers that the stability of the metal/polyelectrolyte complex is the sum of a constant (intrinsic) term and an electrostatic term. The latter depends strongly on the electrolyte concentration. We therefore rewrite the association reaction of divalent cations with the polyanion (4.5) by including monovalent counterions:

$$Zn(II) + K_sP \rightleftharpoons Zn(II)K_{s-v(volt)}P + v(volt)K^+ \tag{4.10}$$
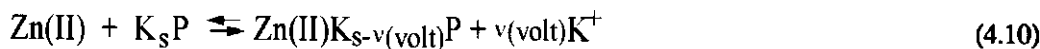
where the subscript s refers to the initial fraction of bound monovalent counterions and, thus, is related to the parameter $f_{M,0}$ as used in conductometry. The voltammetriccally obtained K$^+$/Zn(II) exchange ratio is denoted as v(volt). The exchange equilibrium constant K_{exch} for the exchange reaction (4.10) is

$$K_{exch} = \frac{a_{Zn(II)K_{s-v(volt)}P} \, a_{K^+}^{v(volt)}}{a_{Zn(II)} \, a_{K_sP}} \tag{4.11}$$

where a refers to activities. As long as the concentration of supporting electrolyte is much larger

than the concentration of ligand and metal, i.e. with condition (4.9) obeyed, a_{K^+} is a constant over a whole complexation curve. This condition is obeyed for all experimental data presented. Hence, it is allowed to rewrite equation (4.11) into:

$$K_c = f(\gamma)K = \frac{a_{Zn(II)P}}{a_{Zn(II)} a_P} = K_{th} \frac{1}{a_{K^+}^{v(volt)}} \tag{4.12}$$

where K_c refers to the stability corrected for activity effects and $f(\gamma)$ is some function of activity coefficients. Under the present conditions of large excess of ligand over metal, the degree of coverage, i.e. the number of bound metal ions per charged group on the polyanion, will be small. Hence, it is assumed that the activity correction is equal for both the complex and the ligand so that it cancels from equation (4.12). The remaining activity correction for the heavy metal ion can then be calculated by using expressions for mixtures of electrolytes [e.g. 9].

Since the chemical composition of the sample solutions in conductometry and voltammetry are quite different (cf. equations (4.4) and (4.9)), we should add that it is not obvious that the exchange coefficients v(cond) and v(volt) have to be equal. Unfortunately, exchange coefficients based on theoretical predictions are very scarcely available in the literature. For highly charged polyelectrolytes (ξ=2) under conductometric conditions, Benegas et al. [10] have predicted an exchange coefficient of 1.3 on the basis of a two-state approximation. For the case of excess electrolyte over metal, i.e. under voltammetric conditions, one can deduce from Scatchard plots, based on the same concept, an exchange coefficient of about 1.6 for ξ=4.2 and a degree of coverage of 25% [11]. Taking the Poisson-Boltzmann concept for deriving fractions of free and bound counterions, Fogolari et al. [12] have computed Scatchard variables for a variety of charge densities and an excess of monovalent counterions. Analysis of their data in terms of an exchange coefficient between monovalent and divalent counterions results in a value of approximately 1.7 for ξ=2, a degree of coverage -> 0 and a radius of the polyelectrolyte cylinder of 0.8 nm. The ensuing exchange coefficients for excess of monovalent counterions seem to be somewhat higher than the one predicted for conductometric conditions. Extrapolation, however, to the present case should be done with care, since the voltammetric conditions in our experiments still differ from the ones in the theoretical predictions, i.e. ξ and the degree of coverage. Hence, further extension of theoretical analysis is clearly needed.

4.4 Results and discussion

In the comparison between conductometric and voltammetric speciation, we will use data from the literature [1] as well as experimental results to be presented in chapter 5 of this thesis. For experimental details the reader is referred to the corresponding references. In figure 4.1, some typical conductivity excess curves are presented for the addition of zinc(II) to solutions of polycarboxylate ions with high charge density. The curves for the salt-free systems generally show two distinct linear regions before reaching a more or less constant value, whereas under conditions of "added salt" $(c_K/c_p)>1$, linearity is lost above a certain amount of excess salt.
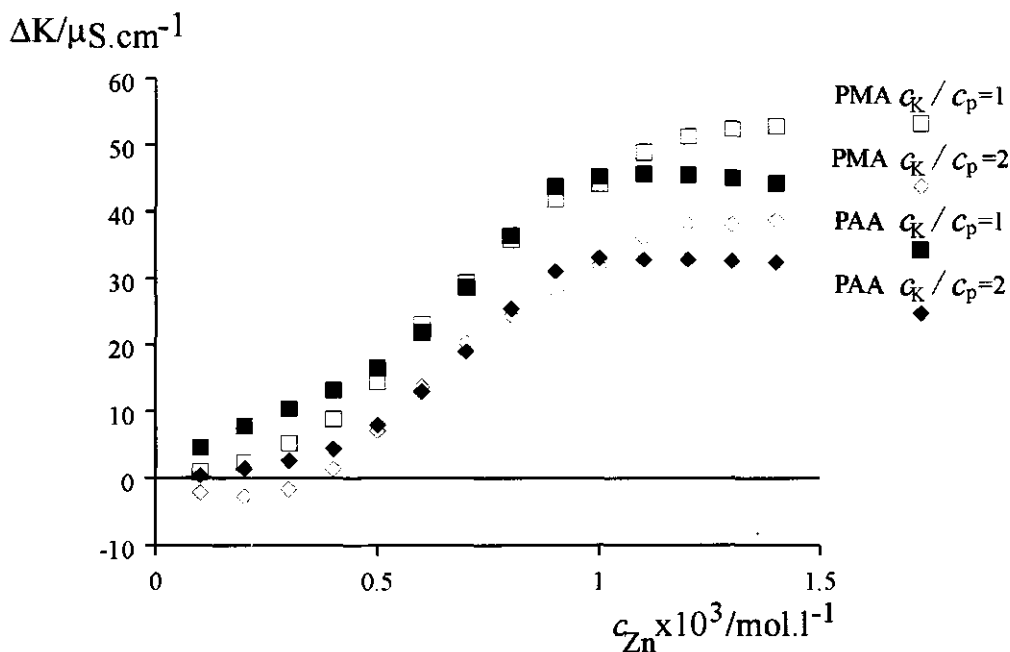
$\Delta K/\mu S.cm^{-1}$

Figure 4.1: Conductivity excess curves for the titration of K/PAA and K/PMA solutions with $Zn(NO_3)_2$ [1,2]. $[PMA]=2.5*10^{-3}$ mol.l^{-1}, $\alpha_n=0.8$ ($c_p=2.0*10^{-3}$ mol.l^{-1}).

Analysis of conductometric data in terms of fractions of free and bound counterions starts with the determination of f_K and λ_p from linear Eisenberg plots (see for example figure 2.1). Once f_K and λ_p are known, the slope of the conductivity excess curve is easily analyzed to yield the fraction of free zinc(II) ions according to equation (4.2). For various Zn(II)/PAA and Zn(II)/PMA systems, the resulting conductometric speciation data are presented in table 4.1. For both the KNO$_3$/Zn(II)/PAA and the KNO$_3$/Zn(II)/PMA systems, the fraction of initially free potassium

counterions increases with decreasing degree of neutralization in accordance with theoretical predictions (cf. equation (2.2) and figure 2.2 in chapter 2). Since the deviations of $(1-f_{Zn})$ from unity are not significant, the fraction of free zinc(II) ions is not measurable for the range where $c_{Zn}/c_p \leq 0.25$. Under these conditions conductometry is only able to measure the exchange of Zn(II) for K^+. For the KNO_3/Zn(II)/PAA and the KNO_3/Zn(II)/PMA systems, the corresponding mean exchange coefficients $v_{KZn(II)}$(cond) are also presented in table 4.1.

Table 4.1: Conductometric speciation data resulting from Eisenberg plots and conductivity excess curves for various KNO_3/Zn(II)/PAA and KNO_3/Zn(II)/PMA mixtures under conditions where $c_{Zn}/c_p \leq 0.25$ with $c_c = 2.5*10^{-3}$ mol.l^{-1}.

	$(1-f_{K,0})$	$(1-f_{Zn})$	v_{KZn}	references
PAA, $c_K/c_p=1$ (no added salt)				
α= 0.8	0.531±0.005	0.99±0.02	1.13±0.04	[1]
0.5	0.429±0.003	1.09±0.05	1.01±0.07	[1]
0.3	0.305±0.005	1.09±0.04	0.74±0.05	[1]
PAA, $c_K/c_p=2$ (KNO_3 added)				
α= 0.8	0.510±0.005	0.94±0.06	1.21±0.08	[1]
PMA, $c_K/c_p=1$ (no added salt)				
α= 0.8	0.499±0.016	0.93±0.03	1.23±0.04	this study
0.6	0.320±0.012	0.87±0.05	0.92±0.08	this study

A typical set of voltammetric complexation curves is presented in figure 4.2, where the normalized peak current Φ is plotted versus the polymethacrylate concentration c_p for various concentrations of KNO_3 for $\alpha_n = 0.8$ and $[Zn(II)] = 10^{-7}$ mol.l^{-1}. The polymethacrylate species have diffusion coefficients much lower than D_{Zn}. Hence, Φ decreases as the result of the association of Zn(II) with the polyanion and reaches a certain plateau value $(D_{ZnP}/D_{Zn})^p$ with further increasing excess of ligand. The Zn(II)/PMA system is definitely labile on the stripping voltammetric time-scale over the whole range of experimental conditions (see for detailed discussion chapter 5). Hence the experimental data represent the equilibrium distribution of zinc(II) ions over the free and bound states. Since lability is obeyed and the metal-to-ligand ratio is very small, the complexation curves can be analyzed in terms of a stability according to equations (4.6) and (4.7). As will be discussed in chapter 5, the exact value of the power of $(\overline{D}/D_{Zn})$ in equation (4.6) affects log K by only 0.1 unit and can therefore be disregarded for the present purpose.

Considering the aim of the present chapter, i.e. a comparison between conductometric and voltammetric speciation data, it is at this point useful to pay attention to the interpretation of the voltammetric peak current in the absence of complexing agents. Let us therefore recall the definition of the term metal speciation as presented in chapter 1: the determination of the distribution of metals over different chemical and/or physico-chemical forms including the free metal ion, metal complexes, adsorbed metals on particles and metal precipitates. Under the present experimental conditions, the initial metal solution contains free (hydrated) heavy metal, potassium and nitrate ions and depending on the pH, protons or hydroxyl ions. Part of the metal ions may be associated with nitrate or hydroxide ions and are therefore by definition not free. Since the diffusion coefficients of these simple inorganic metal species are of the same order of magnitude as the diffusion coefficient of the free metal ion, the voltammetric current will not be significantly affected as compared to the situation with only free metal ions in solution. Ignoring this fact, the voltammetric data may be misinterpreted with respect to free and bound metal ions. Under the present conditions the initial voltammetric response represents undoubtedly the concentration of free metal ions, since association of metal ions with nitrate and/or hydroxide ions will be ignorebly small. Hence, it is allowed to elucidate the voltammetric data in terms of free and bound metal ions. For badly definable natural samples, however, one should be cautious in analyzing voltammetric speciation data into fractions of free and bound metal.

In figure 4.3, the resulting $\log K_c$ values are plotted vs. $\log a_{K^+}$ for the Zn(II)/PMA system for $\alpha_n=0.4$ and $\alpha_n=0.8$. The stability strongly depends on the salt concentration. This behaviour is typical for polyelectrolytes and can be understood in terms of competition between monovalent counterions (K^+) and divalent ions (Zn(II)) for binding by the polyanion, which justifies the using of exchange reaction (4.10). Furthermore, $\log K_c$ and $\log a_{K^+}$ are approximately linearly related, in agreement with equation (4.12). The slopes yield $v_{KZn(II)}$(volt) values which are presented in table 4.2.
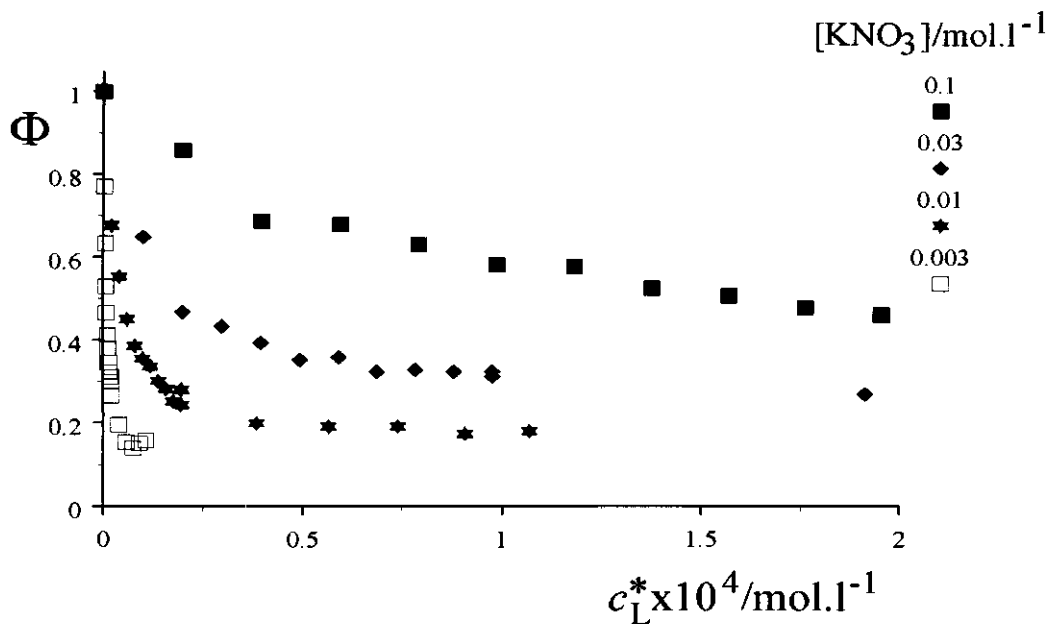
Figure 4.2: Stripping voltammetric complexation curves for the KNO_3/Zn(II)/polymethacrylate system for different KNO_3 concentrations. [Zn(II)]=10^{-7} mol.l^{-1}; α_n=0.8.
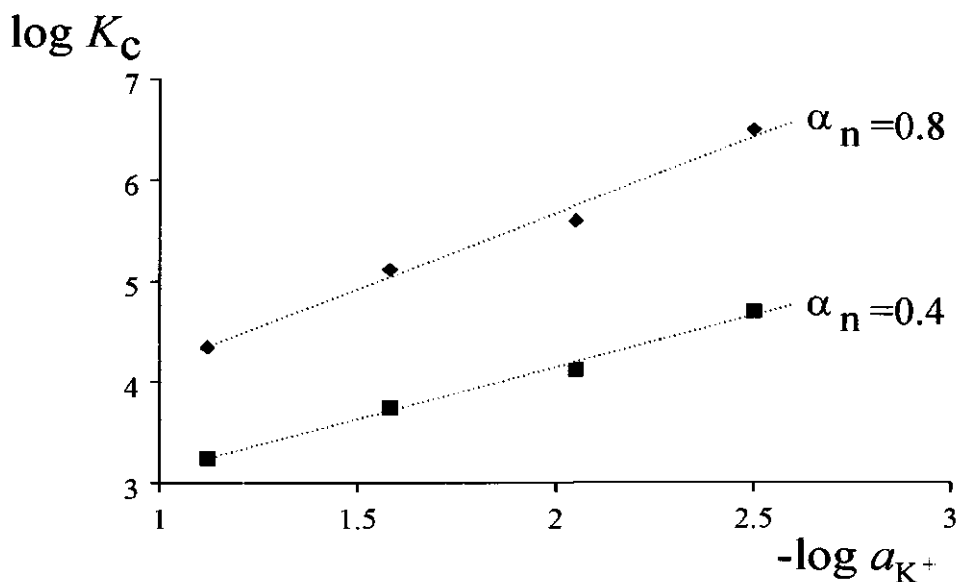

Figure 4.3: Dependence of the stability K_c for the system KNO_3/Zn/PMA on the activity of KNO_3 for [Zn(II)]=10^{-7} mol.l^{-1}.

There is a definite similarity between the voltammetric $v_{KZn(II)}$ values and the conductometric ones (compare tables 1 and 2). For the same α_n values, the voltammetric exchange coefficient seems to be somewhat larger than the conductometric one. The experimentally obtained conductometric exchange coefficients are in close agreement with theoretical predictions based on a two-state approach [10]. This aspect will be discussed in detail in chapter 5. Analogous calculations for the voltammetric conditions (in terms of M/Zn(II) ratio) are not yet available. Still, the global agreement between voltammetric and conductometric results is promising if one realizes that they were obtained under very different conditions with respect to the ratio between the concentrations of the two competing counterions K^+ and $Zn(II)$ and using different techniques. Hence, the experimentally obtained results call for an extensive theoretical analysis.

Table 2: The mean K^+/Zn(II) exchange ratio v(volt) as resulting from the a_{K^+} dependence on the stability parameter K_c for the KNO_3/Zn(II)/PMA system.

α	$v_{KZn(II)}$
0.8	1.42±0.08
0.4	1.00±0.09

Finally, the voltammetric data can be used to check the conductometric values of the fractions free zinc ions in table 4.1. According to equation (4.12), the stability of the metal/complex system is related to the ratio of bound zinc ions over free zinc ions and the activity of the polyion. For the KNO_3/Zn(II)/PMA system with α_n=0.8, the stability is approximately $3.2*10^6$ l.mol^{-1} at an ionic strength level of 0.003 mol.l^{-1}. For the present conductometric conditions with c_p=$2*10^{-3}$ mol.l^{-1}, the ensuing ratio $[Zn(II)_{bound}]/[Zn(II)_{free}]$ is of the order of 10^3. Thus, the deviation of $(1-f_{Zn})$ from unity is too small to be measured by conductometry. Although the stability K decreases with decreasing charge density on the polyion, the fraction free zinc(II) counterions remains below the experimental detectability. Thus the experimental $(1-f_{Zn})$ values in table 4.1, as found to be near unity and insensitive to α, are in agreement with the voltammetrically determined stability of the metal complex system.

4.5 References

1. H.G. de Jong, J. Lyklema and H.P. van Leeuwen, Biophys. Chem. 27 (1987) 173.
2. Chapter 5 of this thesis.
3. H. Eisenberg, J. Polym. Sci., 30 (1958) 47.
4. Chapter 3 of this thesis.
5. D.D. DeFord and D.N. Hume, J. Am. Chem. Soc., 73 (1951) 5321.

6. H.G. de Jong, H.P. van Leeuwen and K. Holub, J. Electroanal. Chem. 234 (1987) 1, 17; 235 (1987) 1; 260 (1989) 213.
7. W. Davison, J. Electroanal. Chem., 87 (1978) 395.
8. H.P. van Leeuwen, Sci. Total Environ., 60 (1987) 45.
9. E. Guntelberg, Z. Phys. Chem. Leipzig, 123 (1926) 199.
10. J.C. Benegas, S. Paoletti, A. Cesàro, M.A.G.T. van den Hoop and H.P. van Leeuwen, Biophys. Chem., 42 (1992) 297.
11. S. Paoletti, J. Benegas, A. Cesàro, G. Manzini, F. Fogolari and V. Crescenzi, Biophys. Chem., 41 (1991) 73.
12. F. Fogolari, G. Manzini and F. Quadrifoglio, Biophys. Chem., 43 (1992) 213.

Conductometry and voltammetry of metal complexes of synthetic polyacids

5.1 Introduction

The results of a variety of conductometric and stripping voltammetric experiments on metal/polyacid systems are presented and discussed. The results concern polyacrylic acid (PAA) and polymethacrylic acid (PMA). Results for naturally occurring complexing agents will follow in chapter 7. The aim of the experiments presented in this chapter is to obtain quantitative information about the association of several heavy metal ions with PAA and PMA in relation to the physico-chemical properties of these polyacids. The complementary character of the information obtained from conductometric and voltammetric data has been discussed in detail in chapter 4. A comparison of the physico-chemical behaviour of the synthetic polyacids with that of complexing agents met in natural systems will be made in chapter 7.

5.2 Experimental

5.2.1 Materials

The polyacrylic acid (PAA) and polymethacrylic acid (PMA) solutions were obtained from Polysciences and BDH, respectively, and used without further treatment. Average molar masses as specified by the manufacturers were 50,000, 150,000 and 500,000 $g.mol^{-1}$ for the PAA solutions and 26,000 $g.mol^{-1}$ for the PMA solutions. Stock solutions of 0.1 $mol.l^{-1}$ (in monomers) were prepared by dilution with water. Concentrations of carboxylic groups were determined by conductometric titration with potassium hydroxide. Stock solutions were stored in the dark at 4°C.

Titrisol potassium hydroxide solutions, Titrisol sodium hydroxide solutions, lithium hydroxide, calcium hydroxide, barium hydroxide, Titrisol hydrochloric acid solutions, potassium nitrate, zinc(II) nitrate, lead(II) nitrate, cadmium(II) nitrate (all from Merck), calcium nitrate, magnesium nitrate and nitric acid solutions (all from Baker) were of analytical-reagent grade. In most of the voltammetric experiments, stock metal standards of 10^{-4} $mol.l^{-1}$ for Cd(II), Pb(II)

and Zn(II) (as nitrates) were prepared by diluting BDH 1000 mg.l^{-1} AAS standards. The exact hydroxide concentrations were determined by conductometric titration with hydrochloric acid. All solutions were prepared using demineralized tap water, produced by a Millipore Super-Q reverse osmosis system. After removing CO_2, the conductivity of this water never exceeded 0.6 μS.cm^{-1}.

5.2.2 Equipment

The conductometric equipment has been described elsewhere [1]. The cell constant was periodically recalibrated.

Voltammograms were obtained using: 1) a Metrohm 663 VA stand controlled by a home-made "Quick Step" polarograph attached to a Hewlett-Packard 3497A data acquisition unit and a Hewlett-Packard 85B programmer, or 2) a Metrohm 663 VA stand controlled by PAR Model 174A polarographic analyzer from EG&G. The system 1) was also connected to a Metrohm 665 Dosimat for the automatic addition of polyacid solutions and to a Knick Multi-Calimatic pH-meter for the pH measurement after each addition. System 2) has only been used in the Zn(II)/PAA molar mass dependency experiments. In all cases, working, reference and counter electrodes were HMDE, Ag/AgCl,KCl$_{sat}$ and glassy carbon, respectively. In the experiments performed with the "Quick Step" polarograph a polystyrene vessel was used. In the other experiments a polyfluoroethylene cell (provided by EG&G PAR) was used. Table 5.1 shows the standard settings of the two voltammetric set-ups used.

Table 5.1: Settings of the two voltammetric set-ups used. System 2 has only been used in the Zn(II)/PAA measurements.

	System 1	System 2
surface area HMDE	≈0.40 mm^2	≈0.52 mm^2
pulse duration	25 ms	40 ms
pulse height	50 mV	25 mV
scan rate	4 mV.s^{-1}	5 mV.s^{-1}
deposition potential		
zinc	-1150 mV	-1200 mV
cadmium	-850 mV	
lead	-650 mV	
pre-electrolysis time	f([Me]$_T$)	60 s
rest period	30 s	30 s

5.2.3 Fitting procedure

For the computation of the fractions of free and bound counterions according to an extended counterion condensation model as described in paragraph 2.2.2, a FORTRAN program (LAHEY compiled) was developed. In order to fit the stripping voltammetric complexation curves to theoretical predictions from equation (3.11), a FORTRAN program was developed. A basic fitting element of the latter program is the subroutine ZXMIN, taken from the IMSL library [2].

5.3 Results and discussion

5.3.1 Conductometry

In order to study the distribution of monovalent and divalent counterions in systems containing PAA or PMA, conductometric experiments have been carried out by adding aliquots of 50 µl of 0.05 mol.l^{-1} M(II)(NO$_3$)$_2$ solution to 50 ml of sample solution. The following metal/poly-electrolyte complexes were studied: Ca/PMA, Mg/PMA, Zn(II)/PAA, and Zn(II)/PMA. Sample solutions of alkali metal polyacrylates and polymethacrylates were prepared by neutralizing the polyacid with the appropriate hydroxide solution to a degree of neutralization of 0.8. Prior to the measurements, the samples were stirred and kept for 60 min in a constant-temperature vessel to achieve thermal equilibrium, while purging with CO$_2$-free, water-saturated nitrogen. All experiments were done in duplicate at $25.00 \pm 0.02°C$.

5.3.1.1 Ca/PMA and Mg/PMA

Figures 5.1a and 5.1b show the conductivity excess for the three alkali metal polymethacrylate solutions as a function of the concentration of Ca^{2+} and Mg^{2+}, respectively, with [PMA]=2.5*10^{-3} mol.l^{-1} and a degree of neutralization of 0.8. Under these conditions, the contributions of H$^+$ and OH$^-$ can be ignored because their conductivities are sufficiently negligible with respect to the other charged species.

From Eisenberg plots, which were found to be linear for the Ca/PMA and Mg/PMA systems at all metal concentrations, the corresponding f_1 and λ_p values have been calculated as described in chapter 2.
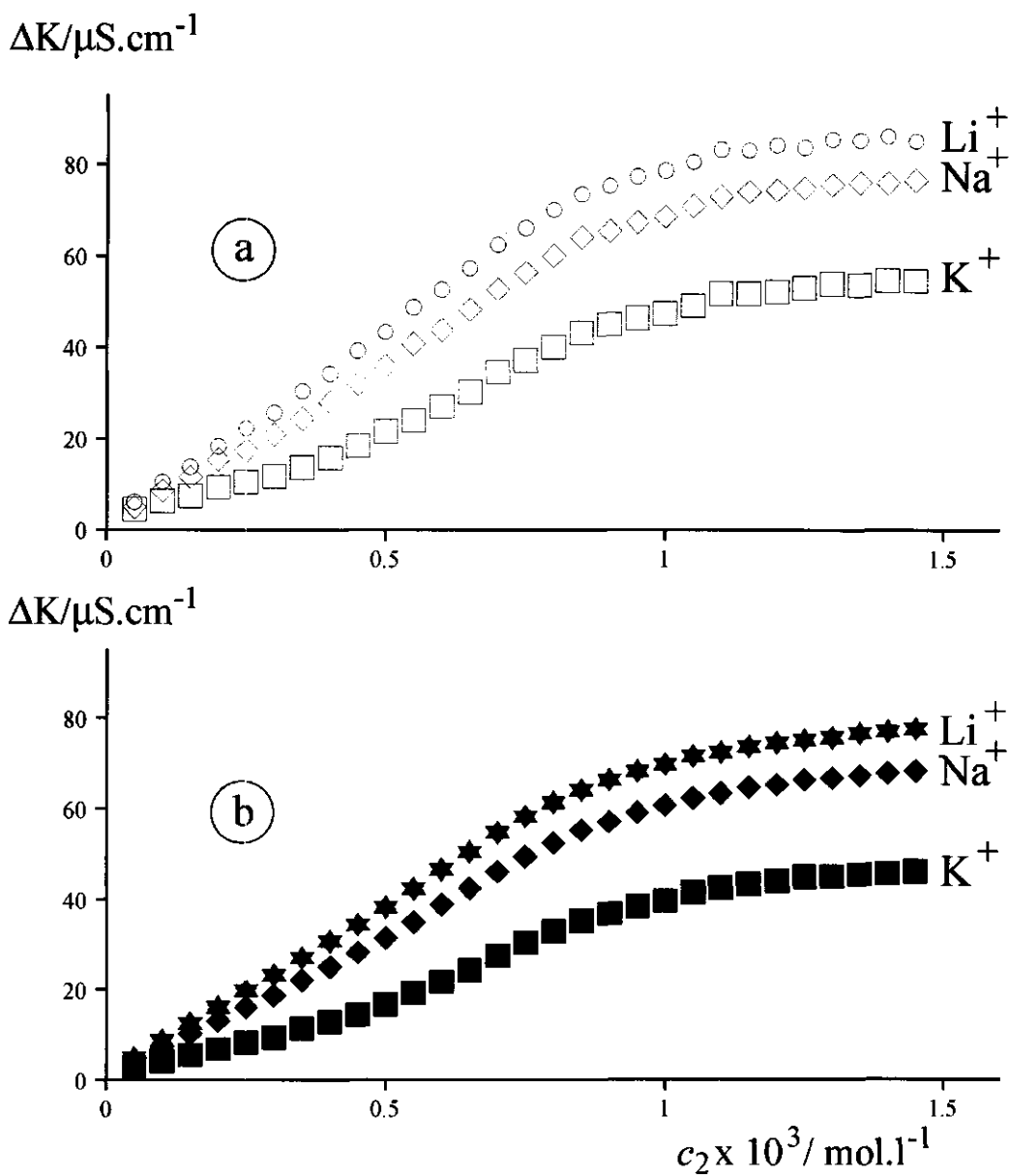
Figure 5.1: Conductivity excess curves of three alkali metal polymethacrylate solutions for various concentrations of Ca^{2+} (a) and Mg^{2+} (b); [PMA]=$2.5*10^{-3}$ mol.l^{-1}; α_n=0.8.

The observed linearity illustrates the non-specific nature of the interaction between the alkali metal ions and the polymethacrylate anion, which also recurs in their competition with both Ca^{2+} and Mg^{2+} for binding by the polyion. This is in agreement with various earlier observations. For example, according to Rinaudo and Milas [3] the binding of Ca^{2+} to carboxymethylcellulose appears to be purely electrostatic. As discussed before by De Jong et al. [1], accurate values of $f_{1,0}$ and λ_p are obtained by extrapolation of f_1 to zero R_2 (figures 5.2a and 5.2b). For the Ca/PMA and Mg/PMA systems, $f_{1,0}$ values were found to be 0.498±0.007 and 0.494±0.004, respectively. Values for λ_p of 46.0±1.4 and 48.9±0.8 $S.cm^2.mol^{-1}$ were obtained for these two samples. From the obtained values of f_1 and $f_{1,0}$, together with the value of λ_p for the blank polyelectrolyte solution [1], the fractions of free divalent counterions can be calculated from the conductivity excess. This can easily be done with equation (2.27), with an apparently constant λ_p [1] over the titration range considered. The calculated f_2 values are average values for the three alkali metal polymethacrylate solutions.

In figures 5.2a and 5.2b, the resulting f_1 and f_2 values are plotted as a function of the ratio R_2 for the Ca/PMA and the Mg/PMA systems, respectively. For the PMA polyion, the results obtained with the Ca system agree with those of Mg within the limits of experimental error. Satoh et al. [4] have studied the activity coefficients as a function of the divalent cation concentration for sodium poly(styrenesulfonate)/$MgCl_2$ or $CaCl_2$ and sodium poly(L-glutamate)/$MgCl_2$ or $CaCl_2$ for the salt-free case. They have also observed the similarity of behaviour between the two alkaline earth metal cations.

The theoretical f_1 and f_2 values are presented as solid curves in figures 5.2a and 5.2b. They have been calculated for $c_p = 2*10^{-3}$ $mol.l^{-1}$ and ξ=2.29 [5]. For both systems the theoretical data agree fairly well with the experimental ones. The theoretical $f_{1,0}$ value is fixed by the limiting-law condition in equation (2.20). According to this equation, only the charge density parameter ξ can account for the observed difference. The difference could be attributed to some uncertainties with respect to (i) the analytical error in α_n and (ii) the value of ξ as taken from the literature [5]. Use of a somewhat smaller value of ξ in the computation, certainly leads to a better fit. Figures 5.2a and 5.2b show that a better agreement between experimental and theoretical f_1 values is obtained for ξ=2.0 (see dashed curves). For this ξ value, however, the model over-estimates the fractions of free divalent counterions for higher values of R_2. It has to be recalled that both the interpretation of the experiments and the model rely on the simplification of the two phase model.
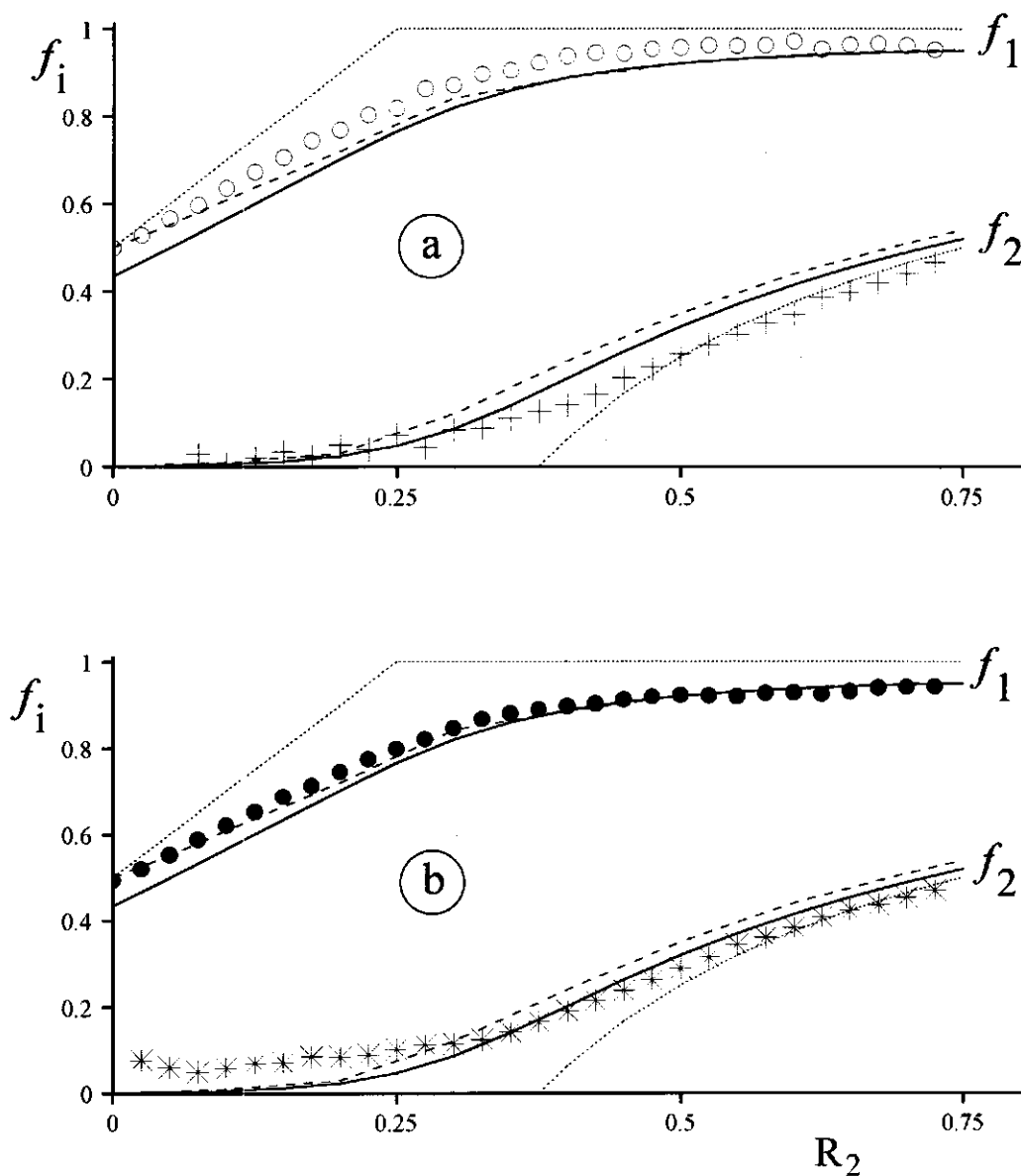
Figure 5.2: Experimental (symbols) and theoretical values (solid curves, ξ=2.29; dashed curves, ξ=2.0; dotted curves, complete charge compensation model) of f_1 and f_2 as a function of the ratio R_2 for the Ca/PMA (a) and Mg/PMA (b) systems; [PMA]=$2.5*10^{-3}$ mol.l^{-1}; α_n=0.8. For discussion see text.

In figures 5.2a and 5.2b, the dotted curves represent the behaviour of the fractions of free monovalent and divalent counterions in the case of exchange with complete charge compensation, as predicted for the salt-free case by Manning's counterion condensation theory [6], for $\xi=2.0$. The salt concentration of the initially salt-free M^+/PMA solution increases along the titration and affects, therefore, the theoretical pattern of exchange with complete charge compensation as plotted in figures 5.2a and 5.2b. Our analysis however, refers to the initial section of the titration curves and the resulting f values hold for the limit $c_{salt} \to 0$. For this limit Manning has shown that the binding of divalent ions approaches the salt-free case of exchange with complete charge compensation [6].

The increase of f_1 with increasing R_2 is due to the exchange of condensed monovalent ions for divalent ions. In the initial part up to $R_2 \approx 0.25$, the liberation of monovalent cations is proportional to the amount of M^{2+} added, and the added divalent ions are practically quantitatively bound (c.f. the prediction according to the case of exchange with complete charge compensation (dotted curves in figures 5.2a and 5.2b)).

Figures 5.2a and 5.2b show that up to $R_2 \approx 0.25$ the release of monovalent counterions is linear upon addition of divalent counterions for both systems (with statistics for the Mg/PMA system: $n=10$, $r^2=0.998$, slope=1.25 ± 0.02). Applying equation (2.28) to the Mg/PMA system in the range $0 \leq R_2 \leq 0.25$, and taking for $(1-f_2)$ an average value of 0.94 ± 0.01 a mean exchange coefficient v has been calculated. Using the same procedure for the Ca/PMA system in the range $0 \leq R_2 \leq 0.25$, the mean exchange ratios v_{1Ca} and v_{1Mg} were found to be 1.39 ± 0.03 and 1.33 ± 0.03, respectively. Using $\xi=2.29$, the mean exchange ratio v_{12} calculated from the theory is 1.38, which is in remarkable agreement with the experimental data. For the PAANa/Mg^{2+} and PAANa/Ca^{2+} with $\alpha_n=1$, Satoh et al. [4] estimated exchange ratios in the range of 1.5-1.8 from activity coefficient data in the same R_2 range. These results seem to confirm that at lower charge densities a divalent counterion replaces less monovalent counterions than at higher charge densities. A similar result has been found for DNA [7].

5.3.1.2 Zn(II)/PMA and Zn(II)/PAA

For the Zn(II)/PMA and Zn(II)/PAA (molar mass 500,000 g.mol^{-1}) systems with $\alpha_n=0.8$, the Eisenberg plots are also linear. By extrapolation of f_1 to zero R_2 (see figure 5.3), $f_{1,0}$ values were found to be 0.488 ± 0.004 and 0.501 ± 0.016 for the Zn(II)/PMA and Zn(II)/PAA systems, respectively. Values for λ_p values were found to be 46.7 ± 0.8 and 26.5 ± 0.3 S.cm^2.mol^{-1} for these

two systems. Assuming λ_p to be constant, the fractions of free monovalent and divalent counterions have been calculated according to equation (2.27). They are plotted vs. R_2 in figure 5.3. Additional results from the literature [1] have been incorporated in figure 5.3. These systems certainly behave differently from the Ca/PMA and Mg/PMA systems. For example, at R_2 equal to 0.5, f_1 reaches unity, indicating that no monovalent cations are bound any more, whereas for the latter systems f_1 approaches unity in a gradual way with increasing R_2 (cf. figures 5.2a and 5.2b). Furthermore, for the region $0 \leq R_2 \leq 0.5$, f_2 seems to be independent of R_2 for both the Zn(II)/PAA and Zn(II)/PMA systems, whereas in the case of the Ca/PMA and Mg/PMA systems f_2 shows a more gradual increase with increasing R_2. It seems that, compared to Ca^{2+} or Mg^{2+} ions, the Zn(II)-ions are bound more strongly. This could be due to some specific binding of the Zn(II)-ions, which is not incorporated in the theoretical model as described in chapter 2. Probably because of this reason, the theoretical f_1 and f_2 values (presented as solid lines; $c_p = 2*10^{-3}$ mol.l^{-1} and ξ=2.29) do not agree very well with the experimental ones.
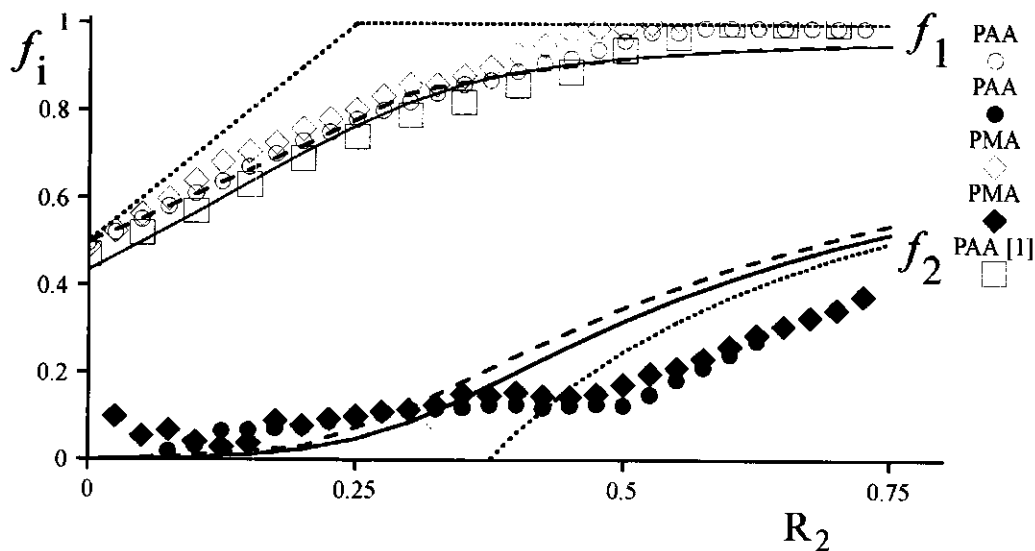

Figure 5.3: Experimental (symbols) and theoretical values (solid curves, ξ=2.29; dashed curves, ξ=2.0; dotted curves, complete charge compensation model) of f_1 and f_2 as a function of the ratio R_2 for Zn(II)/PMA and Zn(II)/PAA (molar mass is 500.000 g.mol^{-1}); [PMA]=[PAA]=2.5*10^{-3} mol.l^{-1}; α_n=0.8. Literature data for Zn(II)/PAA [1] with molar mass of 230.000 g.mol^{-1} have been included.

60

For the Zn(II)/PMA and Zn(II)/PAA systems in the range $0 \leq R_2 \leq 0.25$, the mean exchange coefficients ν have been calculated by applying equation (2.28) and were found to be 1.33 ± 0.05 and 1.23 ± 0.04, respectively. The latter figure is in agreement with the mean exchange coefficient found in the literature for the Zn(II)/PAA system with a molar mass of 230,000 g.mol^{-1}. These values are quite similar to the ones found for the Ca/PMA and Mg/PMA systems. In table 5.2, the conductometric speciation data are summarized for $R_2 \leq 0.25$ for all systems studied.

Table 5.2: Fractions bound monovalent and divalent counterions and the exchange coefficient ν for the Ca/PMA, Mg/PMA, Zn(II)/PMA and Zn(II)/PAA systems under conditions where $R_2 \leq 0.25$; $c_p = 2*10^{-3}$ mol.l^{-1}.

System	$(1-f_{1,0})$	$(1-f_2)$	ν	reference
Ca/PMA	0.502±0.007	0.94±0.01	1.39±0.03	this study
Mg/PMA	0.506±0.004	0.94±0.01	1.33±0.03	this study
Zn(II)/PMA	0.512±0.004	0.93±0.03	1.33±0.05	this study
Zn(II)/PAA	0.499±0.016	0.93±0.03	1.23±0.04	this study
Zn(II)/PAA	0.531±0.005	0.99±0.02	1.13±0.04	[1]

5.3.2 Voltammetry

A systematic study of the stripping voltammetric behaviour of heavy metal ions in synthetic polyacid solutions has been accomplished by varying: 1) the molar mass of the polyacid, in order to deal with different polyionic diffusion coefficients; 2) the concentration of electroinactive supporting electrolyte, in order to investigate the competition between monovalent and divalent counterions; 3) the degree of neutralization, in order to vary the charge density of the polyanion; and 4) the total metal ion concentration, in order to check the chemical homogeneity of the macromolecular complexing agent (this for later (see chapter 6) comparison with natural complexing agents which are generally heterogeneous).

The voltammetric complexation curves have been obtained at $25.0 \pm 0.2°$C as described in chapter 3. The reliability of the results has been verified by periodically remeasuring a standard system, i.e. Zn(II)/PMA at $\alpha_n = 0.8$, [KNO$_3$]=0.01 mol.l^{-1} and [Zn(II)]=10^{-6} mol.l^{-1}. For this standard system, the results remain identical.

5.3.2.1 Shape of voltammogram

In figure 5.4, three sets of differential pulse anodic stripping voltammograms for 10^{-7} mol.l^{-1} Zn(II), Cd(II) and Pb(II) solutions are presented for various points along the experimental complexation procedure. Series 1 represents step 2 of the experimental procedure as described in chapter 3 and shows the voltammetric responses for the initial metal ion solution at pH=3.85 and [KNO$_3$]=0.03 mol.l^{-1}. Regular shapes are obtained with peak width at half height ($W_{1/2}$) equal to approximately 60 mV, indicating the reversibility of the electrode process. For the second series (2) the pH was set close to the pH of the PMA stock solution at α_n=0.3 by adding a small aliquot of KOH (step 3). The resulting pH was 5.70. The peak heights of Zn(II) and Pb(II) decrease. The current decrease of Zn(II) has to be interpreted as a loss of free metal ions due to adsorption onto the surface of the sample vessel [8]. This problem and the way to overcome it are described in detail in chapter 3.
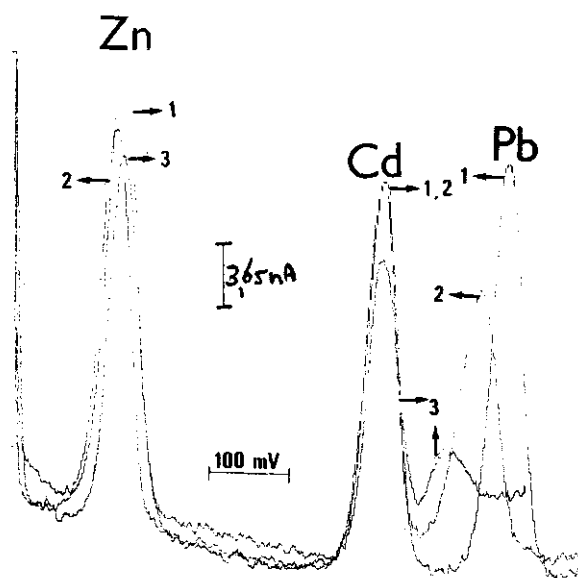

Figure 5.4: Differential pulse anodic stripping voltammograms of Zn(II), Cd(II) and Pb(II) for several steps of the experimental procedure. [M(II)]=10^{-7} mol.l^{-1}; [KNO$_3$]=0.03 mol.l^{-1}; t$_e$=2 min; v$_{scan}$=2.5 mV.s^{-1}. Series 1: pH=3.85; Series 2: pH=5.70; Series 3: [PMA]=4.97x10^{-5} mol.l^{-1}; α_n=0.3. Further explanation in the text.

In the case of Pb(II), the potential shift is significant (approximately 50 mV), indicating some complexation, probably with hydroxide. This can be checked by using equation (3.13). If we assume that under the present conditions $PbOH^+$ is the main complex, the resulting $\log K$ value is found to be in the order of 6.8 with $\Phi=0.6$ and $[OH^-]=5*10^{-9}$ mol.l^{-1}. This is in reasonable agreement with a literature value of 6.3 [9]. Furthermore, the shape of the voltammogram is affected (increase of $W_{1/2}$) and hence, the analysis of complexation curves for Pb(II) under these conditions should be done with special care. These effects become more pronounced for higher pH values (see section 7.3.2.1). For this reason, the present study will be confined to the Zn(II) and Cd(II)/polyacrylate and polymethacrylate complex systems, taking the proper measures to account for adsorption on the vessel wall. Finally, the addition of PMA results in a decrease of all peak heights due to the association of the heavy metals with the polymethacrylate anion (series 3, step 4). The concentration of the PMA in terms of the volume concentration of deprotonated groups equalled $4.97*10^{-5}$ mol.l^{-1}. According to equation (3.11), a larger decrease of the peak current at the same PMA concentration indicates a higher stability (K) of the metal/PMA complex involved.

5.3.2.2 Influence of molar mass of the polyelectrolyte on stability

In figure 5.5, experimental normalized peak currents Φ are plotted as a function of the PAA concentration for three Zn(II)/PAA systems with different molar masses of the polyacid and a constant α_n of 0.8, $[Zn(II)]=10^{-6}$ mol.l^{-1} and $[KNO_3]=0.02$ mol.l^{-1}. Under these conditions the macromolecular ion is certainly in its expanded conformation due to the high charge. As a result of the association of Zn(II) with the polyacrylate ion, Φ decreases and approaches a certain finite plateau value with increasing excess of ligand. This last observation is a clear indication of lability of the metal complex system on the effective time scale of the stripping voltammetric experiment. In the case of non-lability, Φ would decrease to zero. For the three different molar masses, the initial parts of the curves are practically the same, which indicates that the complex stabilities are close to identical (see table 5.3). All stabilities could be satisfactorily calculated after estimating ε from the tail of the complexation curve using either $p=1/2$ or $p=2/3$ according to equation (3.11).

In table 5.3 these stabilities are collected. Invariably, the quality of the fit is acceptable (that is, comparable to or within the experimental error). The differences between the correlation coefficients obtained by using $p=1/2$ or $p=2/3$, are not significant. This is the more general
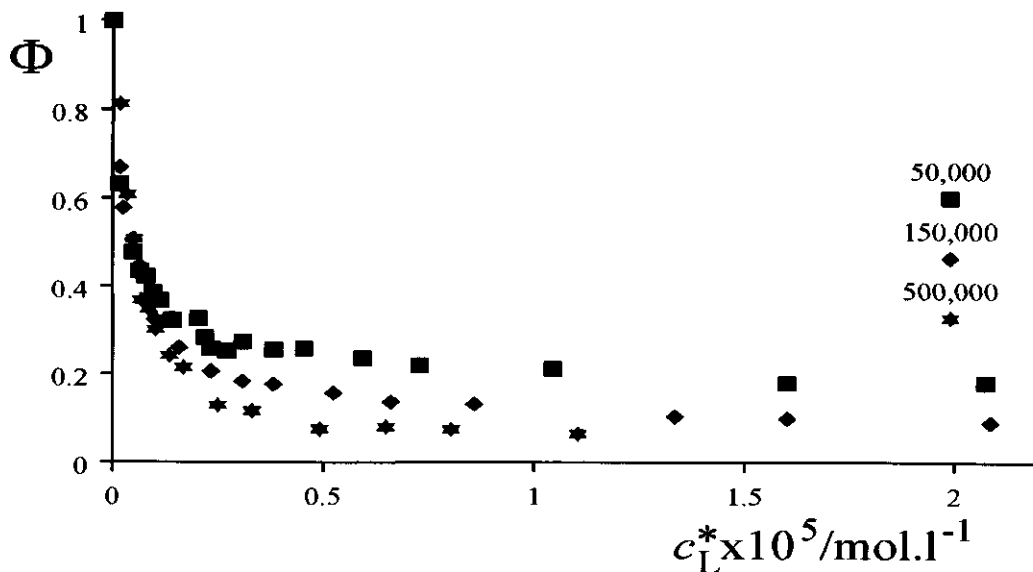
Figure 5.5: Experimental values of Φ as a function of the carboxylate concentration for the Zn(II)/PAA system with different molar masses at $\alpha_n=0.8$.

picture. It is tempting to give preference to the results for p=1/2 because these yield a better constant K (variation 0.01). However, considering all other data [10] and the uncertainties concerning p and ε, this is not very well justified. The conclusion that has to be drawn here is that both sets deserve their credit and that under the given conditions K is approximately $10^{5.8}$ and definitely independent of the molar mass of the polyacid. Thus, the strength of the binding of Zn(II) to the carboxylate group of PAA is not affected by the molar mass of the polyacid, as it should. The results are the more elegant since, unlike the resulting K value, the *shape* of the complexation curve is clearly affected by the molar mass of the polyion. With increasing molar mass, Φ decreases to a lower level, in accordance with a decrease of the diffusion coefficient of the complex with increasing molar mass.

Table 5.3: Stability constants K for the Zn(II)/PAA system as a function of the molar mass of the polyacid at $\alpha_n=0.8$ and $[KNO_3]=0.02$ mol.l^{-1}.

Molar mass	p	ε	log K	r^2
50,000	1/2	0.032	5.92	0.993
	2/3	0.077	5.72	0.989
150,000	1/2	0.006	5.92	0.990
	2/3	0.023	5.68	0.994
500,000	1/2	0.002	5.91	0.938
	2/3	0.008	5.65	0.968

5.3.2.3 Influence of electrolyte concentration on stability of the complexes

Figure 5.6 shows the voltammetric complexation curves for the Cd(II)/PMA system for different concentrations of KNO_3 with $\alpha_n=0.8$ and $[Cd(II)]=10^{-6}$ mol.l^{-1}. For the Zn(II)/PMA system, the corresponding complexation curves are presented in figure 4.2 with $\alpha_n=0.8$ and $[Cd(II)]=10^{-7}$ mol.l^{-1}. In contradistinction to the Zn(II)/PAA systems, the complexation curves have been analyzed in terms of a stability constant according to equation (3.11) without fixing the value of ε. The reason for this is two-fold. First, some of the complexation curves have not yet reached a constant limit and hence, estimations of ε according to equation (3.12) are not allowed. Second, the diffusion coefficient of the complex may be dependent on the concentration of electroinactive electrolyte as has been shown for sodiumpolystyrenesulfonate from quasielastic light-scattering experiments [11].

The resulting K and ε values are presented in table 5.4 using p=2/3. The qualities of the fits are given by the correlation coefficient r^2, which are quite gratifying. It can be seen that the stability of the heavy metal/polymethacrylate complex decreases with increasing KNO_3 concentration. The effect is largely due to the reduction of the electrostatic component of the metal/polyion interaction. This is generally the case for polyelectrolytes with high charge densities and can be understood in terms of competition between the monovalent counterions (K^+) and the divalent counterions (Zn(II),Cd(II)) for binding by the polymethacrylate anion. This aspect has been discussed in more detail in chapter 4. Finally, with one exception, realistic ε values are found, which appear to be somewhat larger than the literature value of 0.023 [10,12]. No clear relationship between the value of ε and [KNO_3] is observed. We note that there is a relative insensitivity of the procedure for the value of ε. Therefore, ε values will not be analyzed in the succeeding experimental results.

Table 5.4: Stabilities K obtained from Φ values for the Zn(II)/PMA and Cd(II)/PMA systems as a function of the concentration KNO_3 with $\alpha_n=0.8$ and $[Zn(II)]=10^{-7}$ mol.l^{-1} and $[Cd(II)]=10^{-6}$ mol.l^{-1}.

[KNO_3] (mol.l^{-1})	Zn(II)/PMA			Cd(II)/PMA		
	$\log K$	ε	r^2	$\log K$	ε	r^2
0.1	4.15	0.058	0.991	4.81	0.046	0.998
0.03	5.11	0.103	0.993	5.74	0.012	0.979
0.01	5.65	0.045	0.991	5.91	0.051	0.993
0.003	6.45	0.013	0.995	6.25	<0.001	0.976

$[KNO_3]/mol.l^{-1}$
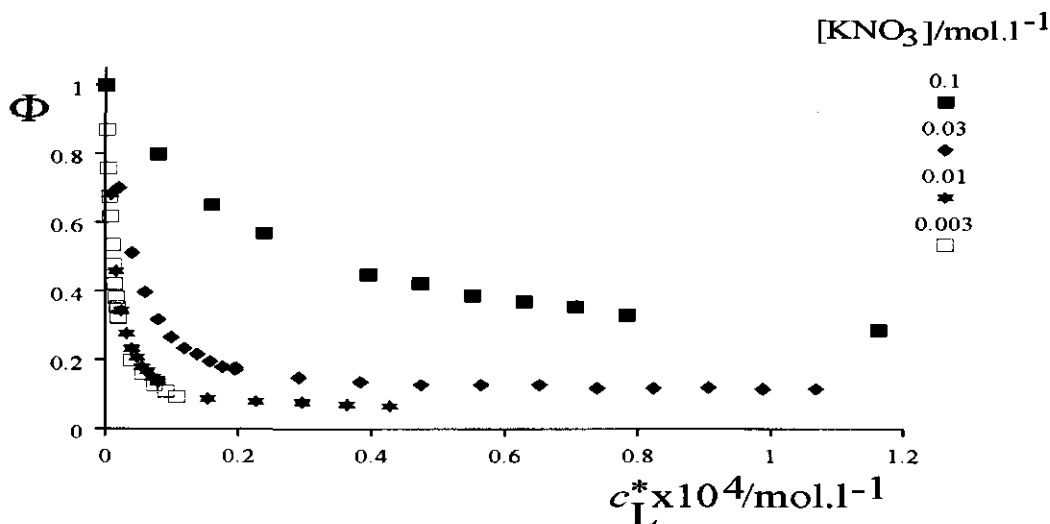

Figure 5.6: Stripping voltammetric complexation curves for the Cd(II)/PMA system for different KNO$_3$ concentrations. [Cd(II)]=10^{-6} mol.l^{-1}; α_n=0.8.

In figures 5.7a and 5.7b, the shift of the peak potential is presented as a function of the polymethacrylate concentration at different KNO$_3$ concentrations. The data are given for the Zn(II)/polymethacrylate and the Cd(II)/polymethacrylate complexes, respectively, with α_n=0.8 and [Zn(II)]=10^{-7} mol.l^{-1} and [Cd(II)]=10^{-6} mol.l^{-1}. In all cases, the peak potential decreases with increasing concentration of the polymethacrylate anion. For the calculation of the stability K from the potential shift, we have used the final five points of the complexation curve to fulfil the condition of having an sufficiently large excess of ligand over metal. The stabilities as obtained from ΔE_{peak} are in excellent agreement with the K values from Φ, except for the Cd(II)/PMA system with [KNO$_3$]=0.01 mol.l^{-1} (see table 5.5).

Table 5.5: Stabilities K obtained from ΔE_p values for the Zn(II)/PMA and Cd(II)/PMA systems as a function of the concentration of KNO$_3$ with α_n=0.8 and [Zn(II)]=10^{-7} mol.l^{-1} and [Cd(II)]=10^{-6} mol.l^{-1}.

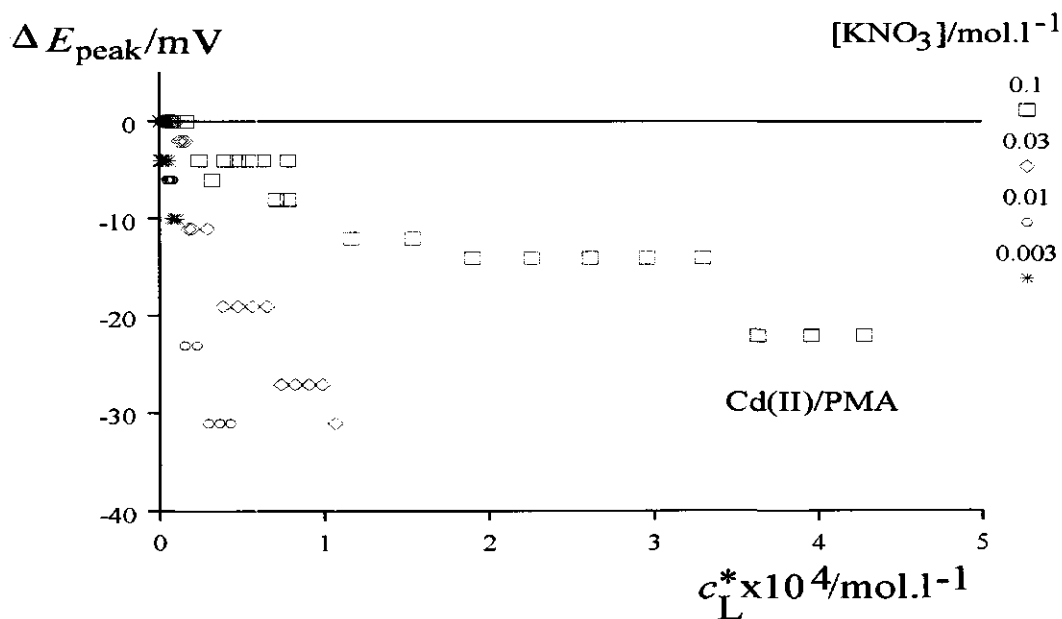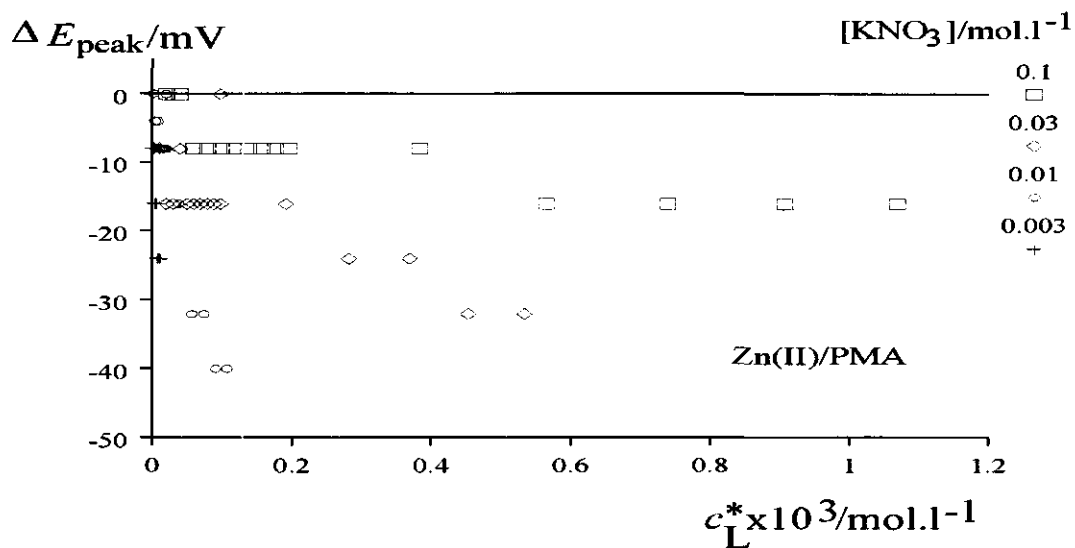|	Zn(II)/PMA	Cd(II)/PMA
[KNO$_3$] (mol.l^{-1})	log K	log K
0.1	4.2±0.1	4.8±0.1
0.03	4.9±0.1	5.9±0.1
0.01	6.0±0.2	6.6±0.1
0.003	6.7±0.1	6.3±0.1

Figure 5.7: The shift of the peak potential as a function of the ligand concentration for the Zn(II)/PMA (a) and the Cd(II)/PMA systems for different KNO_3 concentrations. $[Zn(II)]=10^{-7}$ mol.l^{-1}; $[Cd(II)]=10^{-6}$ mol.l^{-1}; $\alpha_n=0.8$.

5.3.2.4 Influence of the polyelectrolyte charge density

The influence of the charge density on the stability of the Zn(II)/PMA system has been studied by varying the degree of neutralization of the polymethacrylate anion for $[Zn(II)]=10^{-6}$ mol.l^{-1} and $[KNO_3]=0.01$ mol.l^{-1}. In figure 5.8, the corresponding complexation curves are presented for α_n values in the range 0.2-0.8. These curves show that for higher values of α_n, Φ decreases with increasing c_L^* much more strongly than for lower values of α_n. This is due to the appreciably higher value of the stability K and in accordance with the general polyelectrolytic feature that counterion binding is stronger for higher polyionic charge density. The observed plateau values for the higher α_n values or the tendency of reaching a certain plateau value with increasing ligand concentration for the lower α_n values, in combination with a systematic shift of the peak potential (not shown), indicate the lability of the Zn(II)/PMA system for the various values of α_n.
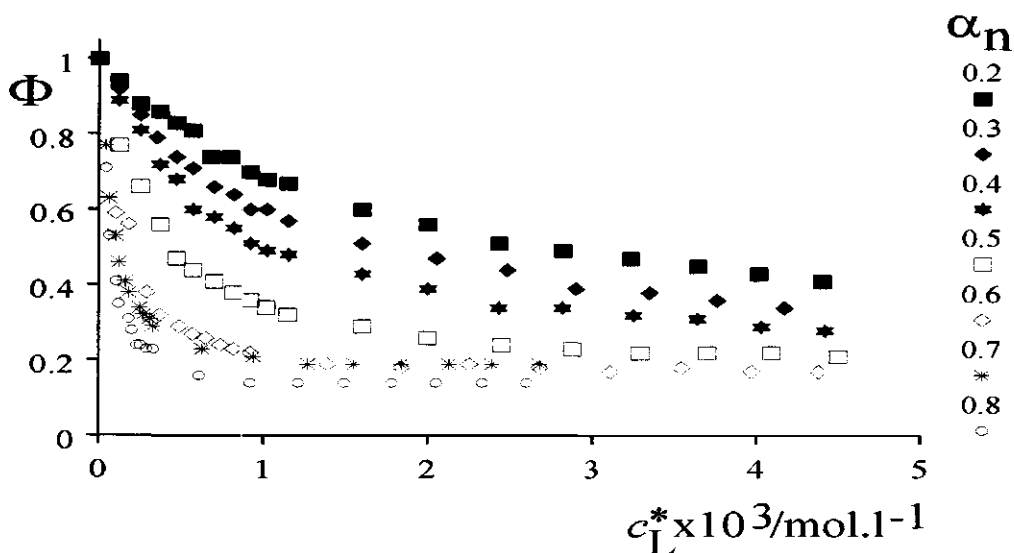

Figure 5.8: Stripping voltammetric complexation curves for the Zn(II)/PMA system for different degrees of neutralization (α_n). $[Zn(II)]=10^{-6}$ mol.l^{-1}; $[KNO_3]=0.01$ mol.l^{-1}.

Hence, analysis of the complexation curves according to equation (3.11) is justified. For the calculation of the stability from the potential shift, the final five points of the complexation curve have been used. The resulting values for K are presented in table 5.6. The log K values obtained from ΔE_{peak} values are very similar to those found from the Φ vs. c_L^* curves.

Table 5.6: Stabilities K obtained from Φ and ΔE_{peak} values for the Zn(II)/PMA system for different degrees of neutralization (α_n). [Zn(II)]=10^{-6} mol.l^{-1}; [KNO$_3$]=0.01 mol.l^{-1}; p=2/3.

α_n	log K (from Φ)	log K (from ΔE_{peak})
0.2	3.92	4.0±0.1
0.3	4.13	4.2±0.1
0.4	4.31	4.3±0.1
0.5	4.69	4.8±0.1
0.6	5.20	5.2±0.1
0.7	5.30	5.3±0.1
0.8	5.54	5.7±0.1

Finally, stabilities K of the Zn(II)/PMA complexes are plotted vs. the degree of neutralization in figure 5.9. It seems that there is an approximately linear increase of the stability with increasing α_n. This finding is in agreement with the results of normal pulse polarographic experiments for the Zn(II)/polyacrylate complex [12]. The linearity might suggest a simple regime of the relationship between α_n and the potential at the metal binding site. From an electrostatic point of view, an increase of the stability with increasing α_n is expected, since the latter is correlated to the charge density of the polyion. According to equation (2.3), ξ increases with decreasing average distance between the charged monomers (l). For fully deprotonated PMA ($\alpha_n=1$), l is approximately 0.24 nm [5], which is well below the Bjerrum length. For the present conditions, where [KNO$_3$]=0.01 mol.l^{-1} and in large excess over the ligand concentration, the reciprocal Debije screening length (κ^{-1}) will be fairly constant for the considered range of α_n and is in the order of 1 nm^{-1}. For smaller values of α_n, l increases and hence, the charge density decreases. However for the range of α_n values covered, κl varies between some tenths and unity, implying a strong electrostatic interaction among the binding sites. It should be noted that in terms of a two-state approximation, for very small values of α_n, i.e. smaller than approximately 0.2, ξ becomes smaller than 0.5 and thus, the dependency of α_n on the stability K may be expected to be less pronounced. We add that measurements are rather difficult to perform in this region of α_n, and hence, validation of the theoretical prediction is not possible with the present experimental method.
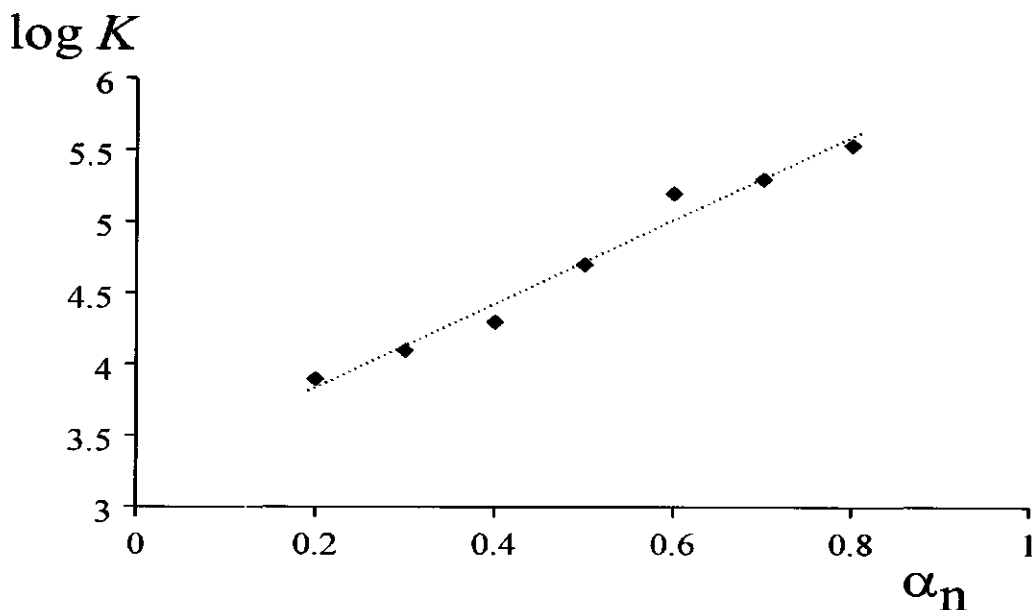
Figure 5.9: Dependence of the stability K obtained from for the Zn(II)/PMA system on the degree of neutralization with $[Zn(II)]=10^{-8}$ mol.l^{-1} and $[KNO_3]=0.01$ mol.l^{-1}.

5.3.2.5 Homogeneity

As discussed in chapter 3, the heterogeneity of the metal/complex system with respect to the metal affinities of the binding sites can in principle be obtained by varying the metal-to-ligand concentration ratio for one ligand concentration, which is always $\gg c_{m_T}$. In order to examine the heterogeneity or, in the present case rather the homogeneity of heavy metal/PMA complexes, we have measured complete complexation curves for different total concentrations of the heavy metal ions but in a range of comparable ligand concentrations. Figures 5.10a and 5.10b show stripping voltammetric complexation curves for the Zn(II)/PMA system and the Cd(II)/PMA systems for different total metal ion concentrations with $\alpha_n=0.8$. The KNO$_3$ concentration is 0.01 mol.l^{-1} and 0.1 mol.l^{-1}, respectively. The shapes of the various curves compare well indicating similar stabilities independent of the metal-to-ligand ratio. Table 5.7 collects the corresponding K values. The stability K appears to be fairly constant over the range of metal ion concentrations employed. Hence, it can be concluded that, at least in the initial range of
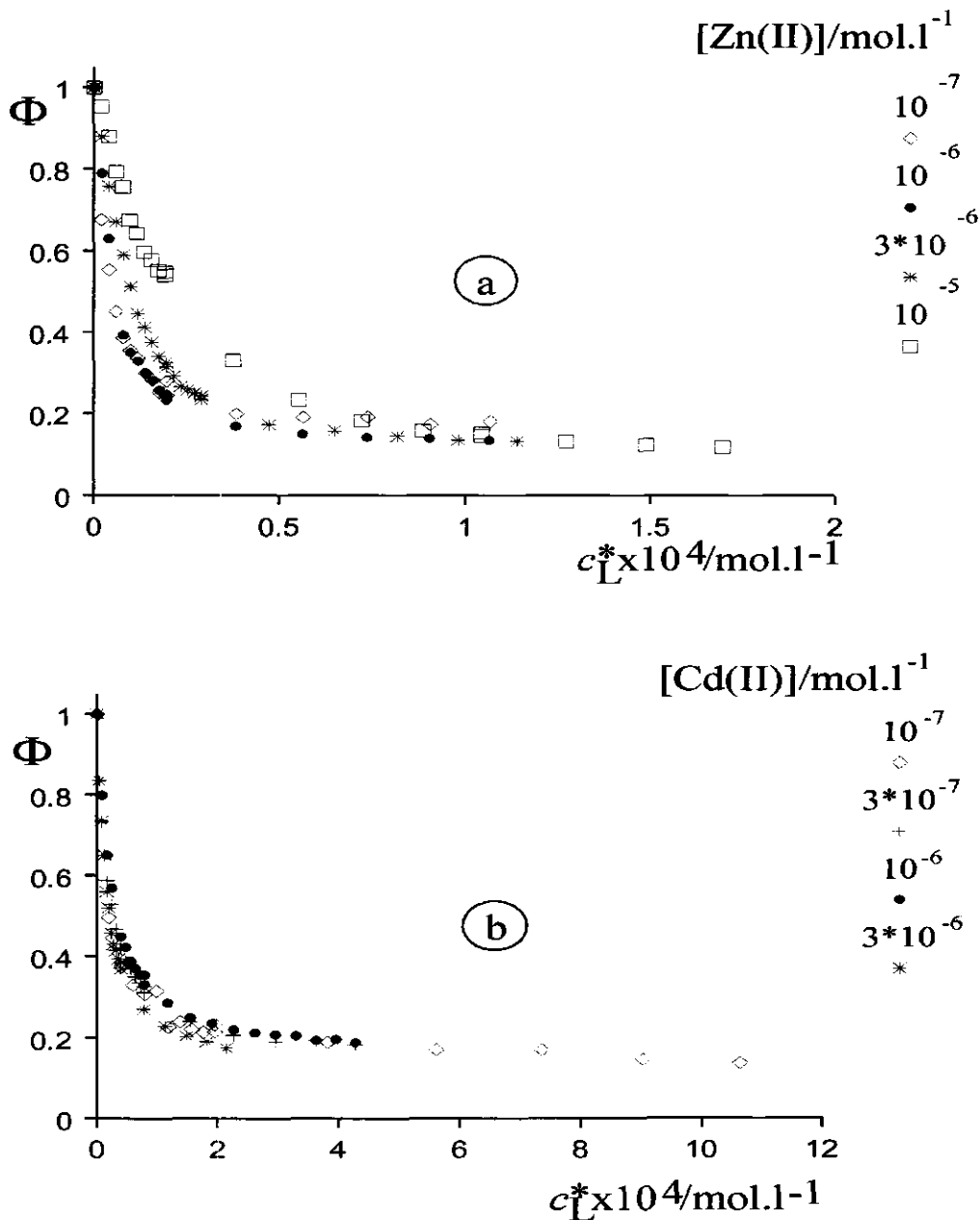
Figure 5.10: Stripping voltammetric complexation curves for the Zn(II)/PMA system (a) and the Cd(II)/PMA system (b) for different total concentrations of the metal ions with $[KNO_3]=0.01$ mol.l^{-1} and $[KNO_3]=0.1$ mol.l^{-1}, respectively, and $\alpha_n=0.8$.

metal-to-ligand ratios, these heavy metal/polymethacrylate complexes have a homogeneous affinity distribution. This is in line with expectation, since these macromolecules consist of only one repeating chemical binding site, i.e. the carboxylate group.

Table 5.7: Stabilities K obtained from Φ values for the Zn(II)/PMA system and the Cd(II)/PMA system for different total concentrations of the metal ions with $[KNO_3]$=0.01 mol.l^{-1} and $[KNO_3]$=0.1 mol.l^{-1}, respectively, and α_n=0.8. (p=2/3)

$[Me(II)]_T$	$\log K$ (Zn(II))	r^2	$\log K$ (Cd(II))	r^2
$1*10^{-7}$	5.65	0.991	5.02	0.993
$3*10^{-7}$	n.d	n.d.	4.91	0.999
$1*10^{-6}$	5.54	0.982	4.81	0.998
$3*10^{-6}$	5.30	0.971	4.65	0.996
$1*10^{-5}$	4.96	0.975	n.d.	n.d.

n.d.: not determined

5.5 References

1. H.G. de Jong, J. Lyklema and H.P. van Leeuwen, Biophys. Chem., 27 (1987) 173.
2. IMSL Library, Edition 9.2 IMSL, Houston 1984.
3. M. Rinaudo and M.Milas, C.R. Acad. Sc. Paris Série C, 271 (1970) 1170.
4. M. Satoh, T. Kawashima and J. Komiyama, Biophys. Chem. 31 (1988) 209.
5. W.P.J.T. van der Drift, PhD Thesis, State University, Utrecht 1975.
6. G.S. Manning, Q. Rev. Biophys., 11 (1978) 179.
7. M.D. Paulsen, C.F. Anderson and M.T. Record, Jr., Biopolymers, 27 (1988) 1249.
8. J.M. Díaz-Cruz, M. Esteban, M.A.G.T. van den Hoop and H.P. van Leeuwen, Anal. Chem., 64 (1992) 1769.
9. W.L. Lindsay, Chemical equilibria in soils, John Wiley & Sons, New York, 1979.
10. M. Esteban, H.G. de Jong and H.P. van Leeuwen, Int. J. Environ. Anal. Chem., 38 (1990) 75.
11. R.S Koene, T. Nicolai and M. Mandel, Macromolecules 16 (1983) 227.
12. R.F.M.J. Cleven, PhD Thesis, Agricultural University, Wageningen 1984.

Pretreatment and characterization of humic acids

6.1 Introduction

In the present chapter we describe (i) a pretreatment procedure for humic substances and (ii) a fractionation methodology based on the solubility characteristics of the humic substances. The resulting material will be denoted as humic acids, purely on an operational basis. Since this thesis is concerned with the interaction of metal ions with naturally occurring polyacids, the humic acid will be characterized in terms of the amount of chargeable groups. Additional information is given with respect to the pH, the conductance and the concentration of the humic acid solutions. The relation between the voltammetric current and the speciation of metal-macromolecular complexes is (largely) dependent on the diffusion coefficients of the free and the bound metal, as described in detail in chapter 3. The diffusion coefficient of the complex is a function of its size and, hence, in some way related to its molar mass. It seems therefore useful to also characterize the humic acids in terms of molar mass distribution and to compare different fractions with different molar mass distributions. For this purpose, we have used flow field-flow fractionation.

6.2 Materials

The humic acids used were commercial samples from Fluka (lot/product number 35069 288/53680), Aldrich (7901816/H1,675-2) and Roth (0411737/7821). Titrisol potassium hydroxide solutions, barium hydroxide, Titrisol hydrochloric acid solutions (all from Merck) and nitric acid solutions (from Baker) were of analytical-reagent grade. The exact barium hydroxide concentration was determined by conductometric titration with hydrochloric acid. All solutions were prepared using demineralized tap water, produced by a Millipore Super-Q reverse osmosis system. After removing CO_2, the conductivity of this water never exceeded 0.6 $\mu S.cm^{-1}$.

6.3 Pretreatment of humic acids

The procedure is largely analogous to that described previously [1]. To prepare a stock solution, 2.5 g of humic acid was added to 1 litre of decarbonated water. The pH of this solution was set at 9.0 by adding 0.1 mol.l^{-1} potassium hydroxide solution and stirred under nitrogen for 24 h. The pH was then reduced to 3.0 by slowly adding 1 mol.l^{-1} nitric acid under continuous stirring. After stirring the solution for 24 h, the resulting precipitate was removed by centrifugation at 7500 rpm for 45 min. The pH of the supernatant was increased to 7 to prevent further coagulation. At this pH, humic acids have the greatest chemical stability [2,3]. The resulting humic acid solution was stored in the dark at 4°C under nitrogen.

Before use, the stock humic acid solution was treated with AG 50W-X4 ion exchanger (Bio-Rad) to transfer the material into the acid form. The solution obtained was dialyzed against pure water, using Spectrapor tubing dialysis with a molar mass cut-off of 1,000. Dialysis was continued until the conductivity of the refreshed dialysate remained constant. The concentration of chargeable groups in the final stock solution was determined by conductometric titration with Ba(OH)$_2$ and is, for convenience, expressed as moles of carboxylic groups per litre. For detailed information on the conductometric titration procedure the reader is referred to chapter 7. The results are typical for humic acids. For example, for Aldrich humic acid Kim *et al.* [4] have found a proton exchange capacity of 5.43±0.16 mmol.g^{-1} by direct potentiometric titration, which is comparable to our results of 5.3 mmol.g^{-1}. The final stock solution was stored in the dark at 4°C under nitrogen. In table 6.1 some characteristics of the final stock solutions (acid form) are presented for the three different humic acid samples.

Table 6.1: Some characteristics of the humic acid stock solutions (acid form).

	Fluka	Aldrich	Roth
concentration (g.l^{-1})	1.7	0.8	1.8
pH	3.15	3.44	3.04
K$_s$ (μS.cm^{-1})	530	376	627
[COOH] (mol.l^{-1})	7.1*10^{-3}	4.2*10^{-3}	8.7*10^{-3}

To check the effectivity of the ion exchange and dialysis in the pretreatment procedure, stock solutions of the Fluka humic acid sample were analyzed for a variety of elements before and after the final treatment step (see table 6.2). To that end, 30 ml of both stock solutions were

concentrated by evaporation and then destructed with a solution containing a mixture of H_2SO_4-Se-salicylic acid-H_2O_2. The remaining solution was analyzed for N and P by spectro-photometry, K and Na by atomic emission spectroscopy, Mg, Mn and Ca by atomic absorption spectroscopy. The experiments were performed in duplicate. Table 6.2 collects the results. The comparison of each elemental concentration in the Fluka humic acid solution before and after ion exchange and dialysis illustrates that for a majority of the impurities the concentrations are substantially reduced. Although Al and Fe are not analyzed, their concentrations are not expected to be high in the Fluka humic acid sample (in its acid form). Using a comparable pretreatment procedure for Aldrich humic acid, Kim *et al.* [4] reported Al and Fe impurities of 35 and 360 μg per g purified Aldrich humic acid. In our case this would result in concentrations of 0.05 to 0.5 mg.l^{-1}. Furthermore, detailed analysis of the conductometric titration curve indicates impurity levels of only a few μS.cm^{-1}. Taking the known impurities of table 6.2 into account, a concentration of 1.5 mg.l^{-1} Al can be deduced for the present sample using the worst case approach. Hence, it can be concluded that the concentrations of the inorganic metal impurities remaining in the Fluka humic acid sample are very small compared to those of the chargeable groups of the sample, i.e. approximately 2% for the alkali metals and about 1% for the alkaline earth metals. Finally, the Fluka humic acid sample appears to contain about 2.4% of nitrogen, which is within the range of 2-6% as observed in the literature [5].

Table 6.2: Element analyses of the Fluka humic acid sample before and after the ion exchange and dialysis treatment. All concentrations are given in mg.l^{-1}.

	N	P	K	Na	Mg	Mn	Ca
before	107.5±4.2	4.82±0.29	327.3±9.3	138.8±2.7	1.46±0.01	<0.01	24.8±2.6
after	40.4±2.6	0.23±0.01	1.3±0.1	1.6±0.1	0.39±0.01	<0.01	1.0±0.1

6.4 Fractionation of humic acids

Fractionation procedures for humic acids are based on differences with respect to (i) solubility as a function of pH, by salting-out, addition of metal ions or organic solvents, (ii) molecular size by using gel permeation chromatography, ultrafiltration, centrifugation, or field flow fractionation, (iii) charge characteristics by using electrophoresis, electrofocusing or ion exchange and (iv) on adsorption by using different types of sorption surfaces [6]. The purpose of our fractionation of humic acids is to obtain different ranges of molecular sizes in order to

study the stability of the metal-complex system as a function of its molecular size. We note that the diffusion coefficient of the complex will decrease with increasing molecular size and, hence, affect the voltammetric current-speciation relationship as explained in detail in chapter 3. Therefore, it seems rather obvious to use one or more techniques as cited under (ii). However, most of these procedures work well only for small volumes (10-100 µl) [e.g. 7] or low concentrations of humic acids (10-200 mg.l^{-1}) [e.g. 8]. Unfortunately, in our approach we have to deal with rather large volumes for conductometric charge characterization and fairly high concentrations to keep the amount of aliquots added in the voltammetric experiments limited. Considering these aspects, we have chosen to fractionate the humic acid samples by pH variation. This procedure is rather crude in terms of separating different molecular sizes, but quick and easy and allows us to handle large amounts of material. Furthermore, it is very often used to fractionate humic material into three main operationally defined classes, viz. (i) humin, (ii) humic acid and (iii) fulvic acid. The first fraction is insoluble in acidic and alkaline media, whereas humic acid is soluble in alkaline but insoluble in acidic media. Fulvic acid is soluble in both alkaline and acidic media. Although this procedure has been extensively used for the fractionation of humic material into the three main fractions, detailed information on the fractional dissolution of humic substances as a function of pH is very scarce [9].
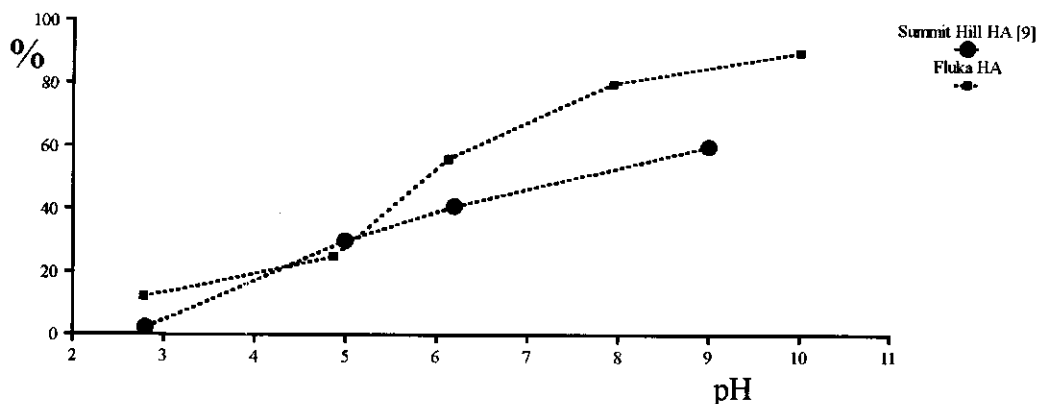

Figure 6.1: Solubility of Fluka humic acid as a function of pH expressed in mass fraction. Data for Summit Hill humic acid at [KNO$_3$]=0.1 mol.l^{-1} are taken from the literature [9].

200 ml of a 1.5*10^{-3} mol.l^{-1} nitric acid solution was added to 0.75 g of solid Fluka humic acid. After stirring the solution for 24 h, the resulting precipitate was centrifuged at 7500 rpm for 45 min. The pH of the supernatant appeared to be 2.78. Further treatment of this first fraction (F1) is described below. The deposit was dried at 40°C to obtain gravimetrically the mass of the

remaining humic acid. This solid fraction was dissolved in 200 ml of Millipore-Q-water by increasing the pH to 4.85 by adding 0.1 mol.l^{-1} potassium hydroxide solution. The resulting solution (F2) was treated in exactly the same way as described for the first fraction. This procedure was repeated for two further pH values, viz. 6.10 (F3) and 7.95 (F4). In addition, to acquire information about the maximum soluble amount of the solid Fluka humic acid, 0.75 g was added to 200 ml of 0.1 mol.l^{-1} KOH. This solution was treated as before. The cumulative solubility of the Fluka humic acid, expressed in mass fraction of the initial material as a function of pH is summarized in figure 6.1. The solubility of Fluka humic acid increases with increasing pH in agreement with many earlier observations. For comparison, solubility data for Summit Hill humic acid at [KNO$_3$]=0.1 mol.l^{-1} [9] are included in figure 6.1.

The first three fractions (solutions) were dialyzed against pure water, using Spectraor tubing with a molar mass cut-off of 1,000. Dialysis was continued until the conductivity of the refreshed dialysate became smaller than 6 μS.cm^{-1}. The humic acid fraction solutions were then transferred into the acid form as described before and finally dialyzed again. Concentrations of chargeable groups were determined by conductometric titration. Table 6.3 collects some characteristics of the three final fractions.

Table 6.3: Some characteristics of three Fluka humic acid fractions as obtained by an acid solubility procedure.

	F1	F2	F3
dissolution pH	2.78	4.85	6.10
pH of the pure solution	4.52	3.74	2.95
K$_s$ (μS.cm^{-1})	133	238	693
[COOH] (mol.l^{-1})	0.5*10^{-3}	1.8*10^{-3}	5.4*10^{-3}

6.5 Molar mass distribution

The molar mass distributions of the humic acids and the humic acid fractions used in this study were determined by using flow field-flow fractionation. These analyses were performed at the Water Studies Centre of the Monash University, Caulfield East, Australia. For an excellent review on the use of field-flow fractionation techniques to characterize aquatic particles, colloids and macromolecules the reader is referred to ref. [10]. A detailed description of the analytical procedure is given by Beckett et al. [11]. In short, the technique includes the following technical details.

Samples were introduced through an injection valve with a 20μl loop and allowed to flow down the channel over a short distance. A schematic representation of the flow field-flow-fractionation channel is shown in figure 6.2 for illustration. The channel flow was stopped while the crossflow was maintained, allowing about 1.5 times the channel void volume of solvent to pass. The channel flow was then resumed. The channel and field flow rates were maintained at approximately 3 ml.min^{-1}. The samples were detected spectrophotometrically at a fixed wavelength of 254 nm and recorded at a chart recorder. The chart recorder output was digitized using a Hewlett Packard plotter and the program GRAPHPAD [12].
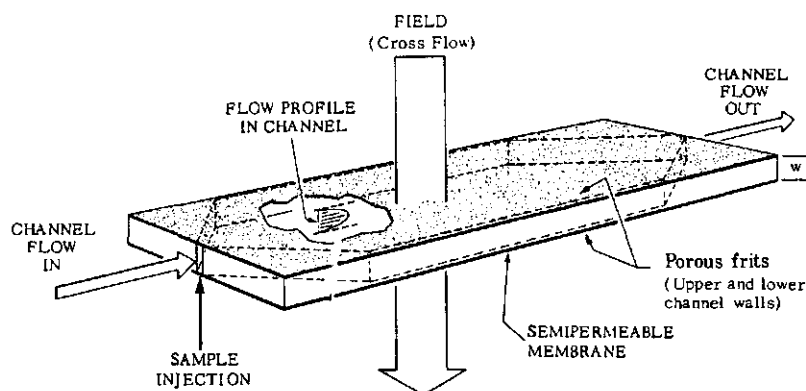

Figure 6.2: Schematic representation of the flow field-flow-fractionation channel [7].

The carrier solvent contained 0.05 mol.l^{-1} tris(hydroxymethyl)aminomethane (TRISMA, Aldrich), 0.0268 mol.l^{-1} HNO$_3$ and 0.00308 mol.l^{-1} NaN$_3$. The pH of the carrier was found to be 7.8. The humic acid samples were dissolved in the TRISMA buffer to give solutions of about 0.25 mg.ml^{-1}. A molar mass calibration procedure was performed using poly(styrenesulfonate) standards (4,500, 6,500, 17,500 and 31,000 Daltons) with a concentration of 1 mg.ml^{-1}, obtained from Polysciences Inc. The flow field-flow fractionation equipment has been described elsewhere [11].

In figures 6.3a-c, three sets of fractograms are presented. Figures a, b and c refer to the set of poly(styrenesulfonate) standards, the unfractionated humic acid samples (Fluka, Aldrich and Roth) and the Fluka humic acid fractions, respectively. The ordinate axis is proportional to absorbance of 254 nm UV radiation. The abscissa axis gives the retention volume, which is approximately inversely proportional to the diffusion coefficient, which, in turn, is a nonlinear function of the molar mass. This means that an increase in retention volume indicates an increase in molar mass, which is clearly illustrated by the fractograms of the poly(styrenesulfonate) standards in figure 6.3a. The fractograms for the Fluka, Aldrich and Roth humic acid samples are quite similar with respect to shape and appearance of the peak maximum. Hence, one might expect comparable molar mass distributions for the three humic acid samples. In figure 6.3c, fractograms of the fractionated Fluka humic acid samples F1, F2 and F3 are presented. Here, the shapes of the fractograms and the positions of the peak maxima are different for the three samples. Thus, from the fractionation of the Fluka humic acid by variation of pH, samples are obtained, which have indeed different molar mass distributions.

For the conversion of fractograms into molar mass distributions, we follow the procedure as described in detail by Beckett et al. [7]. Starting point is the relationship between the retention ratio R and the FFF retention parameter λ by the expression for constant channel flow rate [13]:

$$R = \frac{V^0}{V_r} = 6\lambda\left(\coth\frac{1}{2\lambda} - 2\lambda\right) \tag{6.1}$$

where V^0 is the channel void volume and V_r is the sample retention volume. The channel void volume was estimated from the elution volume required to produce the initial detector response [11] and appeared to be 1.8 ml. For flow FFF, λ is related to the diffusion coefficient of the sample molecules D which in turn can be calculated from [14]

$$D = \frac{V_c' w^2 \lambda}{V^0} \tag{6.2}$$

where V_c' is the volumetric flow rate across the channel (field) and w is the channel thickness (0.0254 cm).
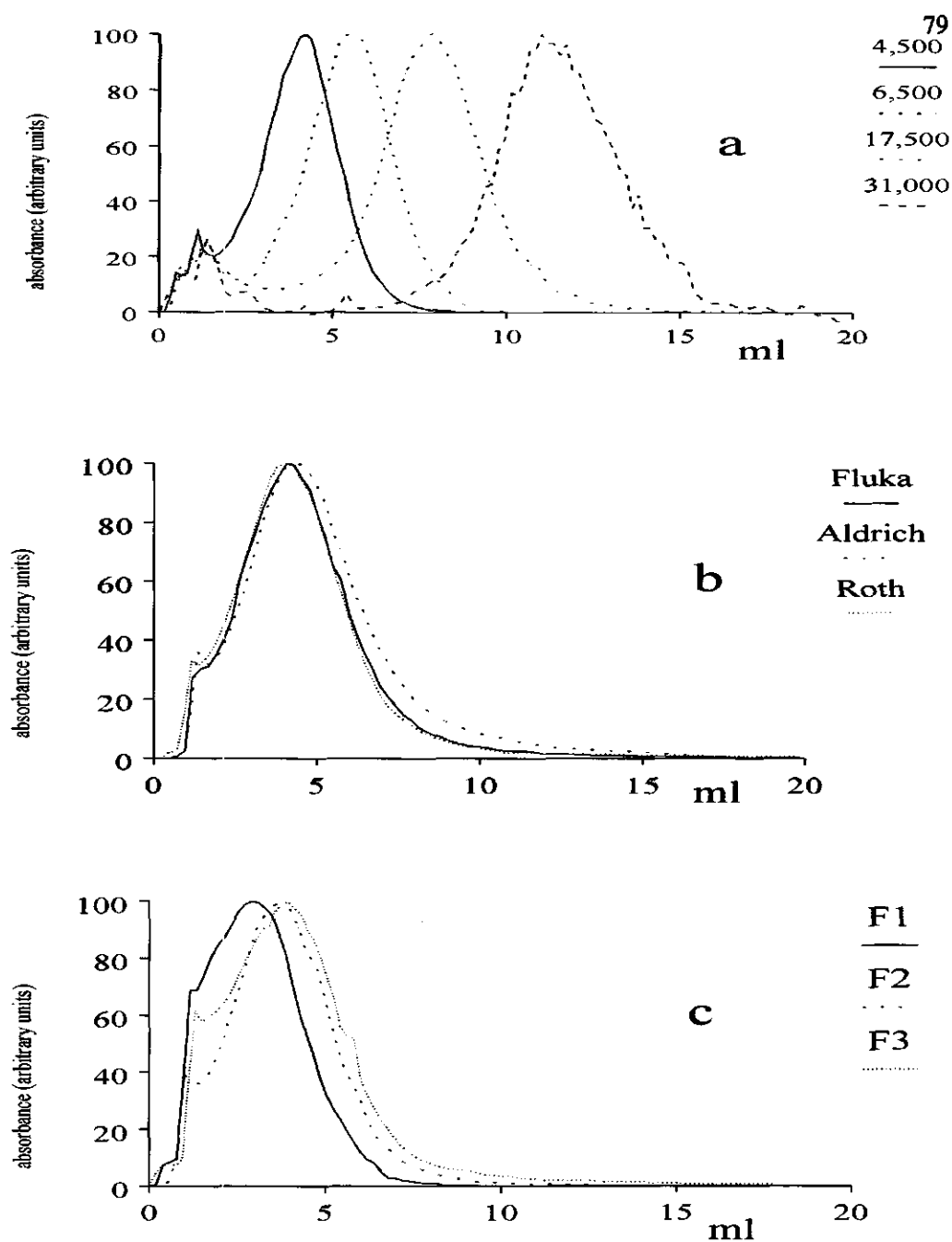
Figure 6.3: Flow FFF fractograms of poly(styrenesulfonate) standards (a), unfractionated Fluka, Aldrich and Roth humic acid samples (b) and fractionated Fluka humic acid samples F1, F2 and F3 (c). The ordinate is proportional to the UV absorbance at 254 nm.

The relationship between D and molar mass is complicated by a dependence of D on the molecular conformation which may change with solution conditions such as pH and ionic strength. For many macromolecules the molar mass M can be obtained from D using the empirical expression [15]

$$\log D = \log A - b \log M \qquad (6.3)$$

where A and b are constants for a given sample, solvent and temperature. For the present experimental set-up and the poly(styrenesulfonate) samples the constants A and b appeared to be $8.19*10^{-5}$ and 0.464, respectively. Beckett *et al.* [7] have shown that poly(styrenesulfonate) samples are appropriate molar mass standards for humic acids.

With the calibration procedure outlined above, the abscissa axis of the fractograms in figure 6.3 were rescaled to molar mass. The ordinate axis was converted into a frequency function by multiplying the original one by $\Delta V_i/\Delta M_i$, where ΔV_i is the difference between the elution volume (minus the extra column dead volume) for consecutive digitized points and ΔM_i is the corresponding difference in molar mass for the same points. Furthermore, since at low elution volumes the void peak interferes with the true sample signal and the resolution is poor in this region, points corresponding to molar masses less than 300 were neglected. Each distribution was normalized so that the total area under the curve between the minimum (300) and maximum molar mass values was set to 100.

In figures 6.4a and 6.4b, the resulting molar mass distributions are presented for the unfractionated humic acids (Fluka, Aldrich and Roth) and the fractionated Fluka humic acid samples (F1, F2 and F3), respectively. The Fluka, Aldrich and Roth humic acid samples appear to have quite similar molar mass distributions, with a peak maximum close to 5,000 Dalton. Furthermore, a substantial part of the samples (20 to 30%) consists of molecules with a molar mass larger than 10,000 Dalton. For the fractionated Fluka humic acid samples a different pattern arises. First, for the fractions F1 and F2, the curves no longer contain distinct peaks. Here the distributions decrease continuously from low to high molar mass. Second, less molecules with a molar mass larger than 10,000 Dalton are present compared to the original unfractionated Fluka humic acid sample. Instead, these samples contain a larger fraction of molecules with a lower
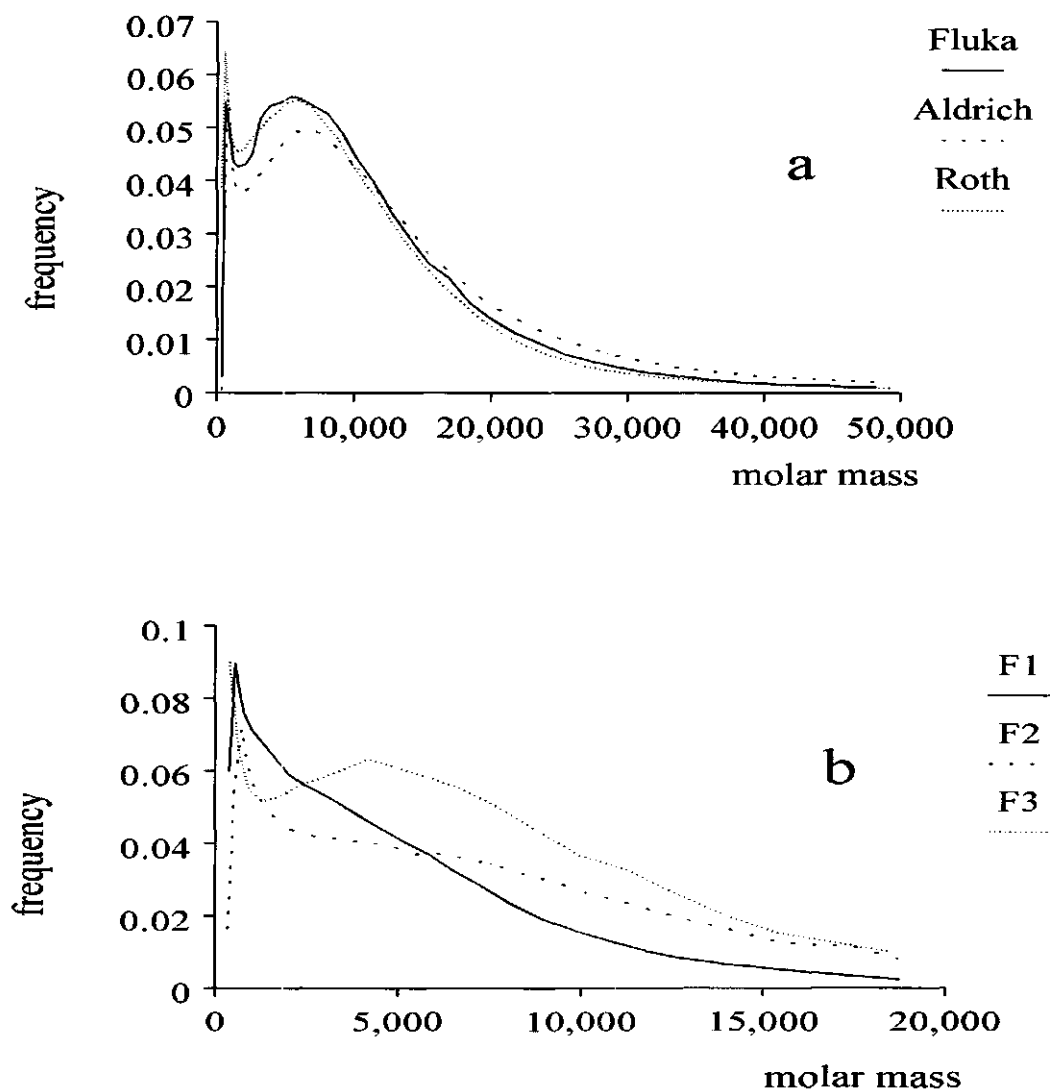
Figure 6.4: Molar mass distributions of unfractionated Fluka, Aldrich and Roth humic acid samples (a) and fractionated Fluka humic acid samples F1, F2 and F3 (b) estimated from digitized flow FFF data. The lower molar mass limit is about 300. The area under the curves between two molar mass limits represents the weight fraction of the sample in that range; i.e., the total area under each curve is normalized to be 100.

molar mass. This is especially the case for fraction F1, which was extracted at the lowest pH value. Thus, although the fractionation by varying pH, results in samples with different molar mass distributions, the separation is far from ideal.

6.6 References

1. R.F.M.J. Cleven, PhD-thesis, Agricultural University, Wageningen, 1984.
2. K. Gosh and M. Schnitzer, Soil Sci., 129 (1980) 266.
3. R.L. Wershaw and D.J. Pinckney, GEol. Surv. Res. Pap., 750D (1971) D216.
4. J.I. Kim, G. Buckau, G.H. Li, H. Duschner and N. Psarros, Fresenius J. Anal. Chem., 338 (1990) 245.
5. F.J. Stevenson, Humus chemistry, genesis, composition, reactions, Wiley, New York, 1982.
6. R.S. Swift, Fractionation of soil humic substances, in G.R. Aiken, D.M. McKnight, R.L. Wershaw and P. Maccharthy (Eds.), Humic substances in soil sediment and water: geochemistry, isolation and characterization, Wiley and Sons, New York, 1985.
7. R. Beckett, Z. Jue and J.C. Giddings, Environ. Sci. Technol., 21 (1987) 289.
8. J. Buffle, P. Deladoey and W. Haerdi, Anal. Chim. Acta, 101 (1978) 339.
9. H.K.J. Powell and R.M. Town, Anal. Chim. Acta, 267 (1992) 47.
10. R. Beckett and B.T. Hart, in J. Buffle and H.P. van Leeuwen, eds., Environmental Particles vol. 2, IUPAC Environmental Analytical and Physical Chemistry Series, Lewis Publishers, Boca Raton, 1993, p. 165-206.
11. R. Beckett, F.J. Wood and D.R. Dixon, Environ. Technol., 13 (1992) 1129.
12. GRAPHPAD, ISI(R) Software, 1987.
13. J.C. Giddings, F.J. Yang and M.N. Myers, Anal. Chem., 48 (1976) 1126.
14. K.-G. Wahlund, H.S. Winegarner, K.D. Caldwell and J.C. Giddings, Anal. Chem., 58 (1986) 573.
15. C. Tanford, Physical Chemistry of Macromolecules, Wiley, New York, 1961.

CHAPTER 7

Conductometry and voltammetry of metal complexes with natural polyacids

7.1 Introduction

In the chapter 5, we have presented metal speciation data for the synthetic polyacids polyacrylic acid (PAA) and polymethacrylic acid (PMA), as obtained by conductometry and voltammetry. In this chapter, we come back to our original objective and focus on systems containing naturally occurring complexing agents. Experiments similar to the ones for PAA and PMA have been performed with commercially available humic acid samples. The pretreatment and character-ization of procedures have been described in detail in the previous chapter. The resulting metal speciation data for the humic systems will be discussed in terms of electrostatic factors, competition effects, and heterogeneity, and compared to the results for the well-defined poly-electrolytes PMA and PAA as described in chapter 5.

7.2 Experimental

7.2.1 Materials

The humic acids used were commercial samples from Fluka (lot/product number 35069 288/53680), Aldrich (7901816/H1,675-2) and Roth (0411737/7821) and treated as described in chapter 6. Titrisol potassium hydroxide solutions, Titrisol sodium hydroxide solutions, lithium hydroxide, calcium hydroxide, barium hydroxide, Titrisol hydrochloric acid solutions, potas-sium nitrate (all from Merck) and nitric acid solutions (from Baker) were of analytical-reagent grade. Stock metal standards of 10^{-4} mol.l^{-1} for Cd(II), Pb(II) and Zn(II) (as nitrates) were prepared by diluting BDH 1000 mg.l^{-1} AAS standards. The exact hydroxide concentrations were determined by conductometric titration with hydrochloric acid. All solutions were prepared using demineralized tap water, produced by a Millipore Super-Q reverse osmosis system. After removing CO_2, the conductivity of this water never exceeded 0.6 μS.cm^{-1}.

7.2.2 Equipment

The conductometric and voltammetric equipment have been described elsewhere [1,2]. The standard voltammetric settings are similar to those used in the case of the synthetic polyelectrolytes and are presented in table 5.1 under system 1.

7.2.3 Fitting procedure

In order to fit the stripping voltammetric complexation curves to theoretical predictions from equation (3.11), a FORTRAN program was developed. A basic fitting element of the program is the subroutine ZXMIN, taken from the IMSL library [3].

7.3 Results and discussion

7.3.1 Conductometry

The association of alkaline and earth alkaline metal ions with humic acid has been studied by conductometric experiments. A dilute humic acid sample (50 ml) was titrated (in steps of 50 μl) with KOH, NaOH and LiOH solutions (all 0.0100 mol.l^{-1}) for the Fluka, Roth and Aldrich samples and (in steps of 53 μl) with Ca(OH)$_2$ and Ba(OH)$_2$ solutions (both 0.0095 mol.l^{-1}) for the Fluka sample only. Furthermore, for the Fluka humic acid only, also a 10 times less diluted sample (50 ml) was titrated (in steps of 50 μl) with KOH, NaOH and LiOH solutions (all 0.100 mol.l^{-1}). Prior to these measurements, the samples were stirred and kept in a constant-temperature vessel for 60 min to achieve thermal equilibrium, while purging with CO$_2$-free, water-saturated nitrogen. All experiments were done in duplicate at $25.00 \pm 0.02°$ C.

7.3.1.1 Analysis of the titration curve

Figure 7.1a shows the conductometric titration curves for the very dilute Fluka humic acid sample using KOH, NaOH, LiOH, Ca(OH)$_2$ and Ba(OH)$_2$ solutions. In figures 7.1b and 7.1c, the corresponding conductometric titration curves are presented for the Aldrich and Roth humic acid samples, respectively. Because the titration curves with the alkali hydroxide solutions for the three humic acid samples are quite similar, we will discuss here the analysis of the titration curve of the Fluka humic acid.

The curves for alkaline metal hydroxides differ markedly from those for earth alkaline metal hydroxides, as previously found by several authors [4-9]. For the alkali metal hydroxide titration curves, three different regions may be distinguished: (A) as for any weak acid, an initial descending part of the curve which predominantly represents the neutralization of free H^+; (B) beyond the minimum, a slow increase of the conductivity owing to the increase in both the number of negatively charged groups on the HA and the concentration of free metal ions; (C) the final part of the curve, where the slope of the conductivity curve approaches the higher level corresponding to the added reagent.

To elucidate the interaction between the added cations and the humate polyion, region B of the titration curve is of primary interest. According to equation (2.25), in this region the conductivity can be completely written in terms of the fraction of free counterions and the molar conductivities of the counterion in pure solvent and the polyion. If no counterion condensation would occur ($f=1$), the slope of the titration curve in this region would increase to a constant value, determined by λ_{metal} and λ_{humate}. It is therefore helpful to carefully analyze the slope of the titration curve ($\Delta K_s/\Delta[OH]$), which is directly related to the molar conductivity of the system (see equation (2.1)). For the most diluted Fluka humic acid sample, figure 7.2 gives the first derivative of the titration curves and this clearly shows that a more or less constant value is obtained in region B. After an apparent equivalence point the slope increases again up to a value of approximately 187, 193 and 217 $S.cm^2.mol^{-1}$ for LiOH, NaOH and KOH, respectively. By way of most direct calibration, we have compared these values with the conductivities for the same hydroxides at the same concentration level. Taking KOH as the reference (for which $\lambda_{K^+}^o + \lambda_{OH^-}^o$ equals 271.1 $S.cm^2.mol^{-1}$ [10]) we found 247 and 237 $S.cm^2.mol^{-1}$ for pure NaOH and LiOH respectively, in excellent agreement with the literature data for molar conductivities at infinite dilution. On this basis it is justified to apply equation (2.1), containing λ_{metal} for infinite dilution, to the values of the slopes of HA titration curves for different cations. It also allows the direct comparison of the slopes of the titration curves in region C with the above-mentioned values for A. Application of equation (2.1) or (2.25) to the analysis of region B apparently requires that $\Lambda \rightarrow 0$ for $c_1 \rightarrow 0$. However, the experimental curves for the Fluka humic acid sample -though quite nicely linear-show distinct positive intercepts of 1.3, 2.2 and 2.9 μS/cm. This is most likely due to occasional impurities. For the Aldrich and the Roth humic acid samples, intercepts were found to be 4.2, 3.9 and 4.2 μS/cm and 1.3, 1.4 and 1.3 μS/cm, respectively.
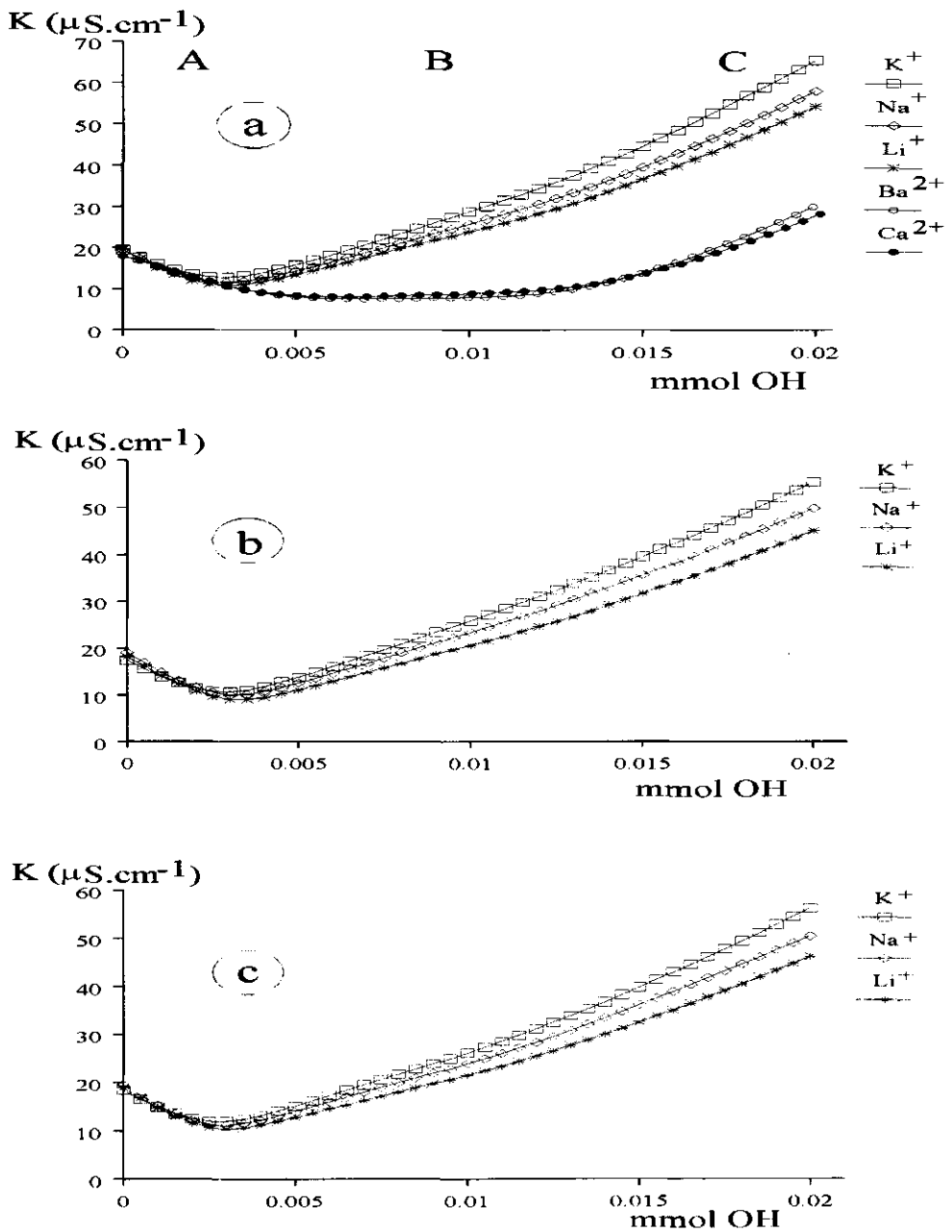
Figure 7.1: Conductometric titration curves of various humic acids for different alkaline and earth alkaline metal hydroxides: symbols (a) Fluka HA, (b) Aldrich HA and (c) Roth HA.

Since the slope of the curve is the essential parameter in our analysis, we have corrected the K_s values by subtracting the value $K_s(0)$, obtained by extrapolation to $OH^-_{added} = 0$. With the sets of Λ values thus obtained, we are in a position to analyze in more detail the nature of the interaction between metal ions and the polyion in region B. We plot Λ for several alkali metal/Fluka humic acid systems and for different stages of the titration (added OH^-) vs. $\lambda^°$ of the alkali metal ions. Figure 7.3 shows a typical set of results. Since the original titration curve is close to linear, the points for different values of added meq OH^- are almost identical. For the three monovalent ions used, a satisfactorily linear relationship between Λ and $\lambda^°_1$ is observed. We recall that analogous results were found for the model polyelectrolytes PMA (see figure 2.1) and PAA [1]. The results show that the interaction between alkali metal ions and the humate polyanion is of a purely electrostatic, non-specific nature. According to the theory, these conditions allow the calculation of λ_p and f_1. In table 7.1, the resulting values are presented for the studied humic acid samples. To illustrate the usefulness of the correction procedure with $K(0)$, table 7.1 also gives the results obtained after analysis of the uncorrected experimental Λ values. Clearly, omitting the correction would result into too high values of λ_p. For the corrected Λ values, f_1 and λ_p are found to be constant over a wide range of amounts of added hydroxide. Their values are 0.91, 0.90 and 0.98 and 78, 92 and 96 $S.cm^2.mol^{-1}$ for the Fluka, Aldrich and Roth humic acid samples, respectively.
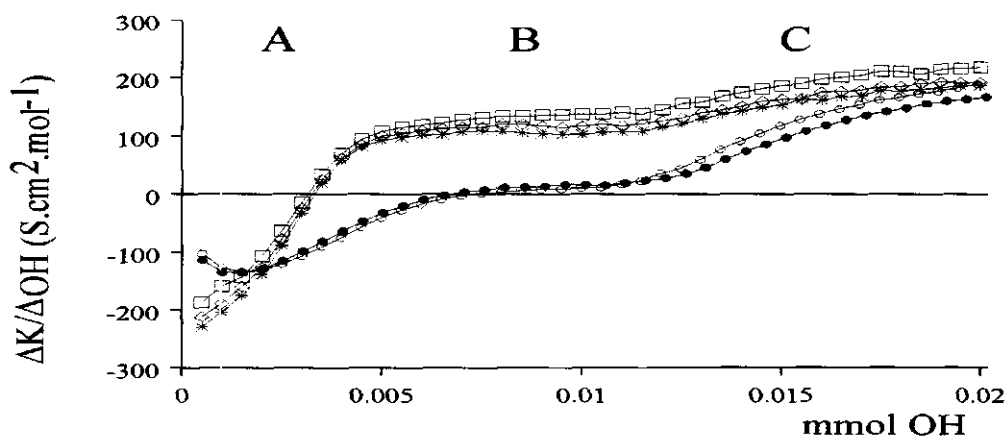

Figure 7.2: Slope of the conductometric titration curve of the diluted Fluka humic acid vs. the amount of hydroxide added for different alkaline and earth alkaline metals. Symbols as in figure 7.1.
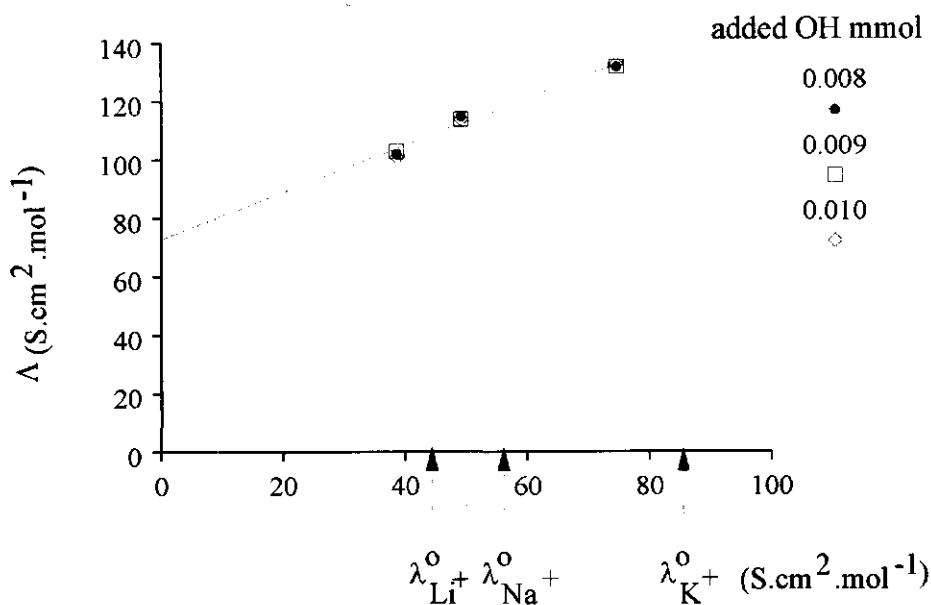
Figure 7.3: Molar conductivity of alkali Fluka humate solutions for different amounts of added hydroxide vs. molar conductivity of the corresponding monovalent counterion. The points for the different additions of hydroxide are almost identical for each ion.

For the Fluka humic acid sample, similar experiments have been performed for a 10 times less diluted sample. The conductometric titration curves (not shown) are analyzed in the same way as before. By extrapolation of the titration curves to $OH^-_{added} = 0$, intercepts were found to be 9, 21 and 21 μS/cm, respectively, which are indeed increased by approximately a factor of 10 compared to the more diluted Fluka humic acid sample. Table 7.1 collects the resulting f_1 and λ_p values, which are found to be quite constant again over a wide range of amounts of added hydroxide. Their values are 0.74 and 53 S.cm^2.mol^{-1}, respectively, and are in agreement with the results of Arai and Kumuda [11]. For comparable humic acid concentrations, they have obtained f_1 and λ_p values in the order of 0.80 and 48 S.cm^2.mol^{-1}, respectively. A decreasing value of λ_p with increasing concentration of chargeable groups is in line with the theory, as predicted for linear polyelectrolytes. According to equation (2.10), λ_p decreases with increasing concentration as a result of the increase of $|\ln\kappa'a|$. At equal stages of the titration, i.e. at comparable charge density of the humate polyion, the association of monovalent counterions with the HA seems to increase with the polyion concentration. The condensation theory, which is for dilute systems, predicts equal f_1 values for any polyion concentration at given charge density, as has been found for PMA (see figure 2.2). For the Fluka humic acid system, the range

of concentrations in terms of chargeable groups is comparable to the one of PMA in chapter 2 and, thus, the binding behaviour differs significantly from that observed in the case of PMA. This means that a two-state approach becomes less appropriate for the description of metal ion binding by the present humic acid.

Table 7.1: Molar conductivities of various humic acid samples and fractions of free counterions for different stages of the titration. For the Fluka humic acid, results for two different concentrations are presented.

OH⁻ added (mmol)	Fluka		Aldrich		Roth	
	λ_p	f_1	λ_p	f_1	λ_p	f_1
0.0080	77.0(154.9)	0.92(0.64)	93.4(129.0)	0.90(0.67)	99.5(113.0)	0.97(0.71)
0.0085	78.3(151.2)	0.91(0.65)	93.2(126.7)	0.90(0.67)	98.2(111.0)	0.98(0.72)
0.0090	78.2(145.6)	0.91(0.66)	91.6(122.9)	0.91(0.68)	98.8(111.0)	0.97(0.71)
0.0095	77.9(140.1)	0.91(0.68)	91.9(121.7)	0.90(0.68)	97.4(108.8)	0.98(0.72)
0.0100	77.4(135.3)	0.92(0.69)	92.3(120.7)	0.90(0.67)	95.9(106.6)	0.99(0.73)
0.0105	77.8(132.3)	0.91(0.70)	91.9(118.8)	0.91(0.68)	94.6(104.7)	1.00(0.74)
0.0110	77.7(128.8)	0.92(0.71)	91.2(116.6)	0.92(0.68)	94.3(103.9)	1.00(0.74)
0.080	53.6(120.5)	0.76(0.53)				
0.085	52.1(112.5)	0.76(0.55)				
0.090	55.2(115.6)	0.73(0.53)				
0.095	53.0(107.5)	0.74(0.55)				
0.100	52.9(104.3)	0.73(0.55)				
0.105	52.7(101.1)	0.73(0.56)				
0.110	53.6(100.2)	0.72(0.55)				

Values in parentheses are those which would have been obtained if no correction for K(0) were applied.

The titration curves obtained with earth alkaline metal hydroxides have quite a different appearance. Region B shows almost zero slope. From this, it can be concluded that there is a strong association of divalent counterions with the humate anions. If we approximate λ_p -by its value for monovalent counterions- 78 S.cm².mol⁻¹, it is possible to estimate the fraction of free divalent ions f_2 on the basis of equation (2.25). In figure 7.4, the resulting fractions of free divalent counterions are plotted vs. the amount of added hydroxide for the very dilute Fluka

humic acid sample. As distinct from f_1, the value of f_2 decreases systematically with increasing amounts of added hydroxide. Thus, the association with these ions increases with increasing number of deprotonated groups, that is with an increasing structural charge density.
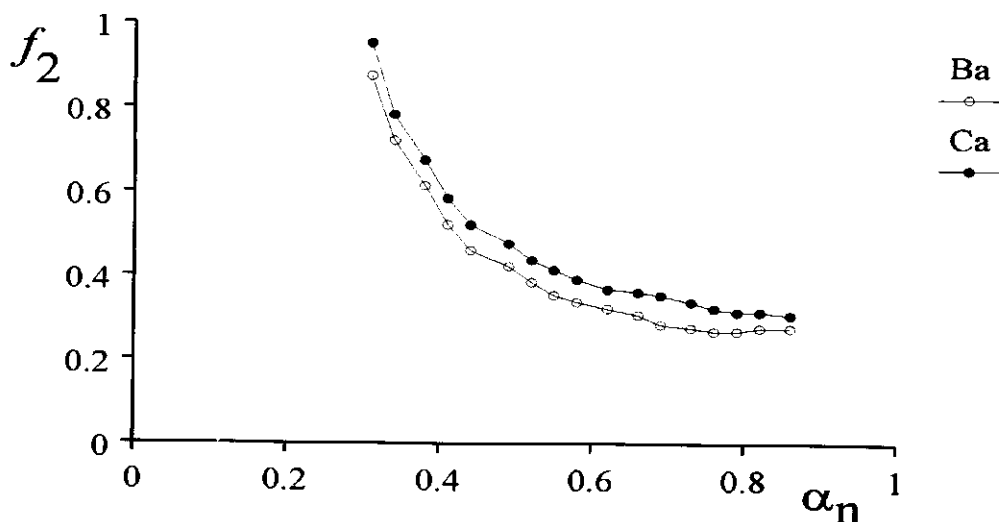

Figure 7.4: Fraction free divalent counterions vs. the degree of neutralization for the diluted Fluka humic acid.

We note that the observed difference in association behaviour between monovalent and divalent metal ions does not agree with predictions according to the counterion condensation theory. For the earth alkaline metal ions, the association with the humate polyanion may be of an intrinsic, specific nature (see also section 7.3.2.3). This assumption seems to be not unreasonable if one considers that stabilities for the association of calcium with simple complexing agents such as acetate and phtalate are found to be in the range of $10^{0.5}$ to $10^{2.5}$ l.mol^{-1} [12].

At this point it is useful to consider the complexation reaction of calcium ions with the humate polyion:

$$Ca + L \rightleftharpoons CaL$$

(7.1)
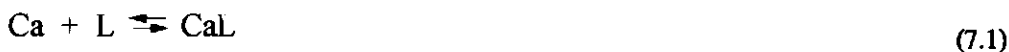
with the corresponding stability K_{Ca} defined as:

$$K_{Ca} = \frac{\overset{*}{c}_{CaL}}{\overset{*}{c}_{Ca}\overset{*}{c}_{L}} \tag{7.2}$$

where $\overset{*}{c}_{Ca}$, $\overset{*}{c}_{L}$ and $\overset{*}{c}_{CaL}$ denote the bulk concentrations of Ca, L and CaL, respectively. The stability K_{Ca} can be deduced from the conductometric speciation data presented in figure 7.4. For example, for the Fluka humic acid with $\alpha_n = 0.6$, approximately 65% of the added calcium is bound by the humate polyanion. The corresponding total amount of chargeable groups is about $2.5*10^{-4}$ mol.l^{-1}. This leads to a stability K_{Ca} in the order of 10^4 l.mol^{-1} for the calcium/humate complex. This value seems to be not unreasonable considering other reported calcium/humic material stabilities in the literature, ranging from $10^{2.6}$ to $10^{4.1}$ depending on the pH, the analytical method, the origin of the humic material and the ionic strength [13-15].

The most common way of determining the number of charged groups from conductometric titration is by extrapolation of the two linear parts of the second and third regions of the titration curve. The point of intersection would give the amount of chargeable groups in the sample. The procedure has to be carried out with care. From figure 7.2 it can be seen that a really linear section ($\Delta K_x/\Delta[OH]$=constant) is indeed observed in the region B, but not easily in region C, unless one would continue till unusually large excesses of reagent. Still, the slope seems to be lower than the theoretically expected one. Although this might indicate that some further deprotonation of very weak acidic groups takes place, there is some uncertainty in this respect. Unexpectedly low slopes are also found (i) at increased salt levels, (ii) with synthetic polyacids, which are definitely known to be fully deprotonated, and (iii) with voltammetric and even potentiometric titration curves [16,17]. Considering complexation reaction (7.1), it is more obvious that there is some increase in the association between the polyion and the counterions, caused by the increased concentration of the latter.

7.3.1.2 Comparison with a linear model polyelectrolyte

In order to compare the results for HA with the properties of a model polyelectrolyte, we performed some comparative experiments with a well-defined synthetic polyelectrolyte. In figure 7.5, the slopes of the curves for the titration of PMA with KOH at different PMA concentrations are shown. Here the equivalence point is known and hence the α_n scale is unquestionable. At low concentrations it is difficult to obtain the intersection point (no sufficiently long linear parts

are observed), but this improves at higher PMA concentrations. An important difference with the HA titration is found in region B. The PMA titration curve clearly shows a *decrease* of the slope with increasing α_n. This has been unambiguously ascribed to condensation of the monovalent counterions. Λ, λ_1^0 plots for PMA (see figure 2.1) for various charge densities show a decrease of f_1 (see figure 2.2), in reasonable accordance with theoretical predictions. Thus, we see that the behaviour of the humate polyions is different from that of the polymethacrylate. The reason for this must be connected with differences in charge density and distribution. A second indication of the different behaviour of humic polyions is provided by the value of λ_p, which was found to be 78 S.cm^2.mol^{-1} for the very dilute Fluka humic acid sample (see above). Considering that the equivalent molar mass of one chargeable group on the humic acid is about 345, the charge density on fully deprotonated humate cannot be extremely high. In terms of a linear polyelectrolyte with a diameter of 1 nm, the corresponding spacing parameter l would also be of the order of 1 nm. One can speculate about different geometrical arrangements, but with a random distribution of the charges, the order of magnitude of l will not decrease drastically.

Substituting such values into equation (2.10) for λ_p, we find 66 S.cm^2.mol^{-1} which is significantly below the experimental value. This again illustrates the limitations involved in the comparison of a linear polyion with randomly distributed charges to the humate entities in the present sample. The same is seen for the counterion binding characteristics: humic acids show hardly any association with monovalent ions, whereas divalent cations are rather strongly bound (see figure 7.4). For polymethacrylate, the difference in association between monovalent and divalent counterions is less extreme. It is too early to draw rigorous conclusions on this point. One might speculate that the overall charge density on the humate polyions is too low to give rise to binding of the low valency counterions, but that the distribution of charges is such that divalent ions are bound rather extensively. The latter might be due to the presence of salicylic-like groups on humate polyions as discussed in the previous section. For analytical purposes this feature is very attractive because the presence (or addition) of higher valency counterions leads to a sharp break in the conductometric titration curve near the equivalence point.
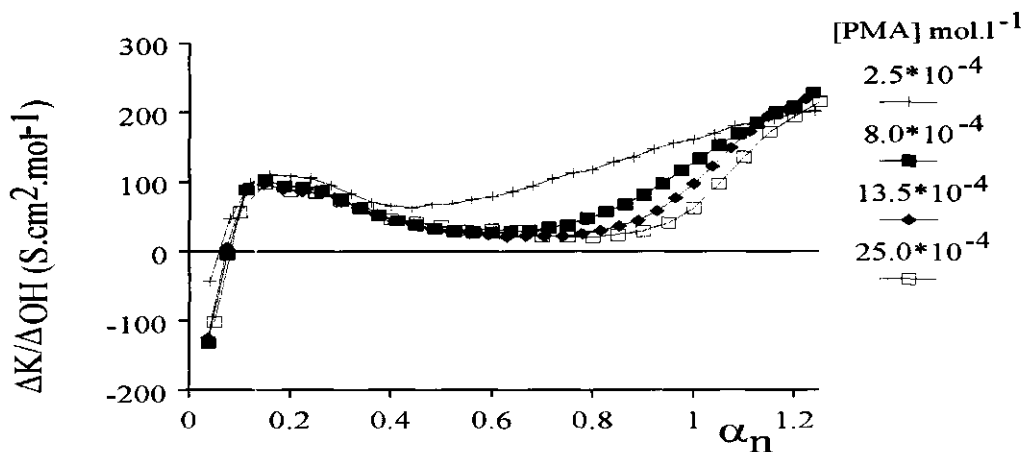
Figure 7.5: Slope of the conductometric titration curve of polymethacrylic acid with KOH vs. the degree of neutralization as a function of the PMA concentrations.

7.3.2 Voltammetry

Voltammetric complexation curves for various heavy metal/humic acid systems have been measured in order to obtain speciation data under different "environmental" conditions. Within this frame, the association of heavy metals with various humic acids has been extensively studied (i) in solutions containing an additional excess of monovalent (potassium) and divalent (calcium) counterions, (ii) for different charge densities of the humic acid by varying the degree of neutralization, (iii) for a range of total metal ion concentrations in order to investigate the chemical heterogeneity of the complexing agent and, finally (iv) for different (solubility-based) fractions of the humic acid.

The voltammetric experiments have been carried out as described in detail in chapter 3 at $25.0\pm0.2^{\circ}$C.

7.3.2.1 Shape of the voltammogram

Before presenting complexation curves for heavy metal/humic acid systems, we will first analyze the stripping voltammetric parameters (current and potential) for several steps of the experimental complexation procedure. To this end, differential pulse anodic stripping voltammograms have been measured for heavy metal solutions (i) as such, (ii) at the pH of the humic acid and (iii) in the presence of humic acid. In figure 7.6, the resulting voltammograms are shown for a solution containing Zn(II), Cd(II) and Pb(II) at total concentrations of 10^{-6} mol.l^{-1}. Series 1 shows the voltammetric responses for the initial metal ion solution at pH=3.8 and [KNO$_3$]=0.03 mol.l^{-1}. Regular shapes are obtained with peak half width $W_{1/2} \approx 60$ mV indicating reversibility of the electrode process. The pH of the second series was set close to the pH of the Fluka humic acid solution (7.4) by adding a small aliquot of KOH. The voltammetric currents for Zn(II) and Pb(II) decrease, but that for Cd(II) remains unaffected. As discussed in chapter 5, in the case of Zn(II) the decreased peak height can be interpreted as a loss of free metal ions due to adsorption onto the surface of the sample vessel. This problem and the way to overcome it are discussed in detail in chapter 3.
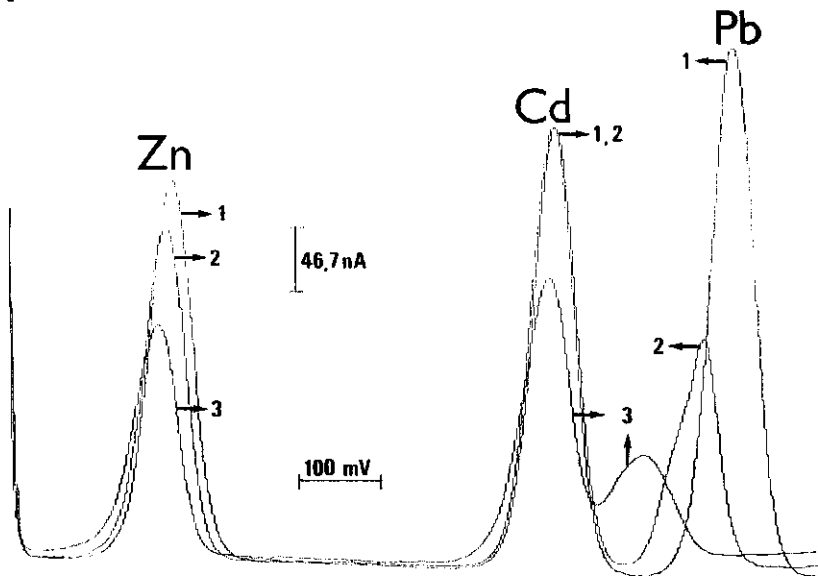

Figure 7.6: Differential pulse anodic stripping voltammograms of Zn(II), Cd(II) and Pb(II) for several steps of the experimental procedure. [Me(II)]=10^{-6} mol.l^{-1}; [KNO$_3$]=0.03 mol.l^{-1}; t_e=1 min; v_{scan}=2.5 mV.s^{-1}. Series 1; pH=3.75. Series 2; pH=7.40. Series 3; [Fluka HA]=10^{-5} mol.l^{-1}; α_n=0.8. Further explanation in the text.

In the case of Pb(II), the potential shift is significant, indicating some complexation with hydroxide (see for further discussion section 5.3.2.1). Hence, it is rather useless to measure the speciation of Pb(II) at such high pH with the experimental procedure as presented in chapter 3. Finally, the addition of Fluka HA results in a decrease of all voltammetric currents due to the association of the heavy metals with the humate polyanion (series 3). The concentration of the Fluka HA equalled 10^{-5} mol.l^{-1} expressed as the volume concentration of deprotonated groups on the HA molecules. According to equation (3.11), a larger decrease of the peak current at the same Fluka HA concentration indicates a higher stability (K) of the heavy metal/Fluka HA complex involved.

7.3.2.2 Influence of electrolyte concentration on the stability of the complexes

For various Zn(II)/humate and Cd(II)/humate systems voltammetric complexation curves are presented for different concentrations of KNO$_3$ with α_n=0.8 at a metal ion concentration of 10^{-6} mol.l^{-1} in figures 7.7a-c and 7.8a-c, respectively. The figures a, b, and c refer to the Fluka, Aldrich and Roth humic acid samples, respectively. Due to the association of Zn(II) or Cd(II) with the humate polyanion, Φ decreases and reaches a certain plateau value with increasing excess of ligand. As explained before (see chapter 5), the latter observation is a clear indication of lability of the metal complex system on the time scale of the stripping voltammetric experiment. In the case of non-lability, Φ would decrease to zero. A second indication of lability of the metal complexes involved is shown by the systematic shift of the peak potential for a sufficiently large excess of ligands (see below). From these results it can be concluded that the Zn(II)/humate and Cd(II)/humate systems are voltammetrically labile under the DPASV conditions employed. Hence, the complexation curves can be analyzed in terms of a stability K according to equation (3.11).

In table 7.2, the resulting values for the stabilities K are presented for the Zn(II)/humate and Cd(II)/humate complexes studied for α_n=0.8 using p=2/3 in the fitting procedure. The qualities of the fit are given by the value of the correlation coefficient r^2, which are quite gratifying. It should be mentioned that, as a consequence of the uncertainties of the mass transport conditions during the pre-electrolysis period, the exact value of p is unknown. However, use of p=1/2 instead of 2/3 affects the value of K by only 0.1 log units (i.e. in the order of the experimental error), which is in agreement with the results for the labile Zn(II)/PAA system (see chapter 5). This is an attractive feature since the experimental procedure is primarily aimed at obtaining stability values, and not so much at collecting values of ε.
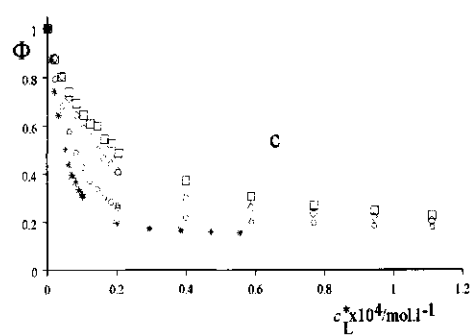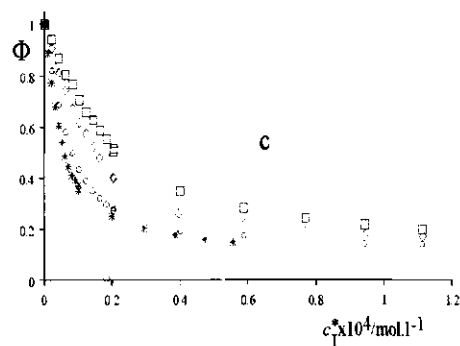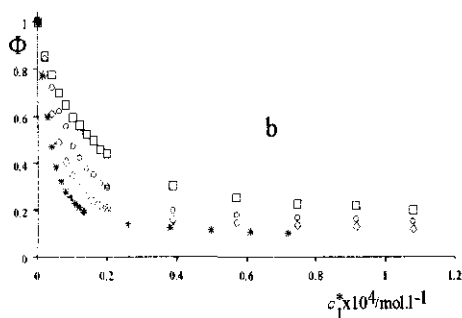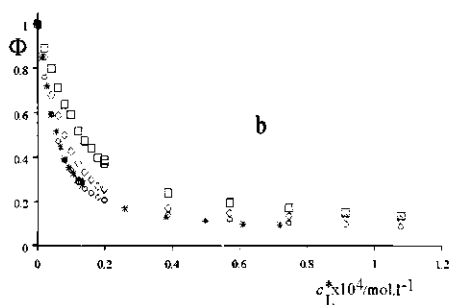
Figure 7.7: Stripping voltammetric complexation curves for various Zn(II)/humate systems for different KNO_3 concentrations. $[Zn(II)]=10^{-6}$ $mol.l^{-1}$; $\alpha_n=0.8$; (a) Fluka, (b) Aldrich and (c) Roth.
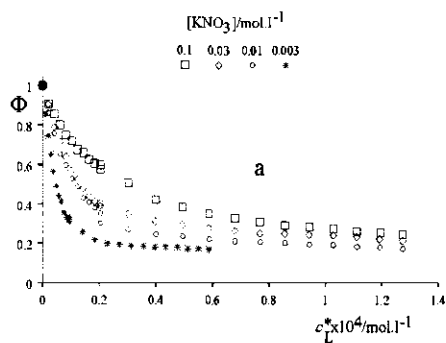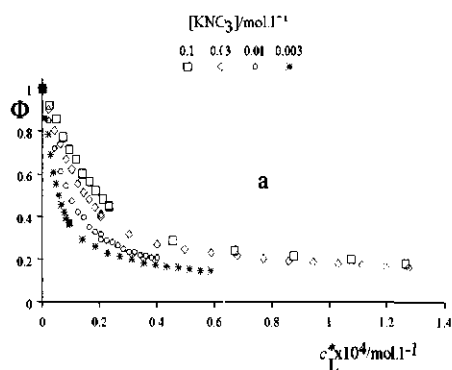
Figure 7.8: Stripping voltammetric complexation curves for various Cd(II)/humate systems for different KNO_3 concentrations. $[Cd(II)]=10^{-6}$ $mol.l^{-1}$; $\alpha_n=0.8$; (a) Fluka, (b) Aldrich and (c) Roth.

For the different types of humate polyanions, the binding of Zn(II) ions and Cd(II) ions is approximately equally strong. This is in agreement with the results of Cleven [1]. He studied the association of several heavy metals (Zn(II), Cd(II) and Pb(II)) with Fluka humics as a function of the charge density on the humate polyanion by varying the degree of neutralization (α_n) for [KNO_3]=0.05 mol.l^{-1}. In this polarographic study, comparable stabilities have been observed for the Zn(II)/humate and Cd(II)/humate systems in the range of $0.2 \leq \alpha_n \leq 0.8$, whereas the stability of the Pb(II)/humate complex was significantly larger (by about two log units) over the whole α_n range employed. On the other hand, Saha $et\ al.$ [18] have observed a significant difference between the stabilities of the Zn(II)/Fluka humate and the Cd(II)/Fluka humate complexes for [KNO_3]=0.1 mol.l^{-1}; the difference increased with increasing pH of the sample solution. The difference between different authors might be due to the heterogeneity of samples as a consequence of their origin and the kind of pretreatment procedure of the humic acid sample employed.

Table 7.2: Stabilities K obtained from Φ values for various Zn(II)/humate and Cd(II)/humate systems as a function of the concentration of KNO_3 with α_n=0.8 and [Me(II)]=10^{-6} mol.l^{-1}. K from ΔE_{peak} is given in parentheses.

[KNO_3] (mol.l^{-1})	Zn(II)			Cd(II)		
	$\log K$ from Φ	r^2	$\log K$ from ΔE_{peak}	$\log K$ from Φ	r^2	$\log K$ from ΔE_{peak}
Fluka humic acid						
0.1	4.93	0.983	(5.5)	4.80	0.999	(5.8)
0.03	5.06	0.986	(5.2)	5.16	0.987	(6.2)
0.01	5.22	0.990	*	5.21	0.990	(6.9)
0.003	5.50	0.993	(6.3)	5.62	0.981	(6.5)
Aldrich humic acid						
0.1	5.14	0.983	(6.5)	5.09	0.999	(5.8)
0.03	5.40	0.976	(6.2)	5.31	0.987	(6.2)
0.01	5.58	0.984	(6.5)	5.54	0.990	(7.0)
0.003	5.54	0.975	(6.4)	5.78	0.981	(7.3)
Roth humic acid						
0.1	4.88	0.987	(5.6)	4.98	0.999	(5.6)
0.03	5.06	0.985	(5.8)	5.10	0.992	(6.5)
0.01	4.98	0.987	(6.1)	5.43	0.977	(6.1)
0.003	5.48	0.989	(6.2)	5.57	0.981	(6.8)

* $\Delta E_{peak}>0$

From table 7.2 it can be seen that the stability of the heavy metal/humate complex decreases with increasing concentration of KNO_3, due to the reduction of the electrostatic component of the metal/polyion interaction. For the K^+/Zn(II)/PMA system, we could interpret this observation in terms of competition between the monovalent counterions (K^+) and divalent counterions (Zn(II)) for binding by the polymethacrylate anion (see chapter 4). However, earlier conductometric speciation data showed that the association of monovalent counterions with the humate polyions is practically absent. Hence, for the present humic acid systems, it is expected that the dependency of K on $[KNO_3]$ is mainly due to screening effects. Studies, which compare the competitive behaviour between monovalent and divalent counterions with theoretical predictions - e.g. from the Poisson-Boltzmann model or from the two-state approximation concept - are mainly concerned with synthetic model polyelectrolytes such as PMA [e.g. 9,19]. Experimental data on the salt concentration dependency of the stability of natural systems are very scarce. Some 15 years ago, Stevenson [20] studied very briefly the stability of several heavy metal/humate complexes as a function of the ionic strength at constant pH (4 and 5) by potentiometric titration. He observed also a decrease of the stability with increasing ionic strength, which was interpreted as the result of an increase in ionization of the humic acid at larger salt concentration.

In figures 7.9a-c and 7.10a-c, the shifts of the Cd(II) and Zn(II) peak potentials are presented as a function of the humate concentration for different KNO_3 concentrations with α_n=0.8 and $[Me]=10^{-6}$ mol.l^{-1}. Except for the Zn(II)/Fluka HA system with $[KNO_3]$=0.01 mol.l^{-1}, a decrease of the peak potential is observed with increasing concentration of the humate polyanion. The potential shift becomes more pronounced with larger excesses of ligand. As before, the calculation of the stability K from the potential shift only involves the last five points of the complexation curve for which the condition of having an extremely large excess of ligand over metal is best fulfilled. In stripping voltammetry, the condition of excess of ligand is related to the metal atom concentration in the mercury drop. For the present experimental conditions, $[M^0]$ will be increased by a factor of about 100 compared to the total metal ion concentration in solution and, hence, becomes about 10^{-4} mol.l^{-1}(Hg). Considering the fact that the humate polyanion is present in approximately comparable concentrations, the condition of excess of ligand is not obeyed. Hence, the calculation of the stability from the potential shift could lead to erroneous results. It might appear useful to make a further inspection of this by applying pseudo-polarography, i.e. stripping voltammetry at various accumulation potentials.
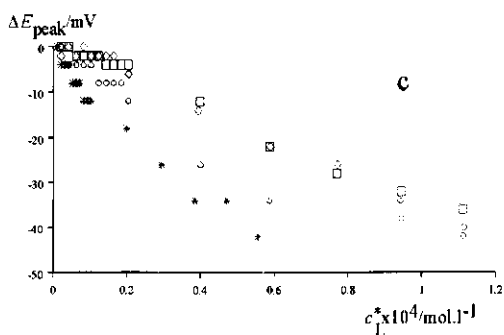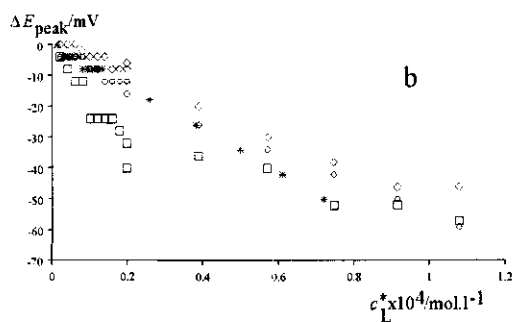
Figure 7.9: The shift of the peak potential as a function of ligand concentration for various Zn(II)/humate systems for different KNO$_3$ concentrations. [Zn(II)]=10^{-6} mol.l^{-1}; α_n=0.8; (a) Fluka, (b) Aldrich and (c) Roth.
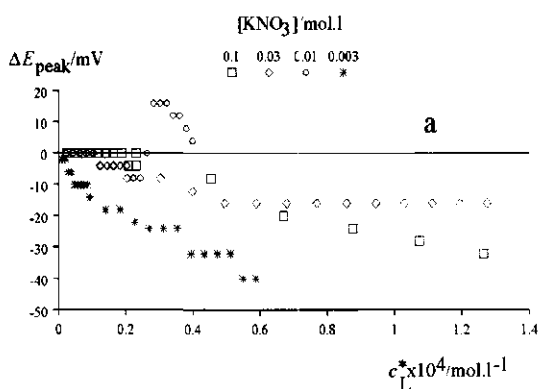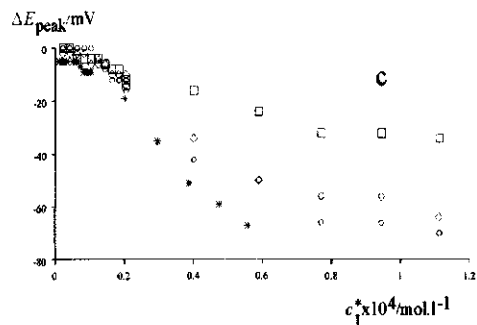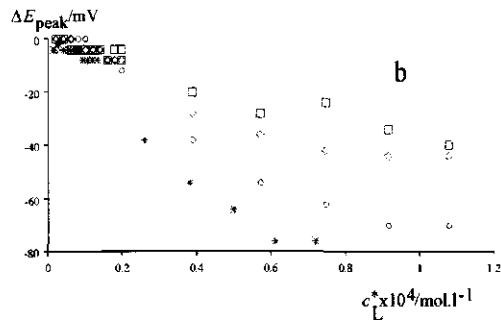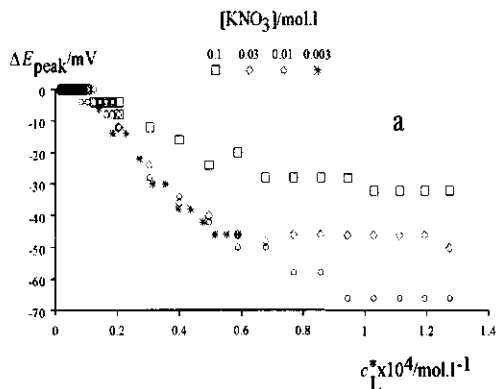
Figure 7.10: The shift of the peak potential as a function of ligand concentration for various Cd(II)/humate systems for different KNO$_3$ concentrations. [Cd(II)]=10^{-6} mol.l^{-1}; α_n=0.8; (a) Fluka, (b) Aldrich and (c) Roth.

$\log K_C$

$-\log a_{K^+}$

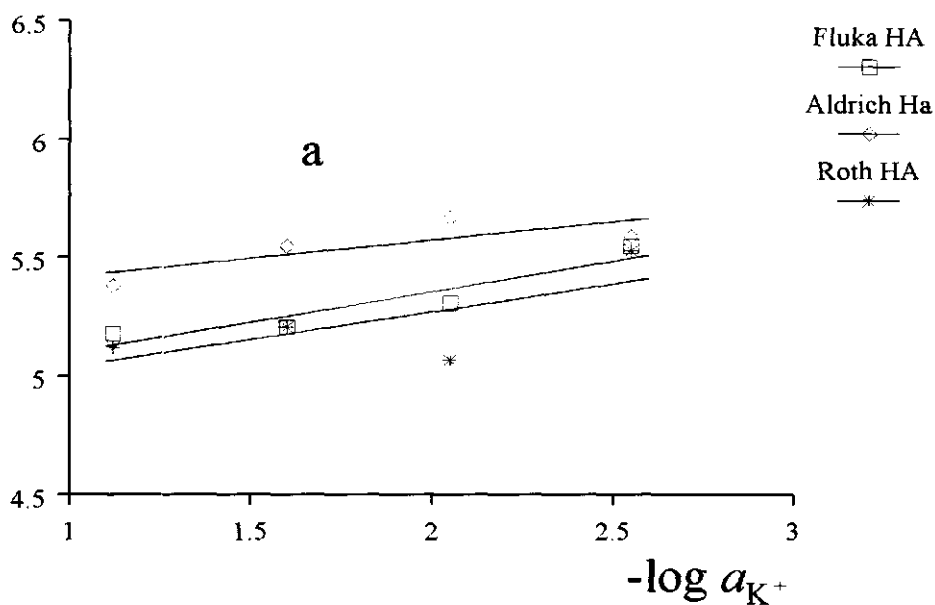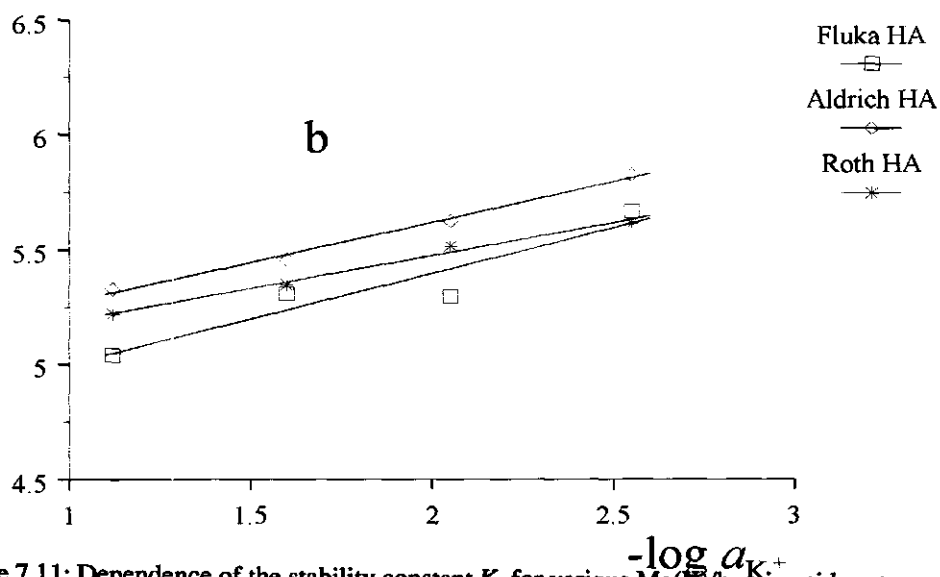$\log K_C$

$-\log a_{K^+}$

Figure 7.11: Dependence of the stability constant K_c for various Me(II)/humic acid systems on the activity of the KNO_3 for $\alpha_n=0.8$. (a) $[Zn(II)]=10^{-6}$ mol.l^{-1}; (b) $[Cd(II)]=10^{-6}$ mol.l^{-1}.

A further difference between the humate complexes and the metal-polymethacrylate complexes is found in the salt dependency of K. For the Zn(II)/PMA and the Cd(II)/PMA systems, the dependency of the stability K on [KNO$_3$] is much stronger than for the corresponding humate systems. As shown in figures 7.11a and 7.11b, log K_c (from Φ) and log a_{K^+} are approximately linearly related for the various humate systems. The values of the slopes are collected in table 7.3 and are much lower than for the corresponding Zn(II)/PMA and Cd(II)/PMA systems, which have been found to be 1.42±0.08 and 0.81±0.21, respectively (see chapters 4 and 5). The findings can be understood in terms of a lower charge density for the humate polyanion. As explained before, the mean separation between sites can be estimated to be not less than 1 nm for the Fluka HA, whereas the separation between individual carboxylate groups on the polymethacrylate is about 0.23 nm [21]. The former is well above the Bjerrum length (about 0.7 nm under the present experimental conditions), the latter is well below it. Thus, for the humic acid systems, it may be concluded that the relative weak dependency of K_c on the salt concentration does mainly reflect screening effects.

Table 7.3: Values for the slopes of the dependency of the stability constant K_c (from Φ) for various Me(II)/humic acid systems on the activity of the KNO$_3$ for α_n=0.8.

	Zn(II)	Cd(II)
Fluka humic acid	0.26±0.07	0.39±0.10
Aldrich humic acid	0.16±0.08	0.35±0.03
Roth humic acid	0.23±0.17	0.30±0.07

7.3.2.3 Competition between calcium and heavy metals

In natural waters, earth alkaline cations are generally present in large excess over heavy metal ions. In the literature earth alkaline cation concentrations are found to be in the range of 10^{-5} to 10^{-2} mol.l^{-1} for fresh waters and open sea waters [22]. Due to competition effects the speciation of heavy metals in humic acid solutions may be affected by the presence of earth alkaline cations. In order to investigate this in some detail, we have performed stripping voltammetric complexation experiments for various calcium/heavy metal/humic acid systems. The experiments are performed for a constant concentration of KNO$_3$ and in large excess over calcium, and, hence, possible screening effects are expected to be eliminated.

In figures 7.12a and 7.12b, voltammetric complexation curves are presented for different concentrations Ca(NO$_3$)$_2$ for Zn(II)/Fluka humate and Cd(II)/Fluka humate systems, respectively,
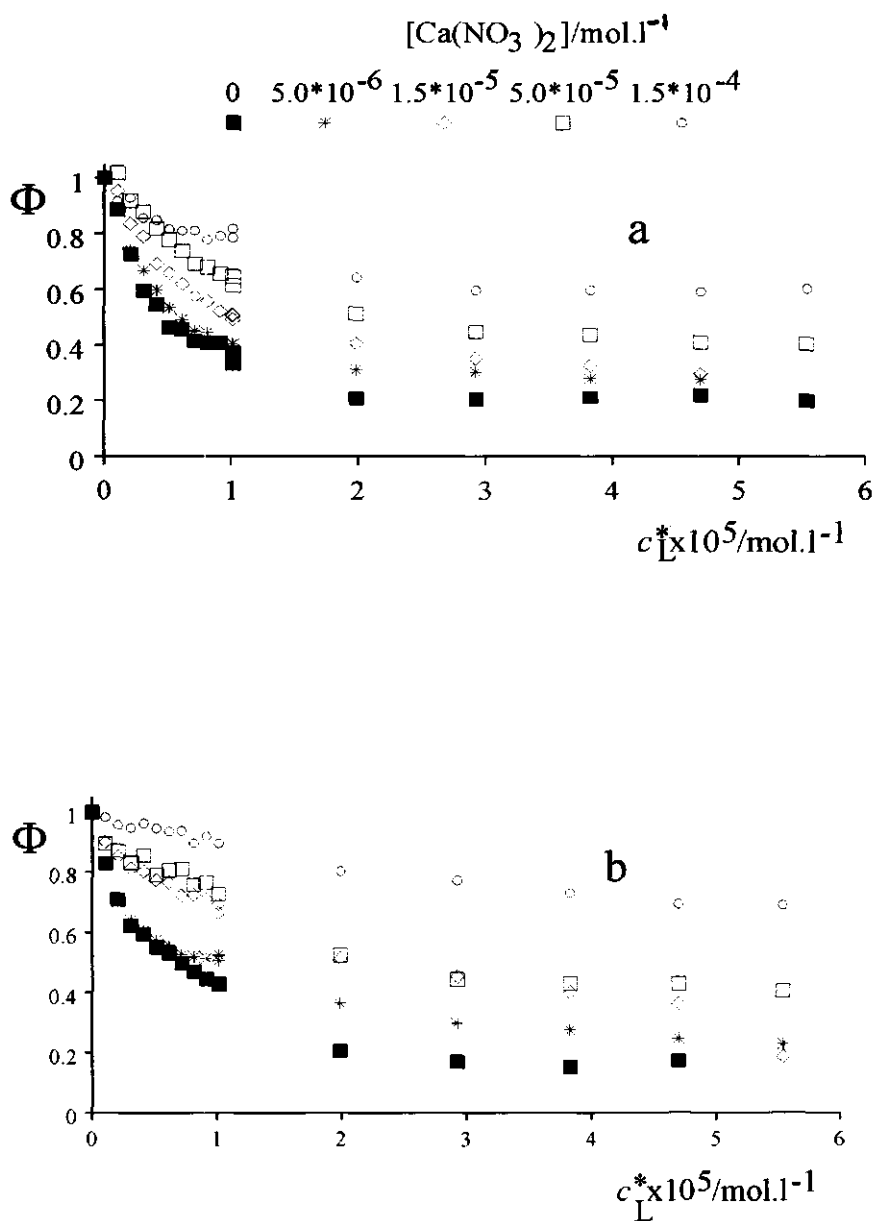
Figure 7.12: Stripping voltammetric complexation curves for the Zn(II)/Fluka humate (a) and Cd(II)/Fluka humate (b) systems for different $Ca(NO_3)_2$ concentrations. $[Me(II)]=10^{-7}$ $mol.l^{-1}$; $\alpha_n=0.6$; $[KNO_3]=0.03$ $mol.l^{-1}$.

with $\alpha_n=0.6$, at a metal ion concentration of 10^{-7} mol.l^{-1} and $[KNO_3]=0.03$ mol.l^{-1}. For both heavy metal/humate systems, a higher Φ is observed for larger calcium concentrations at the same ligand concentration. This indicates a decreased association of heavy metal ions by the humate polyanion. Obviously, calcium ions compete with the heavy metal ions for binding sites at the humic material. Similar observations have been found in the literature [23-25]. For example, Buffle *et al.* [23] measured copper binding by organic matter as a function of added Ca^{2+} in freeze-concentrated marsh water with an ion-specific electrode over the pH range 5-6.5. For all pH values studied, they found a decrease of bound copper with increasing calcium concentration (from 10^{-4} up to $4*10^{-3}$ mol.l^{-1}). The complexation curves in figures 7.12a and 7.12b have been analyzed according to equation (3.11) using p=2/3. The resulting K values are collected in table 7.4. In agreement with the qualitative information obtained from the shape of the complexation curves, the overall stability K decreases with increasing calcium concentration.

Table 7.4: Stabilities K obtained from Φ values for various Zn(II)/humate and Cd(II)/humate systems as a function of the concentration $Ca(NO_3)_2$ with $\alpha_n=0.6$ and $[Me(II)]=10^{-7}$ mol.l^{-1}.

[Ca(NO₃)₂] (mol.l⁻¹)	Zn(II)		Cd(II)	
	$\log K$	r^2	$\log K$	r^2
0	5.59	0.980	5.45	0.993
$5.0*10^{-6}$	5.57	0.985	5.46	0.976
$1.5*10^{-5}$	5.29	0.988	4.97	0.984
$5.0*10^{-5}$	5.07	0.987	4.88	0.969
$1.5*10^{-4}$	5.03	0.956	4.42	0.987

We might understand the observed tendency of K to decrease with increasing calcium concentration by considering an additional complexation reaction of calcium with the metal ion binding sites on the humate polyion (see equation 7.1). In section 7.3.1.1, it was shown that the stability K_{Ca} for the association of calcium with the humate polyion could be satisfactorily calculated from conductometric speciation data. For the present Fluka humic acid with $\alpha_n=0.6$, K_{Ca} was estimated to be in the order of 10^4 l.mol^{-1}. Using this value for K_{Ca}, we have recalculated the complexation curves for the Zn(II)/Fluka humate and the Cd(II)/Fluka humate systems, which are presented for different $Ca(NO_3)_2$ concentrations in figures 7.13a and 7.13b, respectively. The results indeed show that the dependency of Φ with $[Ca(NO_3)_2]$ becomes less pronounced. This tendency seems to become more pronounced by using a somewhat larger value of $\log K_{Ca}$, 4.5 (see figures 7.13c and 7.13d).
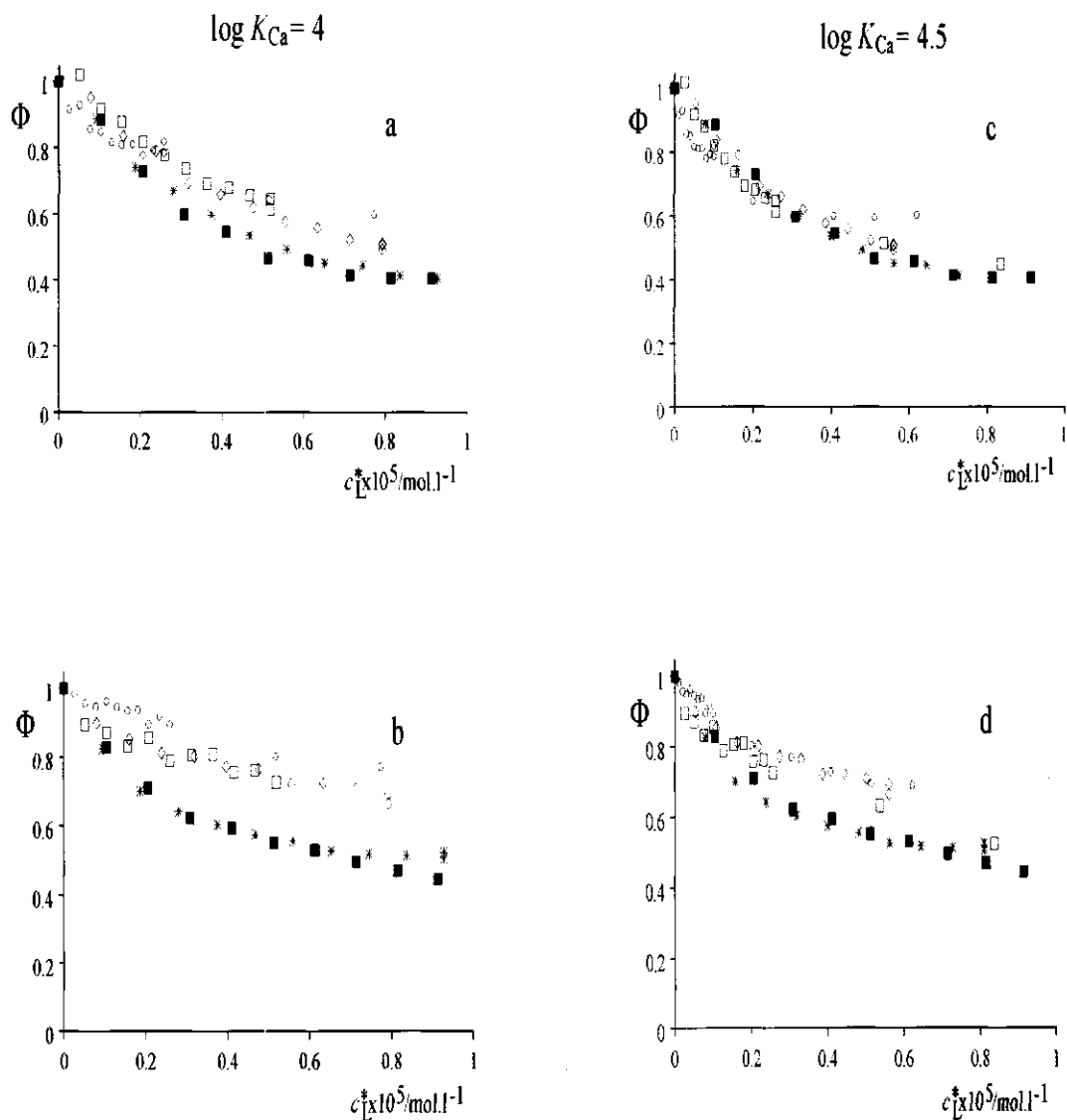
Figure 7.13: Recalculated stripping voltammetric complexation curves for the Zn(II)/Fluka humate (a,c) and the Cd(II)/Fluka humate (b,d) systems for different $Ca(NO_3)_2$ concentrations. $[Me(II)]=10^{-7}$ mol.l^{-1}; $\alpha_n=0.6$; $[KNO_3]=0.03$ mol.l^{-1}. Symbols as in figure 7.12.

Table 7.5 presents the corresponding stabilities K for the various Ca/Zn(II)/Fluka humate and Ca/Cd(II)/Fluka humate systems after correction for the amount of chargeable groups. The data clearly show that after elimination of the calcium complexation, the stability of the heavy metal/humate complex increases to values close to the stability of the corresponding complex in the absence of calcium. For example, using log K_{Ca}=4, an average log K of 5.49 is obtained for the Zn(II)/humate complex, which is in reasonable agreement with the log K value of 5.59 found for the same system in the absence of calcium. It can be concluded that, the introduction of an additional equilibrium properly accounts for for the binding of calcium by the humate polyanion. Hence, we are able to succesfully obtain information of heavy metal speciation in more complex systems, containing such competing cations.

Table 7.5: Stabilities K obtained from Φ values for various Zn(II)/humate and Cd(II)/humate systems as a function of the concentration Ca(NO$_3$)$_2$ for recalculated ligand concentrations with α_n=0.6 and [Me(II)]=10^{-7} mol.l^{-1}.

[Ca(NO$_3$)$_2$] (mol.l^{-1})	Zn(II)		Cd(II)	
	log K	r^2	log K	r^2
0	5.59	0.980	5.45	0.993
log K_{Ca}=4				
5.0*10^{-6}	5.61	0.985	5.50	0.976
1.5*10^{-5}	5.41	0.988	5.09	0.983
5.0*10^{-5}	5.31	0.988	5.19	0.969
1.5*10^{-4}	5.64	0.956	5.05	0.987
average	5.49±0.16		5.21±0.13	
log K_{Ca}=4.5				
5.0*10^{-6}	5.68	0.986	5.57	0.975
1.5*10^{-5}	5.58	0.988	5.26	0.983
5.0*10^{-5}	5.69	0.988	5.51	0.966
1.5*10^{-4}	6.04	0.956	5.46	0.987
average	5.75±0.20		5.45±0.13	

7.3.2.4 Influence of the HA charge density on the stability

In figures 7.14a-b, stripping voltammetric complexation curves are presented for different degrees of neutralization of heavy metal/Fluka humic acid systems with [KNO$_3$]=0.01 mol.l^{-1} with [Zn(II)]=10^{-6} mol.l^{-1} and [Cd(II)]=10^{-6} mol.l^{-1}, respectively. The corresponding shifts of the peak potential are shown in figures 7.15a-b. The lability of the various Zn(II)/Fluka humic

acid and Cd(II)/Fluka humic acid systems is indicated by the observed plateaus for large concentrations of the added humate polyion and the systematic shifts of the peak potential. Analysis of the complexation curves in terms of a stability K is performed according to equation (3.11) by using p=2/3. Table 7.6 collects the resulting values for K.

Table 7.6: Stabilities K obtained from Φ values for various Zn(II)/Fluka humate and Cd(II)/Fluka humate systems for different degrees of neutralization with $[KNO_3]=0.01$ mol.l^{-1} and $[Me(II)]=10^{-6}$ mol.l^{-1}.

	Zn(II)		Cd(II)	
α_n	$\log K$	r^2	$\log K$	r^2
0.4	4.63	0.997	4.77	0.997
0.5	5.11	0.990	5.03	0.992
0.8	5.22	0.990	5.21	0.990

The results show that the stability K increases with increasing α_n. This means that the binding of the heavy metal with the Fluka humate polyion is stronger for higher polyionic charge densities, which runs parallel with the general observation for polyelectrolytes. For example, Cleven [9] found in a comparable polarographic study that for various heavy metal/humic acid complexes the stability increased approximately linearly with increasing charge density. Slopes dlog$K$/dα_n reported by Cleven [9] were inbetween 2 and 4 for the Cd(II)/Fluka humic acid and the Zn(II)/Fluka humic acid systems. We note that Cleven performed his experiments at a relatively high metal-to-ligand ratio which resulted in an overestimation of the dependency of K on α_n. For the present heavy metal/Fluka humic acid systems, it seems that the increase of the stability K with increasing α_n is less pronounced. We recall that the magnitude of the separation between the sites was estimated to be in the order of 1 nm (see section 7.3.1.2). This would mean that for the present experimental conditions, i.e. at relatively low metal-to-ligand ratios, electrostatic effects are negligible and, thus, the value of K is expected to be practically independent on the overall charge density of the humate polyion. Nevertheless, the stability increases with increasing degree of neutralization, which must indicate that the charged sites are rather randomly distributed on the humate polyion.

Figure 7.14: Stripping voltammetric complexation curves for the Zn(II)/Fluka humate system (a) and the Cd(II)/Fluka humatye system (b) for different degrees of neutralization with $[KNO_3]=0.01$ mol.l^{-1} and $[Me(II)]=10^{-6}$ mol.l^{-1}.
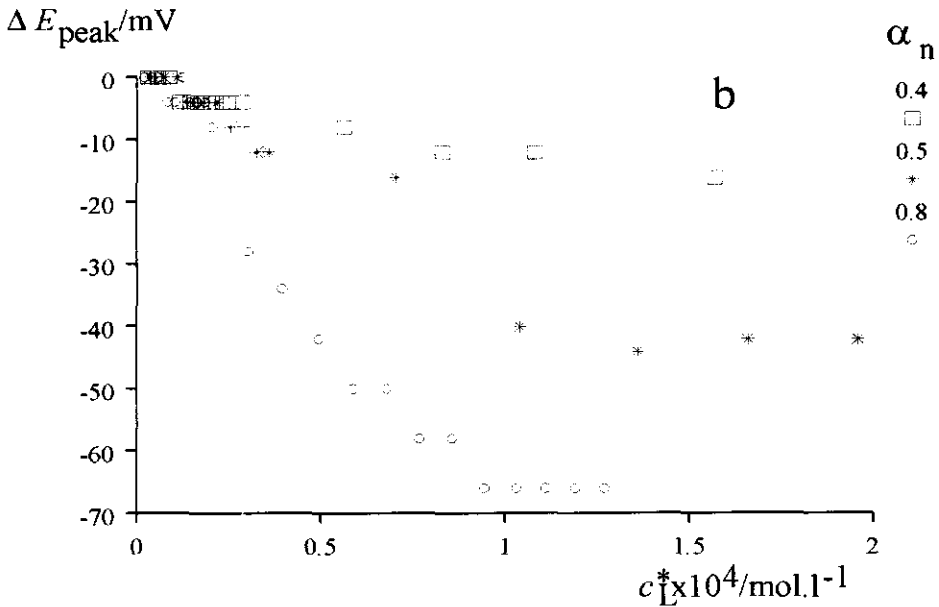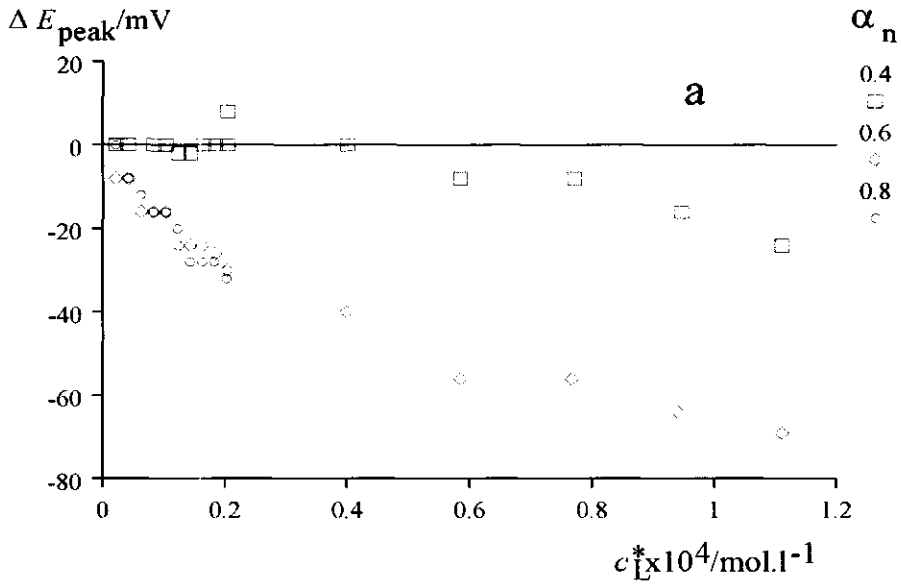
Figure 7.15: The shift of the peak potential as a function of ligand concentration for the Zn(II)/Fluka humate system (a) and the Cd(II)/Fluka humate system for different degrees of neutralization with $[KNO_3]=0.01$ mol.l^{-1} and $[Me(II)]=10^{-6}$ mol.l^{-1}.

7.3.2.5 Heterogeneity

Mainly due to the occurrence of a wide range of functional groups with different affinities for metal ions, natural organic matter appears to be chemically heterogeneous. One of the consequences is that the speciation of heavy metals in solutions containing humic material generally varies with the degree of occupation of the binding sites. With the current voltammetric speciation procedure, we are able to verify this behaviour by varying the metal-to-humic concentration ratio for different total concentrations of the heavy metal ions in a range of comparable ligand concentrations. According to this procedure, we have first verified the absence of heterogeneity of Zn(II)/PMA and Cd(II)/PMA complexes in chapter 5. Then, a similar study has been carried out on the Zn(II)/Fluka humic acid and the Cd(II)/Fluka humic acid systems.

In figures 7.16a and 7.16b, stripping voltammetric complexation curves are presented at different total metal ion concentrations with α_n=0.8 and [KNO$_3$]=0.01 mol.l^{-1} for the Zn(II)/Fluka humic acid system and the Cd(II)/Fluka humic acid system, respectively. The accompanying shifts of the peak potential are presented in figures 7.17a and 7.17b. The present heavy metal/Fluka humic acid systems appear to be voltammetrically labile under the experimental conditions employed, as found for all humic acid systems in the present study. The lability of the metal/complex system is indicated by the presence of a finite plateau value for Φ at high humic acid concentrations and the systematic shift of the peak potential under the same conditions. Hence, stabilities could be calculated according to equation (3.11) using p=2/3. The corresponding K values are collected in table 7.7.

For the Zn(II)/Fluka humic acid and the Cd(II)/Fluka humic acid systems, the stability K significantly decreases with increasing total metal ion concentration at comparable humic acid concentrations. From the data collected one can deduce an average decrease of log K of about 0.5 units per order of magnitude increase in metal ion concentration. For the Zn(II)/PMA and the Cd(II)/PMA systems, the stability K was found to be more or less constant with increasing total metal ion concentration (see section 5.3.2.5). A decrease in K means that the binding with the humate polyion becomes weaker with increasing metal ion concentration, which is in agreement with expectation. Since the metal-to-ligand ratio has been varied for very low concentrations of metal, the electrostatic contribution is constant and, hence, the observed decrease of K with increasing metal concentration
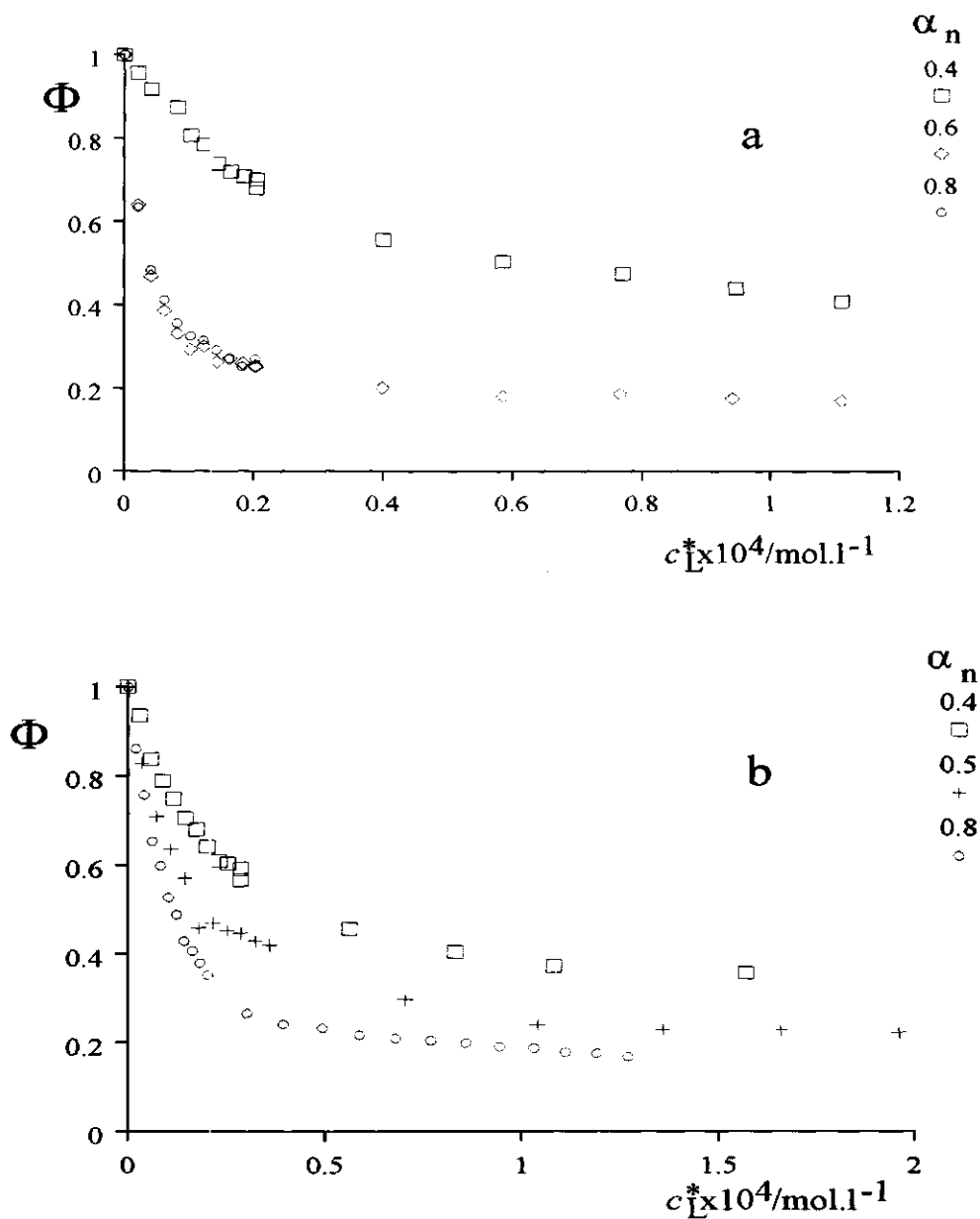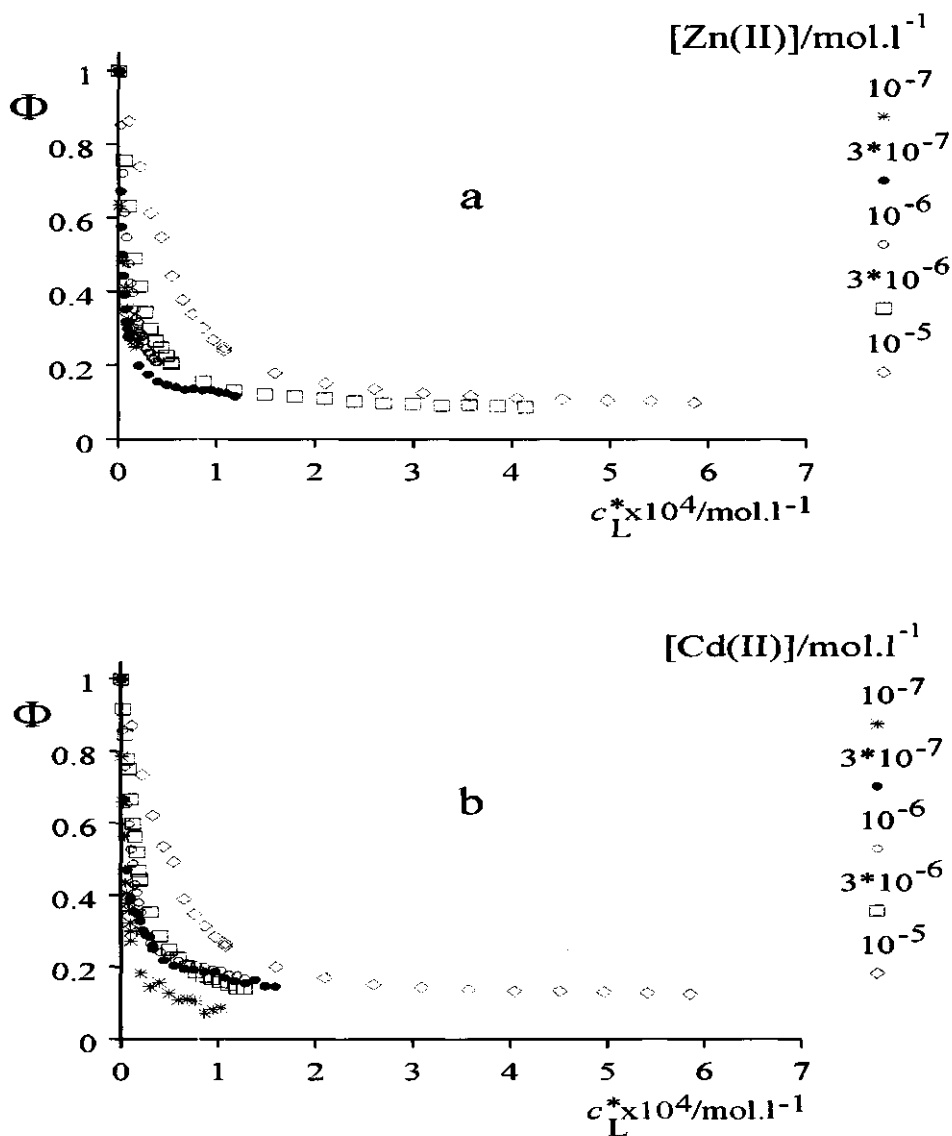
Figure 7.16: Stripping voltammetric complexation curves for the Zn(II)/Fluka humic acid system (a) and the Cd(II)/Fluka humic acid system (b) for different total concentrations of the metal ions with $[KNO_3]=0.01$ mol.l^{-1} and $\alpha_m=0.8$.

Figure 7.17: The shift of the peak potential as a function of ligand concentration for the Zn(II)/Fluka humic acid system (a) and the Cd(II)/Fluka humic acid system (b) for different total concentrations of the metal ions with $[KNO_3]=0.01$ mol.l^{-1} and $\alpha_n=0.8$.

reflects the chemical heterogeneity of the humic acid sample. The stabilities obtained for the metal/humic acid complexes in this thesis should be interpreted as average values for the metal-to-ligand ratio range covered by the experimental conditions.

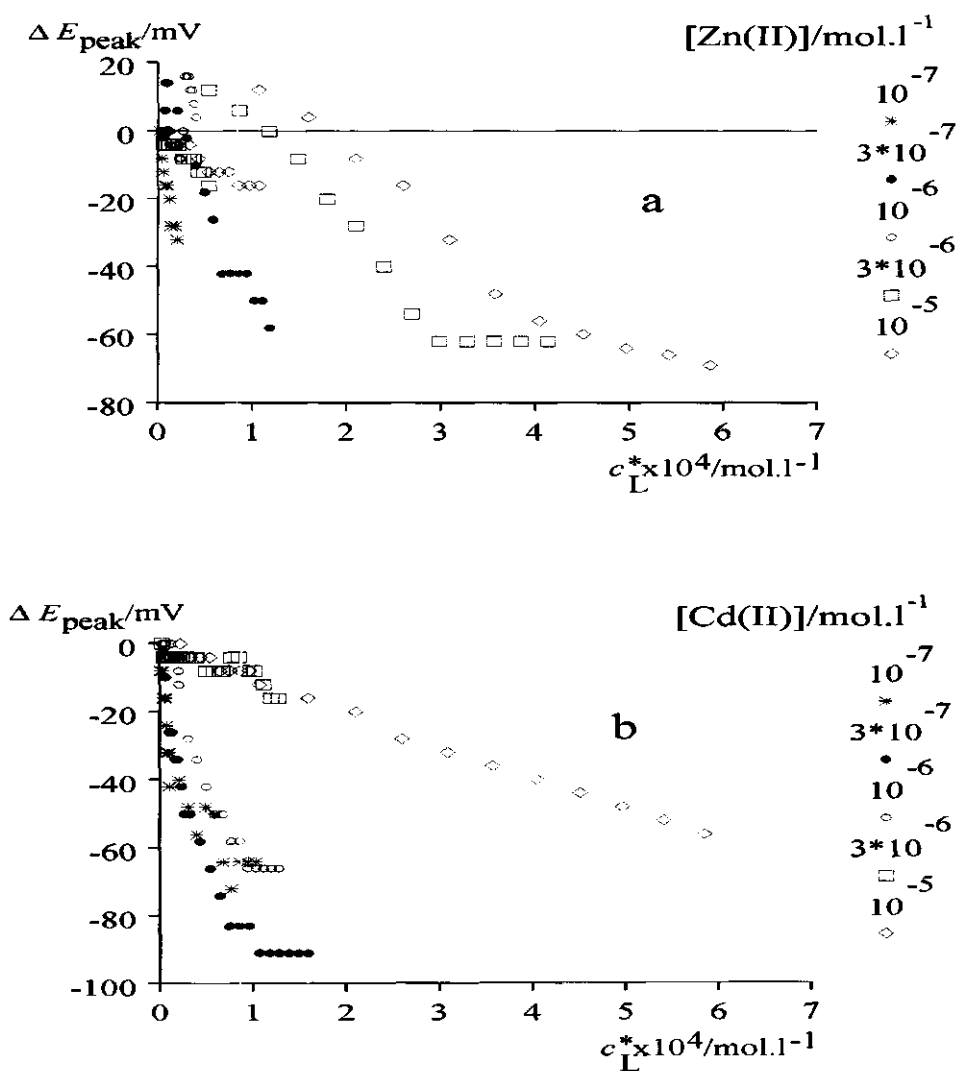Table 7.7: Stabilities K obtained from Φ values for the Zn(II)/Fluka humic acid system and the Cd(II)/Fluka humic acid system for different total concentrations of the metal ions with $[KNO_3]=0.01$ mol.l^{-1} and $\alpha_n=0.8$. (p=2/3)

	Zn(II)		Cd(II)	
$[Me(II)]_T$	$\log K$	r^2	$\log K$	r^2
$1*10^{-7}$	5.74	0.999	5.67	0.996
$3*10^{-7}$	5.72	0.991	5.51	0.994
$1*10^{-6}$	5.22	0.990	5.21	0.990
$3*10^{-6}$	5.12	0.983	5.03	0.976
$1*10^{-5}$	4.67	0.961	4.63	0.967

The stability data may be further transformed into the corresponding adsorption isotherm. For example, one can calculate for each total metal ion concentration the speciation in the metal/humic acid system for one and the same ligand concentration according to equation (3.2). In this way, plots of the degree of coverage as a function of the free metal ion concentration can be constructed. For the present Zn(II)/humic acid and Cd(II)/humic acid systems, the degree of coverage has been plotted vs. $[Me(II)]_{free}$ in figure 7.18 for $[HA]=10^{-5}$ mol.l^{-1}. The isotherm may be further transformed into the distribution of the affinities of the sites according to the procedure outlined by Van Riemsdijk and Koopal [26].
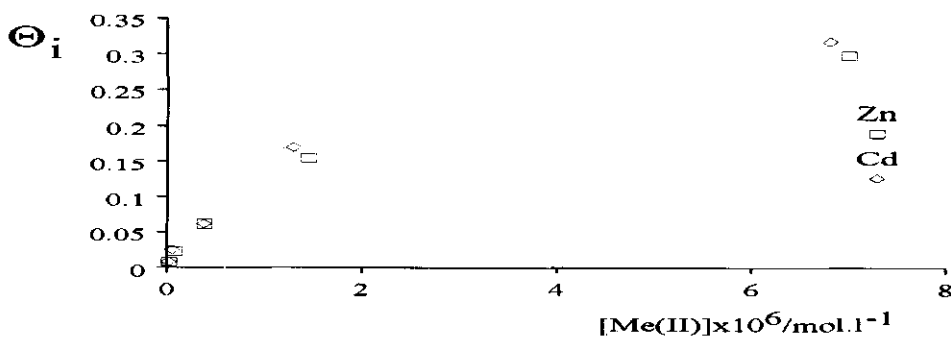

Figure 7.18: Sorption isotherms of the Zn(II)/Fluka humic acid and the Cd(II)/Fluka humic acid systems presented as the degree of coverage versus [Me(II)] with $[KNO_3]=0.01$ mol.l^{-1} and $\alpha_n*[HA]=10^{-5}$ mol.l^{-1}.

7.3.2.6 Influence of the molar mass distribution

In figure 7.19a, stripping voltammetric complexation curves are presented for a set of Zn(II)/Fluka humic acids, including the fractionated humic samples F1 and F2 as well as the unfractionated sample (for comparison), for different values of α_n with $[KNO_3]=0.01$ mol.l^{-1} and $[Zn(II)]=10^{-6}$ mol.l^{-1}. A comparable set of complexation curves with $[Cd(II)]=10^{-6}$ mol.l^{-1} is collected in figure 7.19b. Under the experimental conditions employed, the heavy metal/humate complexes appear to be voltammetrically labile over the whole range of metal-to-ligand ratios. Hence, the complexation curves can be analyzed in terms of a stability K according to equation (3.11).

The shapes of the curves for the fractionated samples are comparable to those for the unfractionated Fluka humic acid sample, indicating approximately equal stabilities. For the Zn(II)/F1 and the Cd(II)/F1 systems with $\alpha_n=0.5$ using p=2/3, log K values were found to be 5.30 and 5.32, respectively. The resulting stabilities for the analogous unfractionated Fluka humic acid, were 5.11 and 5.03, respectively. For the Zn(II)/F2 and the Cd(II)/F2 systems with $\alpha_n=0.4$ using p=2/3, log K values were 4.70 and 4.83, respectively, which are close to 4.77 and 4.63 as found for the unfractionated Fluka humic acid samples. Futhermore, the tails of the curves of fraction F1 seem to be somewhat elevated compared to the one of the unfractionated sample. Here the mean diffusion coefficient of fractionate humate complex may be increased. This pattern is not observed for fraction F2. The results are in line with the molar mass distributions as obtained from the flow field flow fractionation measurements described in chapter 6. The molar mass distribution of fraction F1 showed an increase in low molar mass and a decrease in high molar mass components.

α_n=0.4/Fluka (original) α_n=0.4/F2
□

α_n=0.5/Fluka (original) α_n=0.5/F1
○   +

$$c_L^* \text{x}10^4/\text{mol.l}^{-1}$$
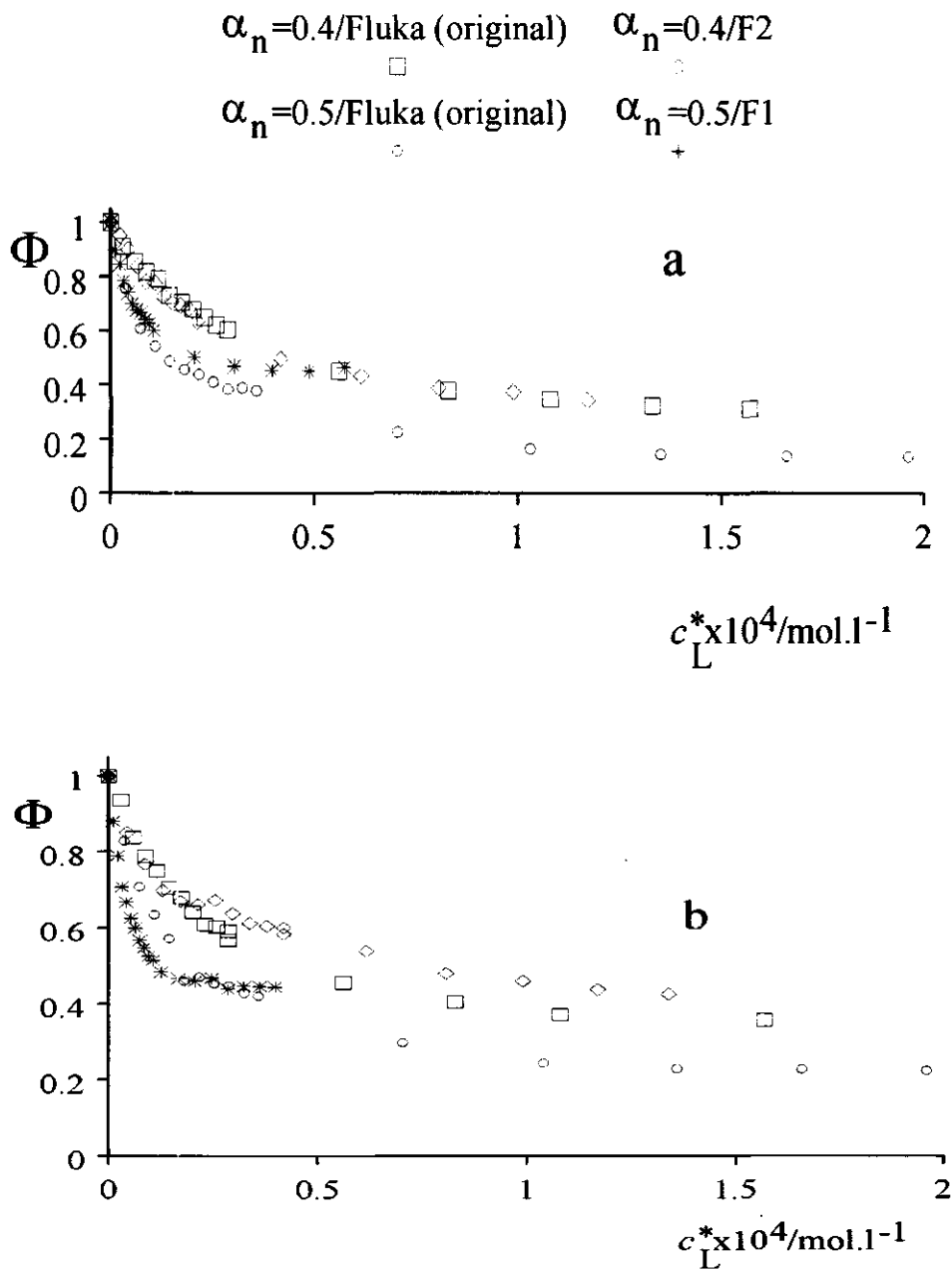

$$c_L^* \text{x}10^4/\text{mol.l}^{-1}$$

Figure 7.19: Stripping voltammetric complexation curves for the Zn(II)/Fluka humic acid system (a) and the Cd(II)/Fluka humic acid system (b) including fractionated and unfractionated samples with [KNO$_3$]=0.01 mol.l^{-1} and [Me(II)]=10^{-6} mol.l^{-1}.

7.4 Concluding remarks

The present section deals with some general conclusions which can be drawn from the speciation data for heavy metal/humate complexes as described in this chapter. First of all, it can be concluded that conductometry and voltammetry are valuable tools in the analysis of ion distributions in metal/humic acid systems. For conductometry, this is especially true for metal ions such as calcium and magnesium, which are present at fairly high concentrations in natural waters. In addition, due to the characteristics of conductometry, it may be well used in supporting model studies. On the other hand, in natural systems the metal-to-ligand ratio for heavy metals is generally very small. Under these conditions, voltammetry appears to be most powerful in the analysis of ion distributions. For the labile heavy metal/humic acid systems, the power of voltammetry is undoubtedly demonstrated by the speciation results presented in this chapter.

The speciation of various metal ions in solutions containing humate polyions has been investigated for different "environmental" conditions. In addition, we have varied the physico-chemical conditions of the metal complex system in order to analyze the association of counterions with polyions in more detail. The results are presented in this chapter and compared to the ones found for the "models" polyacrylic acid and polymethacrylic acid. Several differences in metal association behaviour have been observed. For further discussion, we recall here the main dissimilarities:

(i)   the extent of association of monovalent counterions with the humic material seems to depend on the metal-to-ligand ratio, whereas for the PMA system the fraction of free monovalent counterions is independent on the [PMA] at given charge density;

(ii)   for the humic acid system, the fraction of free monovalent counterions appears to be independent on the charge density of the humate polyion, but it is found in the cases of calcium and barium. On the other hand, for PMA, the fraction of free monovalent counterions is strongly dependent on the charge density of the polymethacrylate polyion at given [PMA];

(iii)   the dependency of K on the salt concentration is found to be significantly less pronounced for the heavy metal/humate systems compared to that for the heavy metal/polymethacrylate systems;

(iv)   for the Zn(II)/HA and the Cd(II)/HA systems, log K decreases with increasing total metal concentration, whereas, in the cases of Zn(II)/PMA and Cd(II)/PMA the stability K remains more or less constant over two orders of magnitude of total metal concentration.

The differences in metal association behaviour between the humics and the synthetic polyacids could be tentatively explained by considering the charge distribution on the polyacids and the chemical heterogeneity of the humate polyions. The mean separation between binding sites on the humate polyion can be estimated to be in the order of 1 nm, which is well above the Bjerrum length for aqueous systems. For $\alpha_n=1$, the linear charge density parameter ξ would then approximately be 0.7. According to the counterion condensation approach for linear polyelectrolytes, no monovalent counterions will be associated by the polyion since the charge density does not exceed its critical value $\xi_{crit} = 1$. This evidence is supported by the relatively small dependency of K on the salt concentration as mainly the result of screening effects. Although most of the experiments have been performed for α_n values ranging from 0.4 to 0.8 (with the corresponding ξ varying from approximately 0.3 to 0.6), the binding behaviour of the divalent counterions, for which $\xi_{crit}=0.5$, differs remarkably from that of the monovalent counterions. This might mean that the association of divalent ions cannot be totally ascribed to electrostatic interaction. Here the chemical heterogeneity of the humate polyion is mainly responsible for the characteristics of the binding of metal ions with the humic acids.

We should add that for the humic acids, uncertainty exists about the conformation of the macromolecule. Furthermore, the spatial distribution of charges on the humate polyion is expected to have a non-uniform character. Although one may speculate about the exact geometry, it is expected to be inbetween the two extremes, i.e. (i) a linear chain with an array of charges, and (ii) a sphere with a distribution of charges on its surface. In describing ion distribution in metal/humic acid systems, we have chosen the former oversimplification. For model systems such as the linear polyelectrolyte PMA, theory with respect to ion binding, which takes into account electrostatic, is available, and this is not the case for cross-linked macromolecules.

Speciation measurements in natural systems according to the methods presented in this study seem not yet suitable for routine purposes. On the other hand, the results give useful (quantitative) information with respect to the speciation parameters of practical importance. For example, it has been shown, that fractionation of naturally occuring complexing agents is of minor concern in understanding the speciation of metal ions in natural waters. The content of this thesis was

limited to metal binding with macromolecules. It seems very useful to extend this type of speciation study to systems containing particles, which are generally also present in natural waters.

7.5 References

1. H.G. de Jong, J. Lyklema and H.P. van Leeuwen, Biophys. Chem., 27 (1987) 173.
2. Chapter 5 of this thesis.
3. IMSL Library, Edition 9.2 IMSL, Houston 1984.
4. B. Chatterjee and S. Bose, J. Colloid Sci., 7 (1952) 414.
5. H. van Dijk, Sci. Proc. R. Dublin Soc., Ser. A, 1 (1960) 163.
6. M. Schnitzer and S.I.M. Skinner, Soil Sci., 96 (1963) 86.
7. F. Halla and W. Ruston, Z. Electrochem., 59 (1955) 525.
8. M.M. Roy, Kolloid-Z., 153 (1957) 174.
9. R.F.M.J. Cleven, PhD-thesis, Agricultural University, Wageningen, 1984.
10. D. Dobos, Electrochemical Data, Elsevier, Amsterdam, 1975, p. 339.
11. S. Arai and K. Kumuda, Geoderma, 19 (1977) 21.
12. L.G. Silèn and A.E. Martell, Stability Constants, Special Publication no. 17, Stability constants of metal ion complexes, The Chemical Society, London, 1964.
13. R.F.C. Mantoura, A. Dickson and J.P. Riley, Estuar. Coast. Mar. Sci., 6 (1978) 387.
14. B.A. Dempsey and C.R. O'Melia, in R.F. Christman and E.T. Gjessing (eds.), Aquatic and Terrestrial Humic Material, p. 239, Ann Arbor, Ann Arbor Science, 1983.
15. A.S. Mathuthu and J.H. Ephraim, Talanta, 40 (1993) 521.
16. G.A. Bhat, R.A. Saar, R.B. Smart and J.H. Weber, Anal. Chem., 53 (1981) 2275.
17. R.E. Truitt and J.H. Weber, Anal. Chem., 53 (1981) 337.
18. S.K. Saha, S.L. Dutta and S.K. Chakravarti, J. Indian Chem. Soc., 56 (1979) 1129.
19. J.C. Benegas, S. Paoletti, A. Cesàro, M.A.G.T. van den Hoop and H.P. van Leeuwen, Biophys. Chem., 42 (1992) 297.
20. F.J. Stevenson, Soil Sci., 123 (1977) 10.
21. W.P.T.J. van der Drift, PhD-thesis, State University Utrecht, Utrecht, 1975.
22. J. Buffle, Complexation Reactions in Aquatic Systems: An Analytical Approach, Ellis Horwood Ltd. Chichister, 1988.
23. J. Buffle, P. Deladoey, F.L. Greter and W. Haerdi, Anal. Chim. Acta, 116 (1980) 255.
24. S.E. Cabaniss and M.S. Shuman, Geochim. Cosmochim. Acta, 52 (1988) 185.
25. J.G. Hering and F.M.M. Morel, Environm. Sci. Technol. 22 (1988) 1234.
26. W.H. van Riemsdijk and L.K. Koopal, in J. Buffle and H.P. van Leeuwen, eds., Environmental Particles vol.1, IUPAC Environmental Analytical and Physical Chemistry Series, Lewis Publisher, Boca Raton, 1992, p. 455-495.

118

LIST OF SYMBOLS AND ABBREVIATIONS

a	cylinder radius of linear polyion
a_i	activity of species i
A	constant in equation (6.3)
b	constant in equation (6.3)
c_c	analytical concentration of total amount of carboxylic groups
c_i, c_1, c_2	analytical molar concentrations of counterions i, of monovalent, divalent counterions, respectively
$(c_-)_j$	analytical molar concentration of co-ions j (for negative polyelectrolyte)
c_p	volume concentration of deprotonated groups on the polyion
c_M^*, c_L^*, c_{ML}^*	bulk concentrations of M, L and ML
D	diffusion coefficient of sample molecule (in equation (6.2))
D_M, D_{ML}	diffusion coefficients of free and bound metal, respectively
$\overline{D}$	mean diffusion coefficient, defined by equation (3.9)
e	elementary charge
E, E_{eff}	electric field; effective electric field
E_{peak}	reoxidation peak potential
ΔE_{peak}	shift of reoxidation peak potential
f	distribution parameter of counterions (in equation (2.1))
f_i, f_1, f_2	distribution parameter of counterions i, of monovalent, divalent counterions, respectively
f_p	charge fraction of polyion
F	Faraday constant
g	reduced molar Gibbs energy, defined by equation (2.14)
g_{el}	reduced molar electrostatic Gibbs energy, defined by (A2.1)
g_{mix}	reduced molar Gibbs energy of mixing, defined by (A2.2)
G	Gibbs energy
H	standard electrophoretic mobility factor defined by equation (2.12)
I	reoxidation peak current
I_e	pre-electrolysis current
J_{diff}, J_{kin}	contribution to the flux under purely diffusion and purely kinetically controlled conditions, respectively
k	Boltzmann constant

k_a, k_d	association and dissociation rate constants, respectively
K	stability of metal complex defined by equation (3.2)
K_c	stability of metal complex corrected for activity effects defined by equation (4.12)
K_{Ca}	stability of calcium complex defined by equation (7.2)
K_{th}	thermodynamic equilibrium constant
K_w	ionic product of water
l	spacing between charged sites on polyion
l_B	Bjerrum length defined by equation (2.4)
L	ligand or site
M	molar mass of macromolecule in equation (6.3)
M, M^0, ML	electroactive metal; metal atom; electroinactive metal complex, respectively
n	number of electrons in charge transfer reaction
n_p	number of moles of polyionic charged groups
p	hydrodynamic parameter
q_{eff}	effective charge
r	total fraction of condensed counterions per fixed charge
r_i, r_1, r_2	fraction of condensed counterions i, of monovalent, divalent counterions per fixed charge, respectively
R	retention ratio, defined by equation (6.1)
R	gas constant
R_1, R_2	molar ratio of the total concentration of monovalent, divalent counterions to the polyion concentration, respectively
t	time scale of experiment
t_e	pre-electrolysis time
T	absolute temperature
u_p^o, u_i^o	electric mobility of the free polyion and the free counterion, respectively
u_p	effective mobility of the polyion in the polyelectrolytic system
v_{scan}	scan rate
V^0	channel void volume
V_r	sample retention volume
V_c'	volumetric flow rate across the channel (field)
V_p	molar condensation volume expressed in liters per mole of fixed charge
w	channel thickness
$W_{1/2}$	peak width at half height

x_i	mol fraction of counterion i in the condensation volume
z_i	valency of counterion i
α_d, α_n	degree of dissociation; degree of neutralization, respectively
γ	activity coefficient
δ	thickness of diffusion layer
ϵ	ratio of diffusion coefficients of free and bound metal
$\epsilon\epsilon_0$	permittivity of the solution
η	viscosity of the solution
ζ^0	electrokinetic potential of the free polyion
κ	reciprocal Debye length
κ'	modified screening length, defined by equation (2.11)
K_s	specific conductivity of solution
ΔK_s	conductivity excess function, defined by equation (2.27)
λ	FFF retention parameter
λ_i^o, λ_1^o, λ_2^o	ionic conductivity of free counterion i, of free monovalent, divalent counterions in pure solvent, respectively
$(\lambda^o)_j$	ionic conductivity of co-ions j in pure solvent (for negative polyelectrolyte)
λ_p	ionic conductivity of polyion (per mol of charged groups)
Λ	molar conductivity
ν	kinematic viscosity of the solution
$\nu_{1,2}$	exchange coefficient for monovalent and divalent counterions, defined by equation (2.28)
Φ	normalized peak current, defined by equation (3.11)
Θ_i	degree of coverage of counterion i, defined by equation (2.22)
Θ_1, Θ_2	degree of coverage of monovalent, divalent counterions, respectively
ξ	structural charge density parameter, defined by equation (2.3)
ξ_{crit}	critical charge density parameter, defined by equation (2.6)
ω	angular frequency
CC	counterion condensation
DPASV	differential pulse anodic stripping voltammetry
FFF	field flow fractionation
HA	humic acid
HMDE	hanging mercury drop electrode
PAA, PMA	polyacrylic acid; polymethacrylic acid

RDE   rotating disk electrode

SV   stripping voltammetry

SUMMARY

The purpose of the research described in this thesis was to examine the applicability of elec-tro-analytical techniques in obtaining information on the speciation of metals, i.e. their dis-tribution over different physico-chemical forms, in aquatic systems containing charged macromolecules. In *chapter 1* a general introduction is given to (i) metal speciation in aquatic systems, (ii) (bio)polyelectrolytes and their counterion distributions and (iii) electrochemical methods emphasizing their apllication to metal speciation.

Chapter 2 deals with the conductometric measurement of counterion association with macro-molecules. First, we have surveyed theoretical developments concerning ion association for purely electrostatic interaction and as reflected in the conductivities of polyelectrolyte solutions. It will be shown that for the salt free case, the distribution of monovalent counterions can be obtained from plots of the molar conductivity of the polyelectrolyte solution versus the molar conductivity of the monovalent counterion, so-called Eisenberg plots. Experimental results for various alkali polymethacrylate concentrations show that the fraction of conductometrically-free monovalent counterions is in close agreement with theoretical predictions, which are based on a two-state appoach. Furthermore, for linear polyelectrolytes a recently proposed model for the case of counterion condensation in systems with ionic mixtures is presented. Finally, the treatment of conductometric data for polyelectrolyte solutions with either one type of counterion or mixtures of two types of counterions in terms of free and bound fractions is discussed.

In *chapter 3* we describe a voltammetric methodology for the analysis of labile homogeneous heavy metal-ligand complexes in terms of a stability K. The method takes into account the difference between the diffusion coefficients of the free and bound metal. Since the relationship between voltammetric current and mass transport properties under stripping voltammetric conditions is not yet well esthablished, we propose a relationship between the experimentally obtained current and the mean diffusion coefficient of the metal-complex system. A sensitivity analysis of this expression for different parameters, such as the stability and the ratio of the diffusion coefficients of the bound and free metal is performed.
Natural complexing agents are often heterogeneous with regard to their affinity to metal ions. Therefore, we will discuss the evaluation of the heterogeneity of these complexes from vol-tammetric data for various metal-to-ligand ratios. For the case of a large excess of ligand over the metal atom concentration, the stability of the metal-complex system may be obtained independently from the potential shift. For this an equation is given similar to the classical one

derived by DeFord and Hume. Finally, we present an experimental procedure based on adding ligand to the solution of the metal and measuring its voltammetric characteristics. The procedure takes into account (i) possible adsorption of metal ions to elements of the equipement and (ii) measuring all protolysis of the polyacids involved.

The characteristic features of applying the two electrochemical techniques conductometry and voltammetry to the study of ion binding by polyelectrolytes are discussed and compared in *chapter 4*. Analysis of data on $K^+/Zn(II)/polyacrylate$ and $K^+/Zn(II)/polymethacrylate$ systems illustrates a certain complementary of the two methodologies. Conductometry primarily measures the $Zn(II)/K^+$ exchange ratio. Voltammetry measures the $Zn(II)/polyion$ binding strength; its dependence on the (excess) K^+ concentration also yields information on the $Zn(II)/K^+$ exchange ratio. The different results seem to be fairly coherent.

Experimental conductometric and voltammetric speciation data of metal-synthetic polyacid systems are presented and discussed in *chapter 5*. The competitive binding of monovalent and divalent counterions has been studied by the conductometric procedure described in chapter 2 for aqueous solutions of alkali metal polymethacrylates in the presence of $Ca(NO_3)_2$ and $Mg(NO_3)_2$. The experimentally obtained fractions of conductometrically free counterions are compared with theoretical values computed according to a new thermodynamic model described in the same chapter. For the systems studied, the fractions of free monovalent and divalent counterions can be fairly well described by the theory. In fact, the results support the assumption that under the present conditions the conductometrically obtained distribution parameters f_1 and f_2 approximate the equilibrium fractions of free monovalent and divalent counterions. The experimentally obtained M^+/M^{2+} exchange ratios agree well with the theoretical ones. Similar experiments have been performed for the $Zn(II)/polyacrylate$ and $Zn(II)/polymethacrylate$ systems. It seems that, compared to Ca^{2+} and Mg^{2+} ions, the $Zn(II)$-ions are bound more strongly. This could be due to some specific binding of $Zn(II)$-ions. Since the theoretical model does not incorporate this mechanisme, the experimental results do not agree well with the theoretical ones.

Furthermore, *chapter 5* collects the results of a systematic study of the stripping voltammetric behaviour of $Zn(II)$- and $Cd(II)$-ions in polyacrylate and polymethacrylate solutions. All metal-ligand complexes involved apprear to be voltammetrically labile over the whole range of metal-to-ligand ratios under the various experimental conditions employed. Hence, the voltammetric data could be analyzed in terms of a stability K according to the methodology presented

124

in chapter 3. The first set of experiments is concerned with the influence of the molar mass of the polyacrylate anion on the stability. Analysis of the data in terms of a mean diffusion coefficient, which decreases with increasing molecular mass, yields a consistent picture with molar mass-independent complex stabilities. The speciation of Zn(II) in such a polyelectrolyte system varies with the concentration of carboxylate groups, but it is invariant with the polyionic molar mass. Secondly, the competition between monovalent (K^+) and divalent (Zn(II) and Cd(II)) counterions has been investigated by varying the concentration of electroinactive supporting electrolyte. The results show that the stability of the heavy metal/polymethacrylate complex decreases with increasing KNO_3 concentration. This effect is largely due to the reduction of the electrostatic component of the metal/polyanion interaction, which is generally the case for polyelectrolytes with high charge densities. For the Zn(II)/polymethacrylate system, a comparison with conductometric data representing the competitive behaviour of monovalent and divalent counterions has been made in chapter 4. The influence of the polyelectrolyte charge density of the polymethacrylic acid on the stability K has been studied by varying the degree of neutralization of the polyanion. For the Zn(II)/PMA complexes, the stability increases approximately linearly with increasing degree of neutralization, i.e. with increasing polyionic charge density. This is in accordance with the general polyelectrolytic feature that counterion binding is stronger with higher polyionic charge density. Finally, for later comparison with natural complexing agents, the chemical homogeneity of the macromolecules involved has been verified by varying the total metal ion concentration for a given polyelectrolyte concentration. The results indeed confirm that the Zn(II)/polymethacrylate and Cd(II)/polymethacrylate complexes have a homogeneous energy distribution. This is in line with expectation, since these macromolecules consist of only one repeating chemical binding site, i.e. the carboxylate group.

Chapter 6 deals with the pretreatment and characterization of humic material. The pretreatment procedure is used to purify the humic material in such a way that (i) the molecules are soluble under the experimental conditions employed in chapter 7, (ii) the amount of impurities is minimized and (iii) the resulting humic material is transferred into the acid form. Furthermore, a fractionation method based on the solubility of the humic substances is described. The humic material is characterized in terms of (i) the amount of chargeable groups by means of conductometric titration and (ii) molar mass distribution by flow field-flow-fractionation. It will be shown that although the fractionation by varying pH results in samples with different molar masses, the separation is far from ideal.

As was done with the synthetic polyacids, experiments have been performed for natural occuring polyelectrolytes. Conductometric and voltammetric results for various metal humic acid systems are presented in *chapter 7*. Solutions of humic acids were conductometrically titrated with potassium, sodium, lithium, calcium and barium hydroxide solutions. The results have been analyzed in terms of fractions of free and bound metal. The conductance properties of humic acids are basically different from those of a linear polyelectrolyte such as polymethacrylate. A marked difference was observed between the shapes of the curves for alkali metal hydroxides and those for alkaline earth metal hydroxides. It appears that monovalent cations are hardly bound by the humate polyion, whereas divalent counterions show a strong interaction. The latter feature may be fruitfully utilized in quantitative analysis.

The association of the heavy metals zinc(II) and cadmium(II) with humic acid samples has been furthere studied by differential pulse anodic stripping voltammetry (i) for various concentrations of supporting electrolyte (KNO_3 and $Ca(NO_3)_2$), (ii) for different degrees of neutralization of the humate polyion, (iii) for different metal-to-ligand ratios and (iv) for different fractions of the humic acid. Under the experimental conditions employed, all heavy metal/humate complexes have been found to be voltammetrically labile over the whole range of metal-to-ligand ratios. Hence, the stability (K) of the complex could be computed taking into account the difference between the diffusion coefficients of the free and bound metal. The dependence of K on the concentration of 1-1 electrolyte (KNO_3) is of comparable extent for various metal-humate complexes, but significantly smaller than in the case of the highly charged linear polyelectrolyte polymethacrylic acid. For the humic acid systems, it has been concluded that the relatively weak dependency of K on the salt concentration mainly reflects screening effects. The influence of the concentration of 2-1 electrolyte ($Ca(NO_3)_2$) on the stability of the heavy metal/humate complex is more pronounced than for the corresponding case of 1-1 electrolyte. By taking into account the association of calcium with the humate polyion, the stability of the heavy metal/humate complex was found to be more or less constant over the range of $Ca(NO_3)_2$ concentrations studied and comparable to the stability of the corresponding complex in the absence of calcium.

The stability of the heavy metal/humate complex has been found to increase with increasing degree of neutralization, i.e. with increasing charge density of the humate polyion. It seemed that the increase of K is less pronounced for higher values of α_n. This observation could not be interpreted from an electrostatic point of view, and is in fact a further indication that the binding of heavy metals with the humate polyion is mainly governed by the chemical characteristics of the humic acid. The chemical heterogeneity of the humic acids was investigated by varying the metal-to-ligand ratio for different total concentrations of the heavy metals but in a range of

comparable ligand concentrations. The results show that the stability K of the heavy metal/humate complex decreases with increasing total metal ion concentration, reflecting a certain chemical heterogeneity of the humic acid. For various heavy metal/fractionated humate complexes, the stability K was found to be comparable to the K value for the corresponding unfractionated humic acid system. This means that the distribution of functional groups is more or less the same for different molar masses of the humic acid.

For the present metal/humate complexes, the general conclusion is that the distribution of counterions over the free and bound states is mainly governed by the chemical heterogeneity of the humate polyion.

SAMENVATTING

In onze hedendaagse samenleving maken wij gebruik van een reeks produkten waarin zware metalen zijn verwerkt. Voorbeelden hiervan zijn loodhoudende benzine, oplaadbare batterijen met cadmium en nikkel, zinken dakgoten, etcetera. Het gebruik van deze produkten brengt zware metalen in ons milieu. Door aparte inzameling en verwerking wordt in bepaalde gevallen getracht deze emissie te minimaliseren. Daarnaast kunnen bij de fabricage van produkten zware metalen vrijkomen. Een zeer bekend voorbeeld is de metaalindustrie. Bij het smelten van ertsen komen zware metalen via de rookgassen in de atmosfeer terecht. Door natte en droge depositie komen ze in een gebied rondom de industriële activiteit in de bodem en het oppervlaktewater terecht. De Kempen zijn op deze manier sterk verontreinigd met cadmium en zink.

Zware metalen zijn in het algemeen zeer toxisch, d.w.z. dat ze reeds in zeer lage concentraties giftig zijn voor plant, dier en mens. Echter sommigen, zoals zink, behoren tevens tot de zoge-naamde essentiële elementen. Deze elementen zijn in nog weer veel lagere concentraties noodzakelijk voor flora en fauna. Een tekort kan leiden tot ziekte bij organismen of slechte groei bij planten. Toxische effecten en deficiëntie verschijnselen worden niet zo zeer bepaald door het aanwezige totaalgehalte van zware metalen in het milieu, maar veeleer door de beschik-baarheid voor opname door flora en fauna. Tegenwoordig spreken we in dit kader over *bio-beschikbaarheid* van de metalen. Ecotoxicologisch onderzoek toont aan dat de concentratie vrije metaalionen in het algemeen een beter inzicht geeft in toxische effecten dan totaalgehalten aan metalen. Kennis van de verdeling van metalen over de vrije en gebonden toestand is daarom zeer gewenst. De verdeling van metalen over verschillende fysisch-chemische verschijnings-vormen wordt aangeduid met de term *metaalspeciatie*.

Metalen kunnen binden aan allerlei deeltjes in de bodem en in het water. Natuurlijke organische stof speelt hierbij een belangrijke rol. We kennen allen de organische stof in de bodem. Het is vrij donker van kleur, maakt de grond vruchtbaar, is in staat om veel water vast te houden en zorgt voor een goede structuur van de bodem. In water oplosbare fracties organische stof worden veelal aangeduid met de termen humuszuren en fulvinezuren. Een gelig tot donker bruine kleur van het water in rivieren en meren wijst meestal op grote concentraties opgelost organische stof. Organische stof ontstaat uit de afbraak van plantaardig en dierlijk materiaal. Het bestaat veelal uit grote moleculen (macromoleculen) met een zeer ingewikkelde chemische structuur en waarin zogenaamde functionele groepen voorkomen. Deze groepen hebben de mogelijkheid om

electrisch geladen te worden. Het gaat hierbij niet om één enkele maar om vele ladingen per molecuul. Stoffen met deze eigenschap worden aangeduid met de term *biopolyelektrolieten*. In de natuur zijn deze moleculen bijna zonder uitzondering negatief geladen en kan dus electrische aantrekking optreden met positief geladen metaalionen. De mate van aantrekking is onder andere afhankelijk van omgevingsfactoren, zoals de zuurgraad van het water, de aanwezigheid van zouten en andere metalen. Deze factoren hebben dus invloed op de verdeling van metalen over de vrije en gebonden toestand en daarmee op de biobeschikbaarheid.

Het meten van de speciatie in natuurlijke systemen is in het algemeen niet eenvoudig. Veel instrumenten ter analyse van zware metalen zijn "slechts" in staat om totaalgehalten te meten. Met behulp van elektrochemische technieken is het daarentegen wel mogelijk om meer te weten te komen over de verdeling van metalen over de vrije en gebonden toestand. De eigenlijke meting is in het algemeen vrij eenvoudig, de interpretatie niet. In het verleden zijn hiervoor theorieën afgeleid. De geldigheid hiervan en de toepassingen in ingewikkelde natuurlijke systemen zijn nog niet in detail bestudeerd. Het doel van het onderzoek, zoals beschreven in deze dissertatie, is het testen van nieuwe mogelijkheden om met elektroanalytische meettechnieken informatie te krijgen over de speciatie van metalen in aquatische systemen met daarin aanwezig biopolyelektrolieten. Daarnaast is getracht om een beter inzicht te krijgen in de processen die verantwoordelijk zijn voor de verdeling van metalen over de vrije en gebonden toestand.

In *hoofdstuk 1* wordt een algemene inleiding gegeven met betrekking tot (i) metaalspeciatie in aquatische systemen, (ii) (bio)polyelektrolieten en hun bijbehorende verdeling van tegenlading en (iii) elektrochemische meetmethoden en hun gebruik in metaalspeciatie onderzoek.

De *hoofdstukken 2* en *3* beschrijven de theoretische achtergrond van respectievelijk conductometrische en voltammetrische speciatiemetingen in (bio)polyelektrolietoplossingen. De opbouw van deze hoofdstukken is ongeveer als volgt: eerst wordt bestaande kennis over de meetgegevens samengevat en in detail geanalyseerd. In het conductometrische geval bestaan die gegevens uit de relatie tussen de concentraties van geladen deeltjes en de gemeten elektrische geleiding. Voor de voltammetrie is dat de relatie tussen de stroom-spannings karakteristiek en het massatransport van stoffen naar het elektrodeoppervlak. Beide relaties bevatten informatie over de verdeling van metalen over de vrije en gebonden toestand (en dus over de speciatie). Vervolgens wordt aangegeven hoe deze informatie zichtbaar gemaakt kan worden. In het algemeen moeten hiervoor titraties worden uitgevoerd, d.w.z. dat een bepaalde stof stapsgewijs aan een uitgangsvloeistof wordt toegevoegd en na elke toevoeging de elektrische geleiding dan

wel de stroom-spanningskarakteristiek wordt gemeten. Bij de conductometrische titratie worden metaalzouten toegevoegd aan de (bio)polyelektrolietoplossing, terwijl in het voltammetrische geval de complexerende stof aan een metaaloplossing wordt toegevoegd. Beide hoofdstukken worden afgesloten met de presentatie van een meetprocedure, zoals deze gebruikt is in het vervolg van dit onderzoek.

In dit onderzoek maken we tevens gebruik van modelstoffen, waarvan de chemische structuur exact bekend is en die kwa eigenschappen lijken op in de natuur voorkomende complexvormers, te weten de humus- en fulvinezuren. We hebben gekozen voor polymethacrylzuur en poly-acrylzuur. Dit zijn macromoleculen met één en dezelfde repeterende functionele groep. De afstand tussen de individuele groepen is bekend. Theorie voor de binding van metalen met deze stoffen is beschikbaar.

In *hoofdstuk 4* vergelijken we voor het kalium/zink/polymethacrylaat complex systeem experimentele speciatiegegevens, die verkregen zijn met conductometrie respectievelijk voltammetrie. De twee meettechnieken leveren stukken informatie die elkaar in zekere zin aan-vullen. Met behulp van conductometrie meten we de uitwisselingsverhouding tussen één- en tweewaardige tegenionen. In het onderhavige geval zijn dat kalium en zink. Voltammetrie meet de bindingssterkte van het tweewaardig metaal/polyelektroliet complex. De relatie tussen de bindingssterkte en de concentratie éénwaardige tegenionen levert ook informatie op over de uitwisselingsverhouding. Voor het kalium/zink/polymethacrylaat systeem blijkt dat de twee technieken vrijwel dezelfde uitwisselingsverhouding opleveren.

Conductometrische en voltammetrische speciatiegegevens voor modelmatige metaal complex systemen staan vermeld in *hoofdstuk 5*. Aan de hand van de in hoofdstuk 2 en 3 beschreven meet- en analyseprocedures zijn conductometrische en voltammetrische experimenten uitge-voerd respectievelijk met de metalen calcium, magnesium en zink en met de metalen zink en cadmium. De algemene trend is dat we binnen zekere grenzen daadwerkelijk in staat zijn om met beide technieken de speciatie in deze systemen te meten. Verder is gevonden dat voor calcium en magnesium in een oplossing van polymethacrylaat de conductometrische specia-tiegegevens heel goed overeenkomen met het in hoofdstuk 2 gepresenteerde theoretische metaalbindingsmodel. De resulaten van voltammetrische experimenten laten zien dat het bindingsgedrag van zink en cadmium met polyacrylaat en polymethacrylaat in overeenstemming is met de algemene verwachting voor polyelektrolieten met eenzelfde repeterende functionele groep; de bindingsterkte is (i) sterk afhankelijk van de concentratie éénwaardige tegenionen,

(ii) niet afhankelijk van de molecuulmassa van het polyelektroliet, (iii) afhankelijk van de ladingsverdeling op het polyelektroliet en (iv) homogeen met betrekking tot de affiniteit van metalen voor de afzonderlijke functionele groepen.

Hoofdstuk 6 is gewijd aan de voorbehandeling van natuurlijke organische stof en de karakterisering van het opgewerkte materiaal. De voorbehandeling heeft tot doel om de natuurlijke organische stof zoveel mogelijk te zuiveren en te transformeren in een zure vorm. Daarnaast is getracht om de organische stof te fractioneren op molecuulgrootte op basis van oplosbaarheidskarakteristieken van de organische stof. De resulterende produkten zijn gekarakteriseerd met betrekking tot (i) de hoeveelheid dissocieerbare groepen aan de hand van een conductometrische titratie en (ii) molecuulmassa verdelingen m.b.v. flow field-flow-fractionation. De fractionering door variatie in zuurgraad resulteert in fracties met verschillende molecuulmassa verdelingen. Toch toonen de resultaten aan dat de scheiding verre van ideaal is.

Ten slotte worden in *hoofdstuk 7* experimentele metaalspeciatiegegevens gepresenteerd voor systemen die natuurlijke organische stof bevatten. Met behulp van conductometrie en voltammetrie zijn we in staat om de speciatie van metalen in deze systemen te meten en te interpreteren. Het bindingsgedrag van metalen aan natuurlijke macromoleculen verschilt behoorlijk met dat van de synthetische polyzuren. Voor de gebruikte humuszuren is gevonden dat de binding van éénwaardige tegenionen, zoals kalium, veel zwakker is dan voor de modelstoffen polyacryl- en polymethacrylzuur. Een verklaring hiervoor is dat voor de onderzochte humuszuren de elektrische ladingen op het molecuul verder van elkaar liggen dan bij de modelstoffen. Hierdoor neemt de onderlinge elektrische wisselwerking tussen de ladingen af. De binding van zware metalen aan de onderzochte humuszuren wordt veeleer bepaald door de chemische heterogeniteit van het humuszuur.

De conclusies zijn van toepassing op verscheidene humuszuren. Wellicht is hier sprake van een algemene trend.

CURRICULUM VITAE

Op 7 februari 1965 ben ik geboren te Kerkrade. In 1983 behaalde ik het diploma Gymnasium β aan het gymnasium Rolduc te Kerkrade. In hetzelfde jaar werd ook begonnen met een studie Bodemkunde aan de toenmalige Landbouwhogeschool te Wageningen. In juni 1988 behaalde ik het doctoraal met als afstudeervakken Bodemscheikunde en Grond- en Gewasanalyse. Mijn praktijktijd bracht ik door bij het Forest Research Institute te Rotorua, Nieuw-Zeeland.

Van juni 1988 tot juni 1992 was ik in dienst bij de vakgroep Fysische en Kolloidchemie van de Landbouwuniversiteit. In deze periode vond het onderzoek plaats dat tot dit proefschrift leidde. Sinds 1 juli 1992 verricht ik bij het Laboratorium voor Ecotoxicologie van het Rijksinstituut voor Volksgezondheid en Milieuhygiëne onderzoek naar het fysisch-chemisch gedrag van zware metalen in de compartimenten bodem, sediment en water. Dit onderzoek vindt plaats in het kader van de afleiding van integraal afgestemde milieukwaliteitsdoelstellingen.